EFFECTS OF MIXTURE OF GRINDING MEDIA OF DIFFERENT SHAPES ON MILLING KINETICS

Kalumba Pascal Simba

A dissertation submitted to the Faculty of Engineering and the Built Environment, University of the Witwatersrand, in fulfilment of the requirements for the degree of Master of Science in Engineering.

Johannesburg, 2010

Declaration

I declare that this dissertation is my own unaided work. It is being submitted for the Degree of Master of Science in Engineering to the University of the Witwatersrand, Johannesburg. It has not been submitted before for any degree or examination to any other University.

_____

Kalumba Pascal Simba

06th Day of November 2010

Abstract

This dissertation focuses on the determination of breakage parameters in order to describe the performances of mixtures of grinding media of different shapes.

A series of batch grinding tests were carried out using the same mass of spherical balls, Eclipsoids^{TM} and cubes to break coarse, medium and fine sizes of quartz material. Then, mixtures of the same mass made of spherical balls and cubes, spherical balls and Eclipsoids^{TM} were successively considered. The breakage parameters were determined and used to evaluate the grinding performances of the mixtures of grinding media.

It was found that mixtures of grinding media shapes can increase the breakage rate in a particular milling environment. But, spherical balls remain the most efficient grinding media.

Finally, an optimal mixture made of grinding media of different shapes cheaper to manufacture can be used in the grinding process alternatively to 100 % balls.

Dedication

To The Almighty God

by

Kalumba Pascal Simba

Acknowledgements

Firstly, I thank the Almighty GOD who gave me the abilities to fulfill this Master's project.

Secondly, I thank my wife Debora and my son Joshua for the love, all the support and sacrifices endured. My in-depth acknowledgement and appreciation to my father Jean-Réné Simba, to maman Yvonne and to all my brothers and sisters for their unconditional support and encouragements.

Thirdly, I thank Professor Michael H. Moys, the supervisor of my Master of Science Dissertation. His advice, assistance, guidance and availability are highly appreciated.

Fourthly, I present my gratitude to Dr Murray Bwalya for the support, help and multiple advices during the data analysis process of the laboratory results. Mr. Gerard Finnie is acknowledged for his help during my research. I am also grateful to all colleagues, members of the comminution group, workshop staff and all the staff in the School of Chemical and Metallurgical engineering. While it is not possible to name every person, many thanks to all of you without which this work would not have been possible.

Lastly, I would like to thank the University of the Witwatersrand for supporting this work and allowing the publication of the results.

Kind regards.

K. P. Simba

Table of contents

List of figures

List of tables

List of symbols

a or $a(d)$	Breakage rate parameter characteristic of the material.
A	Material-dependent constant.
A_i	Material-dependent constant.
B	Material-dependent constant.
B_i	Material-dependent constant.
b'_{ii}	Parameter defined in Equation (2.11).
$b_{i,j}$	Mass fraction arriving in size interval i from breakage of size interval j.
$b_{i,j,k}$	Fractional breakage into size i from breakage of size j by size k balls
$B_{i,j}$	Cumulative breakage function of particles of size x_j into size x_i.
C	Material-dependent constant.
C_i	Material-dependent constant.
D	Internal mill diameter.
d	Ball diameter.
f_c	Fraction of mill volume occupied by the bulk volume of powder charged.
J	Fraction of the mill volume filled by the ball bed.
$m(x,t)$	Mass fraction of the primary breakage products less than x_i when particles in class j break.
M_i	Mass fraction in class i.

N	Mill speed in rpm.
P	Power drawn by the mill.
$P_{expt}(t)$	Retained mass fraction on top size screen x at grinding time t as experimentally measured.
$P_i(t)$	Weight fraction of the material less than size x_i at time t.
$P_{model}(t)$	Predicted mass fraction retained on size screen x after grinding of single-sized material of initial size x for a total grinding time t.
$Q(x)$ or $Q(x_i)$	Correction factor of the selection function equation in the abnormal breakage region.
S_i	Rate of disappearance of material of size i or specific rate of breakage of particles of size x_i, also known as selection function
S_A	Selection function of component A of the material.
S_B	Selection function of component B of the material.
S_C	Selection function of component C of the material.
SSE	Objective function known as the Sum of Squares Errors.
t	Grinding time.
x_i	Size of particles in class i; for a size interval the upper size used to represent the particle size.
x_j	Size of material in the top size.
x_m	Particle size for which S_i is maximum for given ball and mill diameters.
U	Fraction of the spaces between the grinding media at rest which is filled with powder.

V_M	Mill volume.
$w_i(t)$	Mass fraction of unbroken material of size i in the mill at time t.
W	Total charge mass.
α	Parameter characteristic of the material.
β	Breakage parameter characteristic of the material used.
γ	Breakage parameter characteristic of the material whose values typically are found to be between 0.5 and 1.5.
Λ	Positive number representing an index of how rapidly the rate of breakage falls as size increases in the abnormal region.
φ_i	Fraction of harder material.
τ	Torque exerted by the mill minus friction in the bearings.
μ or $\mu(d)$	Particle size at which the correction factor $Q(x)$ is 0.5 for a ball diameter d, it varies with mill conditions.
Φ_j	Fraction of the fines produced.
ϕ	Breakage parameter characteristic of the material used, it represents the fraction of fines that are produced in a single fracture event.

Chapter 1 Introduction

1.1 Background

Grinding media have a direct effect on the operation of industrial mills. The effect of grinding media on milling kinetics has been studied using different shapes of grinding media (Kelsall *et al.*, 1973, Herbst and Lo, 1989, Shi, 2004, Lameck *et al.*, 2006, Ipek, 2007, Cuhadaroglu *et al.*, 2008).

Spherical balls or spheres (here referred as "balls") were found to be more efficient than other grinding media shapes. Balls produced the finest products and used the least power for constant batch grinding time (Norris, 1953). But, alternative shapes to balls have been suggested to reduce the grinding costs and increase the milling efficiency. These early works focused on one shape and, sometimes compared the performances of two or more different media shapes. From then on, the role of media shape on grinding performance gained some attention.

However, very little work has been done on investigating mixtures of media of different shapes. The study of these mixtures could enlighten the behaviour of grinding media after breaking and wearing out as well as to improve the grinding efficiency of media shapes which are easy to manufacture and of poor grinding performance when used alone.

Generally, the performance of the grinding process can be satisfactorily measured using the population balance model technique. In this model, milling

is expressed in terms of the selection function and the breakage function. For this study, the selection and breakage functions are determined by batch grinding tests performed on single particle sizes for grinding media charge consisting of a single size for each shape, and for charge of mixture made of grinding media of different shapes. The selection and breakage functions parameters obtained are compared, and the performances of the mixture of grinding media shapes are eventually evaluated.

1.2 Statement of the problem

The spherical balls which are predominantly used in ore grinding change shape through breakage and wear. They can even break during the grinding process. These balls constitute a section which moves slowly but does no effective grinding. Possible remedies are a lower ball charge, higher lifters or an increase in mill speed (Napier-Munn, *et al.*, 1996). The movement of these irregularly shaped components through the mass of the charge is believed to differ significantly from the behaviour of initial grinding media shapes. Additionally these worn balls experience surface and linear contacts with each other, while spherical ones have only point contact interactions. The breakage is then done more with mixture of grinding media of different shapes than with a defined single shape of media.

Also, the need to minimize the costs of the grinding process may lead to the use of an alternative grinding media shape to balls. The introduction of the new grinding media shape may be done gradually to avoid the regrading costs or may just be used in association with the balls. Moreover, the change in the entire size

distribution of balls charged in a grinding system is determined assuming that ball wear was equal to the loss in ball mass, ball wear was a function of ball size, and fresh balls replacing the worn balls had the same characteristics (Austin *et al.*, 1985).

An investigation of mixtures of grinding media of different shapes is worth it to understand how they affect the milling kinetics. Our hypothesis is that the volume of grinding zones can be increased when there is an optimal mixture of two grinding media with different shapes and, therefore the milling kinetics will be improved.

1.3 Research objective

The mean objective of this research is to investigate the Population Balance Model which requires a complete breakage characterization of the material being described in terms of selection and breakage functions. In order to achieve this, a series of laboratory tests was carried out on quartz material sample.

In this dissertation the breakage parameters are estimated for mixture of grinding media of different shapes, and then compared to the parameters of individual grinding media shapes. The overall impact of the mixture of grinding media shapes is then evaluated in terms of their grinding performances.

1.4 Layout of the dissertation

This dissertation is organized into six chapters. The first chapter introduces the Research; the importance of grinding media shapes is discussed and the

motivation behind this study is stated. The organization of the dissertation is also covered in this chapter.

The second chapter presents a literature review. The importance of grinding media in comminution is reviewed. The Population Balance Model (PBM) is discussed as well.

The third chapter provides a detailed description of the laboratory work and equipment used to achieve the objective. Experimental procedures that were used are also presented.

The fourth chapter characterizes the milling kinetics as a function of media shapes used for this study. The specific rate of breakage and breakage distribution parameters of the feed material are estimated. A comparison between these media shapes performances is done as well.

The fifth chapter presents the effects of mixtures of grinding media of different shapes on milling kinetics. Their performances are respectively compared to those obtained with the different media shapes used in the previous chapter.

The last chapter summarizes the conclusions drawn from this work and some recommendations for future investigation.

Chapter 2 Literature Review

2.1 Introduction

The reduction of particle size of an ore material is usually achieved progressively, different methods being applied at different stages in the comminution process (Woollacott and Eric, 1994). Particularly, the tumbling grinding mill has been found to apply a small force to a large number of particles by using grinding media (Kelly, 1982). And grinding media have a significant impact on the performance of tumbling mills in terms of product size distribution, energy consumption and grinding costs (Mineral Processing Handbook, 2002).

On the other hand, grinding media costs compared with overall grinding costs are usually high and need to be minimized. As a consequence, many surveys have been conducted to study the influence of different grinding media shapes on the grinding process (Kelsall *et al.*, 1973, Cloos, 1989, Allen *et al.*, 1993, Lameck *et al.*, 2006).

Despite the fact that balls were found to be the most efficient, the use of other grinding media shapes as an alternative to balls has often been suggested to reduce the specific energy consumption and grinding costs, to increase throughput and the milling efficiency. These early works focused on one shape without exploring possible advantages of the use of mixtures of media shapes. Thus, this research extends to the use of mixture of media shapes to enhance grinding.

A review of previous works is presented in this chapter. The population balance model, which satisfactorily describes the grinding process, is also discussed.

2.2 Grinding media in comminution

The grinding media do impact on the operation of industrial mills. They hence are a critical component of tumbling mills. Therefore, it is important to understand their contribution in the grinding process. Ideally, grinding media should have the largest possible surface area to provide suitable contact with the material being ground and they should be heavy enough to have sufficient energy required for breaking the ore particles. These requirements must be balanced, since the larger the individual grinding media, the less the specific surface.

As the grinding proceeds, the grinding media become worn or break. As a result, fresh grinding media must be added in the mill. Grinding media form a significant part of the operating costs of the mill operation. To reduce grinding media consumption, several approaches were proposed: the use of higher-quality, wear-resistant grinding media, the use of cheaper grinding media, or yet the use of large lumps of material being ground (Woollacott and Eric, 1994).

2.2.1 Grinding media shape

The role of grinding media shapes on grinding performance had recently gained attention. The manufactures of the grinding media have made conflicting claims regarding their milling performance. Many surveys on grinding media were then conducted in that regard.

In 1924, Fairchild made a comparison of spheres and cubes in two full-scale ball mills operating in parallel. Considering similar feed and product size distribution, he found that cubes were more efficient. The assessment was based on iron consumption and power drawn per ton of ore reduced (Kelsall *et al*, 1973).

In 1945, Taggart concluded that balls were the most effective and cheapest size reduction media for the particle size ranges normally ground by mills (Kelsall *et al*, op cit).

Norris (1953) reported the results of a laboratory scale wet batch-grinding tests with mixed and uniformly sized spheres, cubes, discs, cylinders and more complex shapes, and of a plant test comparison of cubes and spheres (Kelsall *et al*, op cit). He concluded that for constant batch grinding time spheres produced the finest products and used the least power, while cubes and discs were the least efficient. However, each cube was approximately 34 % heavier than each ball in the uniform charges. Consequently, it was not possible to quantify the effects caused by a change in shape alone.

Then, in 1970, Howard pointed out the controversy around grinding media. He recommended an understanding of autogenous grinding mechanisms since ore lumps were of varied shapes.

Later, in 1973, Kelsall *et al* studied the influence of different grinding media shapes (steel spheres, cubes, long, short and equi-cylinders, and hexagonal "cylinders") on grinding in a small continuous wet ball mill. They showed that grinding media shape had a significant effect on both the selection function *S*

and the breakage function *B*. These media shapes had a marked effect on the average residence time, but little effect on the type of flow through the mill. They also showed that spherical media handled the greatest throughput and produced the most correctly sized product.

In 1988, Howat and Vermeulen experimentally investigated the fineness of grind, the consumption and wear rate of balls, cones, pebbles and cylpebs. The fineness of grind was determined by measurement of the harmonic mean size of the product and the fraction of material smaller than 75 microns. They concluded that for equal charge masses of balls and cones, conical media produced coarser grind at all feedrates.

Cloos (1989) suggested the use of cylpebs as an alternative media to balls for fine grinding. He argued that the mill power is determined by the weight of the grinding charge and, for the same total weight of media charge, irrespective of size or shape, the mill would require the same power as such the specific energy consumption could be reduced as shapes and size can increase throughput.

Herbst and Lo (1989) found that balls were more efficient than truncated cones with an energy advantage of 5-20 %. They attributed this difference to the probability of capture for cones because of their increased surface contact being higher than the point contact made between balls. The methodology they developed for comparison of the grinding efficiency of a tumbling mill using balls and truncated cones as grinding media showed no difference in breakage functions, but significant differences in specific selection functions.

In 1993, Allen *et al.*, from Armco Mineral Processing, conducted industrial tests comparing grinding efficiency of forged balls and cylpebs at plant grinding silica. Their results indicated that spherical forged balls have advantages of lower wear rates, lower specific energy consumption and increased throughput.

Shi (2004) conducted comparatives tests using balls and cylpebs in a laboratory Bond mill at various conditions such as same media mass, same size distribution, same surface area and same input specific energy. Single-stage batch grinding tests revealed that, depending on the conditions, one grinding media shape was advantageous than the other, the greater surface area of cylpebs being balanced by the line contact and area contact grinding action. The scale-up to predict cylpebs performance reached the same conclusion. His research concluded that, according to the simulations, fine generation rate is more dependent on the media size distribution than the media shape.

In 2006, Lameck *et al*. compared spherical balls and worn balls. They found that spherical balls had slightly higher rates of breakage. And, considering the proportion of worn balls inside the balls charge (15-40 %), there were no benefit to justify the removal of worn balls from the mill.

Lameck *et al*. (2006) also investigated the effects of cylpebs, spherical and worn balls on load behaviour and mill power drawn at various load filling and mill speeds. Toe and shoulder positions were used to account for the load behaviour and mill power. They found that the power drawn was sensitive to media shape and gave a valuable insight of the behaviour of the three grinding media shapes.

In 2007, Ipek also compared cylpebs and balls in a laboratory ball mill under the same conditions of mass and feed. The results showed faster breakage rates for the coarse fractions with cylpebs as charge, these differences being more significant for coarser fractions than for fine fractions. His results suggested also that cylpebs produced slightly finer size products than balls. In addition, the primary breakage distribution function proved to be dependent on the feed size, but independent of the grinding media shape.

In 2008, Cuhadaroglu *et al*. investigated the effect of balls and cylinders on the breakage parameters of colemanite. They concluded that the use of cylinders has resulted in higher breakage rates compared to balls due to the fact that both rod mill and ball mill actions are provided in the same grinding system. In term of production of fines, they found that cylinders produce more fines at shorter grinding time while the amount of fines for ball grinding exceeds that of cylinders after progressive grinding.

2.2.2 Grinding media action

Grinding within the tumbling mill is influenced by the size, quantity, the type of motion, and the spaces between the individual pieces of medium in the mill (Wills and Napier-Munn, 2006). Also, the degree of grinding of a particle depends on the probability to enter the grinding zone between the media shapes and the probability of some breakage to occur in that grinding zone. Therefore, the grinding can be done by several mechanisms which distort the particles and change their shapes beyond their degree of elasticity, which causes them to

break. In a ball mill, particles break primarily by impact and attrition (King, 2001).

2.2.2.1 Impact breakage

Breakage by impact, also referred as breakage by compression, occurs when forces are normally applied to the particle surface. This mechanism of fracture encompasses shatter and cleavage (King, 2001). Fracture by cleavage occurs when the energy applied is just sufficient to load comparatively few regions of the particle to the fracture point, and only a few particles result. The progeny size is comparatively close to the original particle size. This fracture occurs under conditions of slow compression where the fracture immediately relieves the loading on the particle.

Chipping is a special case of cleavage whereby a relatively small piece is cleaved off the particle, leaving a particle of essentially the original size (Kelly and Spottiswood, 1990).

On the other hand, fracture by shatter occurs when the applied energy is well in excess of that required for fracture. Under these conditions many areas in the particle are over-loaded and the result is a comparatively large number of particles with a wide spectrum of sizes. This occurs under conditions of rapid loading such as in a high velocity impact (Kelly and Spottiswood, 1982).

2.2.2.2 Abrasion impact

Abrasion fracture occurs when insufficient energy is applied to cause significant fracture of the particle. It is a surface phenomenon which takes place when two particles move parallel to their plane of contact. In this case, localized stressing

occurs and a small area is fractured to give a distribution of very fine particles (effectively localized shatter fracture) (Kelly and Spottiswood, 1982).

2.2.2.3 Breakage by attrition

Breakage by attrition is explained as the rubbing together of two media. This occurs between two similar mediums, such as quartz particles, or two separate media such as quartz and steel. Attrition is assumed to be largely responsible for the breaking of particles that have become smaller than the voids between the grinding media. Attrition can also be seen as the act of wearing or grinding down by friction.

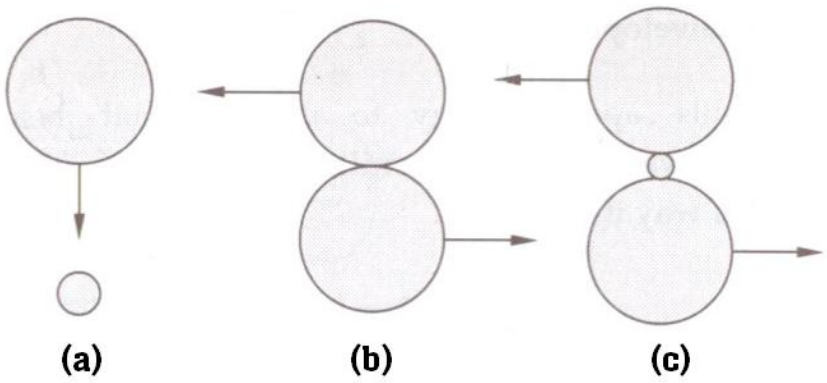

Figure 2.1 Breakage mechanisms in a ball mill: (a) impact, (b) abrasion, (c) attrition (Napier-Munn *et al.*, 1996)

2.2.3 Grinding media motion in a tumbling mill

The relative motion of the media is determined by the tumbling action which in turn is strongly influenced by the lifters and liners. The tumbling mill rotates and the grinding media are lifted along the rising side of the mill until they cascade and cataract down to the toe of the mill charge. The speed at which the mill is

run is important, since it governs the nature of the product and the amount of wear on the shell liners. And, it is common to define the critical speed at which the grinding media will just hold against the shell for the full cycle. The following figure presents the motion of the charge in the tumbling mill.

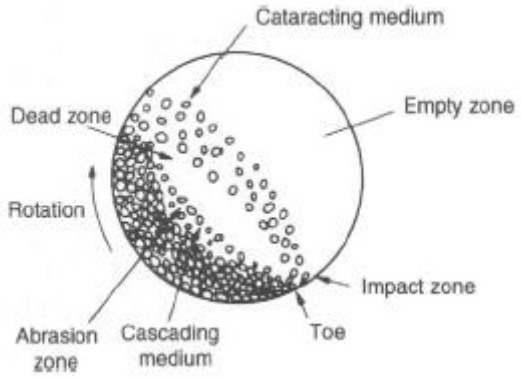

Figure 2.2 Motion of charge in a tumbling mill (Wills *et al.*, 2006).

The grinding media tumble relatively gently at low rotational speeds. They tend to be raised and to slip back as a locked mass. As the tumbling action increases with the increasing of the speed, grinding media emerge from the bed, roll down and reenter the mass. The bed is then expanded, allowing particles to penetrate between the grinding media. This series of collisions while the grinding media are tumbling down is called cascading. This cascading leads to finer grinding with increased slimes production and increased liner wear. Therefore, the dominant size-reduction mechanism in this case is attrition.

On the other hand, at higher rotational speeds, grinding media are ejected from the shell and from the main body of the load and are thrown into free flight before impacting on the toe of the load or on the mill liners. This tumbling

action is called cataracting, and the dominant size-reduction mechanism is impact breakage.

At higher speeds still, the load in the mill starts to centrifuge and the relative motion between the grinding media, particles and mill liners is insignificant. Consequently, the grinding rate is reduced drastically.

The speed at which the load just starts to centrifuge is defined as the critical speed. The critical speed of the mill is expressed as (Austin *et al.*, 1984):

$$\text{critical speed, rpm} = \frac{42.3}{\sqrt{D-d}} \tag{2.1}$$

where D is the internal mill diameter and d is the maximum ball diameter, both in meters.

The fraction of critical speed at which these processes occur depends on the filling conditions and the type of lifters (Austin *et al.*, 1984).

2.2.4 Media size

The selection of media size is a compromise between two conflicting factors. On one hand, the surface area for grinding increases giving a higher capacity while the relative size of the media decreases. On the other hand, as the media size increases, the force between the grinding surfaces increases so that larger particles can be broken (Kelly and Spottiswood, 1982).

The efficiency of grinding depends on the surface area of the grinding medium. The angle of nip is important and grinding media sizes must be carefully chosen in relation to the largest and hardest particles in the feed. Various formulae have been proposed for the required ratio of ball size to ore size, however, none of

which is entirely satisfactory; the practice of charging balls to a tumbling mill is a matter of experience as well (Concha *et al,* 1992). The capacity of a mill increases with decreasing ball diameter, due to the increase in grinding surface, to the point where the required angle of nip between contacting balls and particles is exceeded.

During mill operation, grinding media are reduced in size because of wear. And, the grinding characteristics change. The extent of wear would depend on the characteristics of the rock present, such as density, composition and surface hardness. It is also affected by the speed of mill rotation, the mill diameter, the specific gravity of the mineral and the work index of the mineral (Gupta and Yan, 2006). According to Austin *et al,* (1984), the variation of breakage function values for crystalline quartz changed slightly with ball diameter, with larger ball diameters giving proportionally more fines. A lower specific rate of breakage due to larger balls is partially compensated by the production of a bigger proportion of fines fragments per impact.

Kotake *et al,* (2002) investigated the effect of feed size and ball diameter on the grinding rate constant of material being ground when the mass of balls, mass of feed and the rotational speed of the mill were kept constant. They found that the variation of the grinding rate constant with feed size was roughly similar, for all feed materials used.

2.3 Population balance model

During mill operation, coarse feed enters the mill, undergoes breakage actions and exit the mill with a finer size distribution. The energy input is converted to mechanical breakage action to form the broken finer size particles (Yekeler, 2007). The modelling of such a mechanism necessitates a detailed understanding of the grinding process itself. This process is apparently a combination of two actions taking place simultaneously inside the mill: a selection of the particle for breakage, and a breakage of the selected particle resulting in a particular distribution of fragment sizes (Gupta and Yan, 2006).

The complexity of the breakage environment in a tumbling mill preludes the calculation of parameter values given in the models developed for this process. Parameter estimation techniques can be classified in three broad categories (Wills *et al.*, 2006):

- Graphical methods which are based mainly on the grinding of narrow size distributions.
- Tracer methods which involve the introduction of a tracer into one of the size intervals of the feed and the analysis of the product for the tracer.
- Non-linear regression methods, which allow all parameters to be computed from a minimum of experimental data.

The Population Balance Model (PBM) which is a non-linear regression method has been used for our investigation. In this method, the grinding process is fully described using a size-mass balance inside the mill that takes into account the

two abovementioned actions. This population balance uses mass that is experimentally measured rather than numbers of particles (Yekeler, 2007).

2.3.1 Selection function

The Selection function or the rate of breakage is the fractional rate at which a given size of particle disappears, having been broken into smaller particles. It usually assumed that it obeys a first-order breakage pattern (Austin *et al.*, 1973). For batch grinding of brittle material in various types of small laboratory mills, the rate of breakage can be expressed as:

$$Rate\ of\ \ breakage = S_i w_i(t) W \tag{2.2}$$

where S_i is a specific rate of breakage of particles of size i, $w_i(t)$ is the mass fraction of the total charge and W is the total charge at time t of grinding. Throughout batch grinding, the total charge is constant. Then, this equation can be rewritten for $i = 1$ as:

$$\frac{dw_1(t)}{dt} = -S_1 w_1(t) \tag{2.3}$$

which gives, after integration:

$$\log[w_1(t)] = \log[w_1(0)] - S_1 t / 2.3 \tag{2.4}$$

This is an integrated form of the batch grinding equation for the breakage of larger sizes prepared in narrow size fractions, where $w_1(t)$ is the weight fraction of the mill hold-up in class 1 at time t (Austin *et al*, 1984).

The formula proposed for the variation of the specific rate of breakage S_i with particle size is:

$$S_i(d) = a(d).[\frac{x_i}{x_0}]^{\alpha}.Q(x) \text{ with } Q(x) = \frac{1}{1+[\frac{x_i}{\mu(d)}]^{\Lambda}}, \quad \Lambda > 0 \qquad (2.5)$$

where $a(d)$ is a parameter defining the breakage rate in a particular mill under defined operating conditions;

α is dependent on the material ground;

x_i is the particle size in mm;

x_0 is a reference size, usually 1 mm;

$\mu(d)$ defines the particle size at which $Q(x)$ is 0.5;

and Λ is an index of how rapidly the rate of breakage falls away.

Λ is found to be primarily characteristic of the material, but $\mu(d)$ varies with the mill condition (Austin *et al.*,1984).

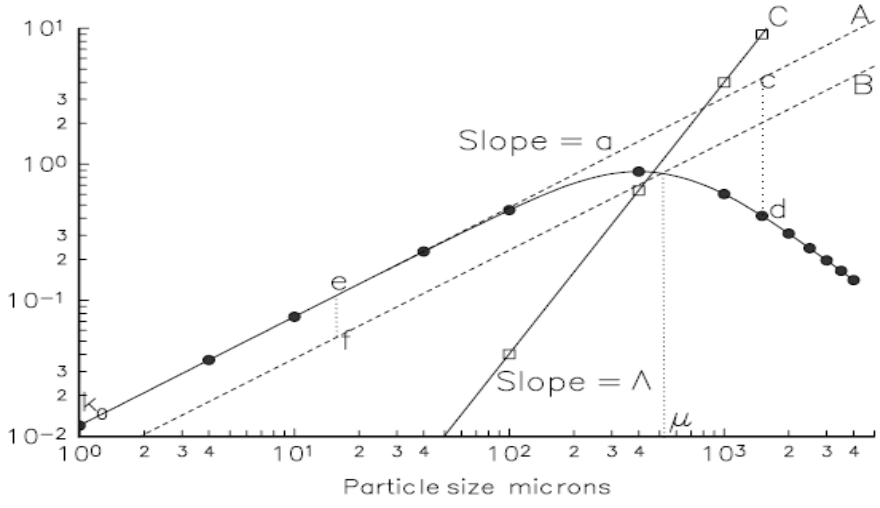

Figure 2.3 Graphical procedures for the determination of parameters in Austin's selection function (King, 2000).

2.3.2 Breakage function

The breakage function describes the size distribution of the products of breakage. The primary breakage distribution function of a particle of size j to size i is defined as follows:

$$b_{i,j} = \frac{mass\ of\ particles\ from\ class\ j\ broken\ to\ size\ i}{mass\ of\ particles\ of\ class\ j\ broken} \tag{2.6}$$

The values of the primary breakage distribution function are deduced from the size distributions at short grinding times. The general empirical fitting model of the breakage function, $B_{i,j}$, is given by:

$$B_{i,j} = \phi_j [\frac{x_{i-1}}{x_j}]^{\gamma} + (1-\phi_j)[\frac{x_{i-1}}{x_j}]^{\beta} \tag{2.7}$$

Where γ, β and ϕ_j are all characteristic of the material being ground and are parameters which can be adjusted to ensure that $B_{i,j}$ represents the experimental data. The parameter γ characterises the size distribution of fines produced from breakage of the top size material, β characterises the size distribution of coarse progeny and ϕ_j indicates the fraction of fines produced, x_i is the top size and $B_{i,j}$ is the weight fraction of the primary breakage products less than x_i when particles in class j break (Austin *et al.*, 1984).

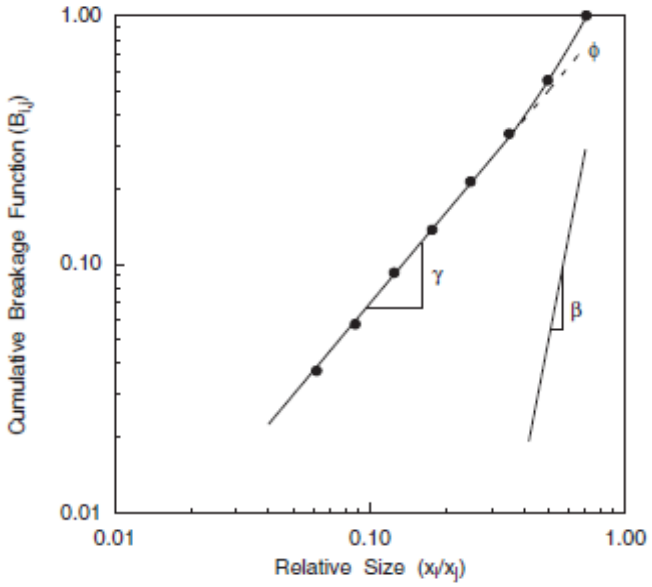

Figure 2.4 The cumulative primary daughter fragment distribution of any material ground (Yekeler, 2007).

The $B_{i,j}$ values are said to be normalizable when the fraction appearing at sizes less than the initial feed size is independent of the initial feed size. For non-normalizable breakage, the distribution parameters are calculated using the nonlinear regression method. Equations (2.8) and (2.9) are then used (Austin *et al.*, 1984).

$$B_{i,j} = \phi_j [\frac{x_{i-1}}{x_1}]^{\gamma} + (1-\phi_j)[\frac{x_{i-1}}{x_1}]^{\beta}, \qquad 0 \leq \phi_j \leq 1 \tag{2.8}$$

$$\phi_j = \phi_1 [\frac{x_i}{x_1}]^{-\delta} \tag{2.9}$$

where δ characterizes the degree of non-normalization.

If $B_{i,j}$ values are independent of the initial feed particle size, then $\delta = 0$.

2.3.3 Abnormal breakage

In laboratory mills, some materials are subjected to abnormal breakage which is defined as departure from first-order kinetics, and occurs particularly for the larger feed particle sizes (Austin *et al.*, 1973).

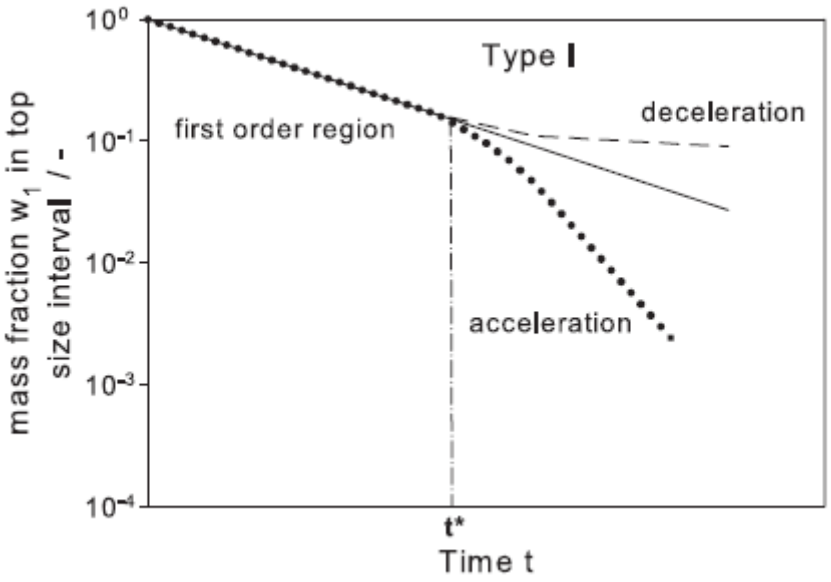

Figure 2.5 Characteristic deviations from the linear kinetic approach for breakage of monodisperse material (Toneva and Peukert, 2007).

Several models were proposed to explain it. First, they assumed the material to consist of an initial material A that breaks to produce another material B. The two materials are different only on a breakage point of view. The component A is breaking to component B during the grinding. Thus, they found the following model:

$$w_i(t) = \frac{m(t)}{m(0)} = (1-\varphi_i)e^{-S_A t} + \varphi_i . e^{-S_B t} \qquad (2.10)$$

where $\varphi_i = \frac{b'_{ii} S_A}{S_A - S_B}$; S_A is the selection function of component A of the material and S_B is the selection function of component B of the material. The system behaves as if the A material consists of a fraction $(1-\varphi_i)$ of soft material and a fraction φ_i of harder material.

In general the effective mean value of the selection function is given by:

$$S_i = \frac{1}{\frac{1}{S_{Ai}} + \frac{b'_{ii}}{S_{Bi}}} \tag{2.11}$$

Austin *et al.* (1984) suggests that the mean effective specific rate can be defined by the time required to break 95% of the material when a particle size presents an abnormal behaviour. Alternatively Equation (2.11) can be used.

If the non-first-order grinding batch grinding cannot be fitted with Equation (2.10), another more elaborated equation is proposed. They assumed the feed A is breaking into an intermediate material B which in turn breaks to a final material C. The corresponding model is as follows:

$$w_i(t) = \frac{m_i(t)}{m_i(0)} = \left\{1 + S_A t + \left(\frac{S_A}{S_A - S_C}\right)^2 \left[(S_C - S_A)t - 1\right]\right\} . e^{-S_A t} + \left(\frac{S_A}{S_A - S_C}\right)^2 e^{-S_C t} \tag{2.12}$$

The effective mean value of the milling rate is given by

$$S_i = \frac{1}{\frac{1}{S_{Ai}} + \frac{1}{S_{Bi}} + \frac{1}{S_{Ci}}} \tag{2.13}$$

The disappearance of larger sizes material from a given top size interval is often not first order. It can be modeled as consisting of a faster initial rate and a slower following rate.

2.3.4 Beyond the first-order kinetics

The population balance modeling is widely used to analyse, simulate, control and optimize grinding processes. Additionally, population balance models enable to elucidate the breakage mechanisms (Bilgili *et al.*, 2004). A formulation of the population balance model for a well-mixed batch grinding process is given by Bass (1954):

$$\frac{\partial m(x,t)}{\partial t} = -S(x)m(x,t) + \int_{x}^{\infty} b(x,y)S(y)m(y,t)dy \quad \text{with} \quad m(x,0) = m_0(x), \qquad (2.14)$$

where the first term describes the first-order disappearance rate of particles of size x, the second term is the generation rate of particles of size x due to first-order breakage of all particles of size $y \geq x$, $m(x,t)$ is the mass fraction of particles within a differential size range $x + \partial x$ at time t.

To account for discrete form in which experimental data for batch grinding is, the following size-discrete form of Equation (2.14) was introduced (Austin, 1971):

$$\frac{dM_i(t)}{dt} = -S_i M_i(t) + \sum_{j=1}^{i-1} b_{ij} S_j M_j(t), \quad N \geq i \geq j \geq 1 \quad \text{with} \quad M_i(0) = M_{i0} \qquad (2.15)$$

where i and j are the size-class indices running up to N, M_i is the mass fraction in class i, S_i is the specific breakage rate parameter and b_{ij} is the

breakage distribution parameter. Equations (2.14) and (2.15) are referred to as the linear, time-invariant population balance models because the specific breakage rate of particles of size x depends only on size x, but not on population density and/or time. Austin (1971) stated that Equation (2.15) which recognizes the "apparent non-linearity" does not hold for long milling times.

Austin and Bagga (1981) introduced a time-dependence to the specific breakage rate parameter S_i:

$$\frac{dM_i(t)}{dt} = -S_i(t)M_i(t) + \sum_{j=1}^{i-1} b_{ij}S_j(t)M_j(t) \quad \text{with} \quad M_i(0) = M_{i0} \tag{2.16}$$

This linear, time-variant model accounts for non-first-order kinetics that originates from truly time-dependent phenomena. Phenomenon such as the slowing-down of the specific breakage rate observed in dry grinding are not explained explicitly and thoroughly. The traditional population balance models neglect the effects of the temporally evolving materials properties and multi-particle interactions (Bilgili *et al.*, 2005).

Consequently, the context of non-linear population balance models was introduced to explain the non-first-order breakage rates that originate from multi-particle interactions. Particularly, a non-linear model for batch grinding process was proposed by Bilgili *et al.* (2004):

$$\frac{\partial m(x,t)}{\partial t} = -k(x,t)F\left[\int_0^\infty P(x,z)m(z,t)dz\right]m(x,t) + \int_x^\infty k(y,t)F\left[\int_0^\infty P(y,z)m(z,t)dz\right]b(x,y)\times m(y,t)dy$$

$$\text{with} \quad m(x,0) = m_0(x) \tag{2.17}$$

where z is a generic particle size surrounding particles of size x, $z \neq x$.

The general non-linear framework is then derived in four non-linear size-discrete population balance models A, B, C and D with varying complexity. This non-linear framework reduces to the traditional models under certain limiting conditions.

2.4 Summary

In this chapter, the significant impact of grinding media on the performance of milling process in terms of product size distribution, energy consumption and grinding costs is underlined (Mineral Processing Handbook, 2002). A review of a wide range of research on grinding media is done. It is clear that very little work has been done to investigate mixtures of grinding media of different shapes.

The population balance model, which satisfactorily describes the grinding process, is also discussed. The specific breakage rate and the breakage distribution are both defined.

The specific breakage rate parameters are obtained using the following equation (Austin, 1984):

$$S_i(d) = a(d).[\frac{x_i}{x_0}]^{\alpha}.Q(x)$$

$a(d)$ and $\mu(d)$ which are dependent of the mill conditions are the main focus of this investigation.

The breakage distribution parameters which are less sensitive to the change on the operating conditions and the feed size distribution than the specific breakage rate parameters are given by:

$$B_{i,j} = \phi_j \left[\frac{x_{i-1}}{x_j}\right]^{\gamma} + (1-\phi_j)\left[\frac{x_{i-1}}{x_j}\right]^{\beta}$$

The breakage function parameters, which are assumed to be ore dependent, are considered the same for all the different grinding media shapes.

The abnormal breakage which occurs particularly for the larger feed particle sizes in laboratory mills (Austin *et al.*, 1973) is also explained.

The linear, time invariant and time variant population balance models are reviewed. Eventually, the non-linear population balance framework is introduced in order to explain the physical or mechanical multi-particle interactions which the assumed first-order breakage rate cannot thoroughly explain (Bilgili, 2004).

Chapter 3 Experimental Equipment and Programme

This chapter describes the laboratory grinding mill. Also, the grinding media and the feed samples used for the batch tests are presented. Additionally, the tests performed to generate the experimental data are explained and the method used to characterize the breakage properties of the quartz defining the milling kinetics of the grinding media shapes and the mixtures of these grinding media shapes is presented.

3.1 Laboratory grinding mill

The Wits small laboratory mill was used to carry out the batch grinding tests on the quartz sample. This mill was fitted with eight equally spaced lifters. The mill has 0.302 m diameter and 0.282 m length. And, it is driven by a 0.25 kW mono-phased variable speed motor.

This laboratory mill is equipped with safety switch which allows to monitor the correct use of this equipment. The speed controller is used to set the operational speed at which the mill is run. The motor is connected to a torque arm to enable measurement of forces exerted on the beam, allowing the mill power to be obtained. A series of known weights was hung to the load beam to calibrate the torque required to turn the mill. The load beam is mounted on the frame of the mill rig and connected to the mill axle.

Eventually, the maker signal and the voltage signal are recorded via the data acquisition card on the control room computer using the WaveView software.

Figure 3.1 presents a photograph of the laboratory mill used for our investigation.

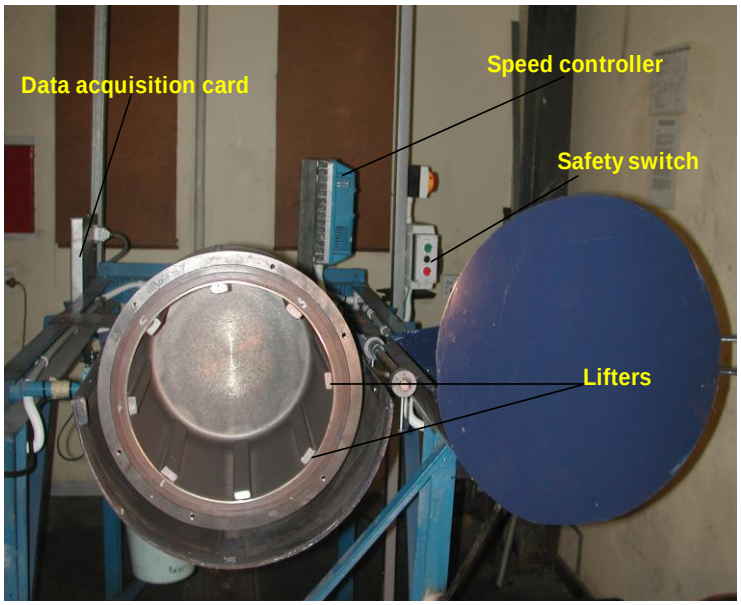

Figure 3.1 Snapshot of the Wits small laboratory mill.

The basic mill power drawn equation described by Hogg and Fuerstaneu (1972) is given by:

$$P = \frac{2\pi N \tau}{60} \tag{3.1}$$

where N is the mill speed in rpm,

τ is the torque exerted by the mill charge minus friction in the bearings.

The laboratory operating conditions used for our batch tests are presented in Table 3.1 below.

Table 3.1 Laboratory operating conditions.

Mill dimensions	
Diameter	*0.302 m*
Length	*0.280 m*
Volume	*0.0202 m^3*
Lifters	
Number	*8*
Material	*Mild steel*
Profile	*parallelepiped*
Height	*10 mm*
width	*20 mm*
Tests conditions	
Ball filling, J [a]	*20 %*
Powder filling, U [b]	*75 %*
Mill speed	*75 % of critical speed*

([a]) $J = \left(\frac{mass\ of\ balls / ball\ density}{mill\ volume} \right) \times \frac{1.0}{0.6}$ (3.2)

([b]) $U = \frac{f_c}{0.4J}$ where $f_c = \left(\frac{mass\ of\ powder / powder\ density}{mill\ volume} \right) \times \frac{1.0}{0.6}$ (3.3)

U is the fraction of the spaces between the grinding media at rest which is filled with powder. Efficient breakage in the mill is obtained with a powder grinding media ratio ranging from 0.6 to 1.1.

3.2 Grinding media and test materials

3.2.1 Grinding media

Balls, cubes and Eclipsoids made of cast iron were used for the batch tests. Eclipsoids are semi-prolate spheroid (stretched ellipsoid of revolution). Their shape is similar to that of a half rugby football (Figure 3.2). The pictures of grinding media shapes used in this study are presented in Figure 3.3.

Figure 3.2 Scaw Metals Eclipsoids^{TM} used for the batch tests.

Figure 3.3 Photographs of spherical balls, cubes and a mixture of grinding media shapes used in this study.

40 mm balls, 40 × 40 mm Eclipsoids and 32 mm cubes were used. The total load mass was kept constant for all grinding media shapes, as well as for the mixtures of grinding media for an average porosity of 0.4 (Austin *et al.*, 1984). However, the material properties such as coefficient of friction, size and shape affect media

packing (Zhou *et al*, 2002). Various mixtures of grinding media of different shapes constituted of percentage mass were used for our experiments. Table 3.2 below gives the physical properties of the grinding media used.

Table 3.2 Physical properties of the grinding media.

Grinding media	Balls	Eclipsoids	Cubes	Mix B-E*	Mix B-C 1*	Mix B-C 2*
Mass (kg)	0.256	0.256	0.260	-	-	-
Specific gravity (g/cm^3)	7.64	7.64	7.93	-	-	-
Surface area (cm^2)	50.27	62.84	61.44	-	-	-
Volume (cm^3)	33.51	33.51	32.77	-	-	-
Grinding media number	72	72	71	36 - 36	36 - 35	54 – 18
Mass charge (kg)	18.432	18.432	18.460	18.432	18.432	18.504
Total surface area (cm^2)	3619.58	4524.48	4362.24	4072.03	3987.60	3820.61
Total Volume (cm^3)	2413.06	2413.06	2326.53	2413.06	2368.03	2399.62

(*): Mix B-E is the mixture made of 50% balls and 50% eclipsoids, Mix B-C 1 is the mixture made of 50% balls and 50% cubes and Mix B-C 2 is the mixture made of 75% balls and 25 % cubes.

The grinding media used present different contact mechanisms during grinding action. These contact mechanisms are function of their geometry.

The following figures show these different contact mechanisms. Balls are subjected to point contact only between them, while cubes and Eclipsoids present point, line and flat facets contacts in grinding action. Eclipsoids are mostly subjected to line contact mechanisms whereas cubes are mostly subjected to flat facets contact in grinding action.

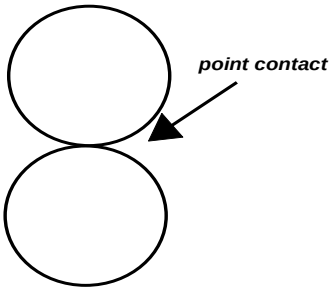

Figure 3.4 Point contact mechanism of balls.

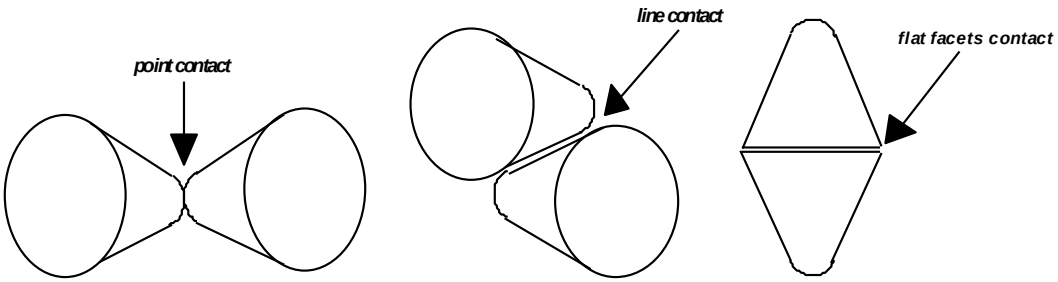

Figure 3.5 Contact mechanisms of Eclipsoids.

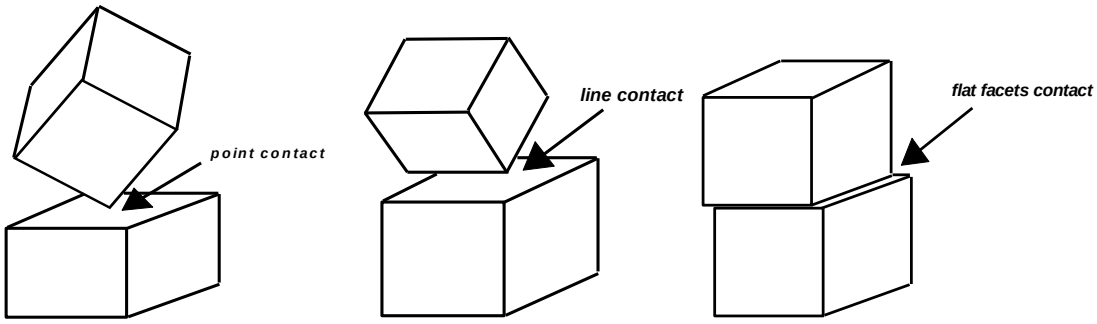

Figure 3.6 Contact mechanisms of cubes.

3.2.2 Test materials

Mono sized feed fractions of quartz with a specific density of 2.64 g/cm^3 were used for all the batch tests done with each grinding media shape alone, and then with the mixtures of these grinding media shape. The size fractions chosen for the tests were ranging from -16000 to 300 µm.

A total of 135 batch tests on 11 mono-sized feed class materials were carried out for the intended series of grinding tests (Table 3.3).

After defining the laboratory conditions in Table 3.1, the mass of material necessary per test was calculated to be 1.920 kg. Then, the mono-size feed materials were prepared for the batch tests (Table 3.3). The quartz material was collected from bags of 40 kg approximately and screened using a standard Tyler series of screens. The retained quartz fractions of interest were labelled and stored.

Another screening using nested screens in decreasing order in interval of $\sqrt{2}$ was done for 20 minutes in order to get mono-sized fraction more carefully prepared.

Eventually, 1.920 kg quartz feed samples were constituted from the screened material.

Table 3.3 presents the experimental design including the feed size considered per grinding media shape used.

Table 3.3 Experimental design.

Feed size (microns)		Grinding media shape charge considered					
Upper	Lower	Balls	Eclipsoids	Cubes	Mix B-E	Mix B-C1	Mix B-C2
16 000	13 200				×	×	×
13 200	9 500	×	×	×			
9 500	6 700				×		
6 700	4 750					×	
4 750	3 350	×	×	×			
3 350	2 360	×	×		×		×
2 360	1 700	×	×			×	
1 700	1 180	×	×	×			
850	600	×	×				
600	425			×			×
425	300	×	×		×	×	

3.3 Experimental methods

The one-size-fraction method (Austin *et al.*, 1984) was used to perform our batch grinding tests. Four grinding times were considered: 0.5, 1, 2 and 4 min. For every test, a blank sieving test was done on the prepared feed material. After that, the quartz sample was placed in the mill with the grinding media. Then, the feed material was ground for 30 seconds to determine the primary breakage distribution function. After this grinding period, the mill contents were discharged.

A full particle size distribution was done on the collected product using nested screens in decreasing order of size from the top screen down to the 75 microns screen in interval of $\sqrt{2}$. Firstly, the product was screened down to 1700

microns for 20 minutes. Then, the undersize material was split to constitute approximately 100 g of representative sample. The 100 g sample was washed on a 75 microns screen to remove the slimes, and then dried in the oven. Finally the dried quartz was screened for about 20 minutes to complete the size analysis. For materials of size smaller than 1700 microns, a representative sample was directly prepared for wet screening, then dry screened after being dried in the oven. After all this, the screen fractions were then recombined for batch grinding for 30 seconds to reach a total time of 1 min, then for 1 min to reach 2 min, and finally for 2 min to reach 4 min. Each grinding process was followed by a full particle size analysis.

The mass fraction retained on each screen was weighed on a scale. Same set of screens were used in order to be consistent throughout the experiments. The dried weight of the washed sample was checked against the starting mass sample before wet screening. The difference in mass was then added to the one in the pan to ensure that masses balance out.

3.4 Data collection and processing

The Wits small laboratory mill with a data acquisition system (WaveView) was used to collect the grinding data. The mill torque was recorded using the torque beam attached to the mill rig. Signals from the torque beam and marker probe were transferred to the computer through the WaveView interface. These data were used to calibrate the mill torque and the speed.

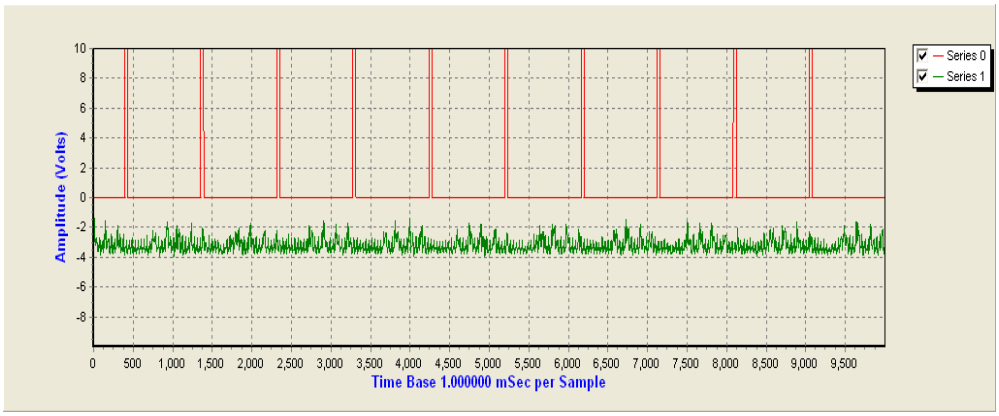

Figure 3.7 Typical signals of the voltage and the marker probe recorded using WaveView.

Figure 3.8 presents one of the calibration curve obtained after manipulating torque informations of the laboratory mill.

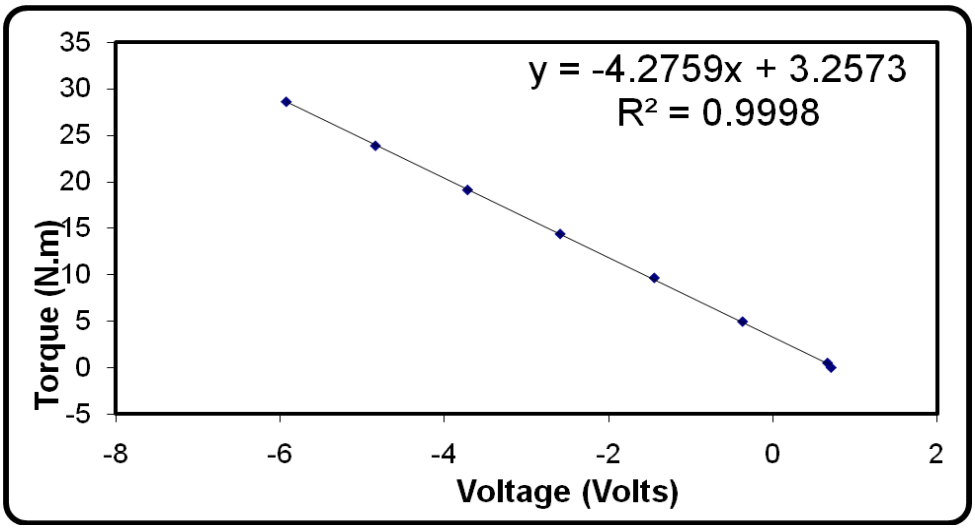

Figure 3.8 Torque calibration curve of the mill (23th January 2009).

The torque calibration of the mill was found to be reliable with coefficients of determination ranging between 0.9980 and 1.

The grinding raw data were recorded and compiled. Then a spreadsheet programme was developed to generate different particle size distributions. The manipulated data obtained from the batch tests were then used to work out the grinding parameters of the different grinding media shapes. This detailed analysis aimed at bringing to light the effects of mixing grinding media of different shapes on the milling kinetics.

Based on the estimated breakage parameters, the selection functions were estimated and compared to explain in much detail the milling performances of the grinding media.

3.5 Summary

The Wits small laboratory mill was regularly calibrated before running the batch tests. Four grinding times were used to monitor the selection function of feed size material, while 0.5 minutes were used for the breakage function. These grinding times were recorded at each step for future processing of data. The quartz was ground and screened to complete the particle size analysis. The compiled raw data was stored on a computer. Eventually, these data were manipulated and analyzed to determine the milling kinetics of the grinding media.

Chapter 4 Milling Kinetics of Grinding Media of Different Shapes

Austin *et al.* (1984) have shown that the breakage characteristics of any materials could be determined using single-size-fraction batch grinding tests. Basically, mono-size balls are used to batch-grind single size materials for several time periods to get an estimate of the grinding kinetics.

In this chapter, raw data collected from laboratory batch tests performed using balls, Eclipsoids and cubes are processed to provide different breakage parameters necessary to the description of the selection function and the breakage function of the quartz material used.

4.1 Introduction

Comminution or size reduction of solids is one of the oldest and most widely used particulate unit operations in many industries. To know how fast each size breaks, and in what sizes the primary breakage products appear gives the concept of size-mass balance or population balance of the mill (Austin et al., 1984). The Size reduction involves, mainly, two breakage mechanisms; impact and attrition which depend on grinding media and feed material characteristics such as size, shape, weight and composition.

The specific breakage rate constant has been investigated widely using grinding mills under different conditions, and this is of great interest when considering

the grinding efficiency, the design of the circuit of grinding, and classification processes (Kanda, et al., 2007). Thus, the selection function is used to evaluate the effectiveness of a milling process.

In this chapter all the breakage parameters are determined numerically starting with the milling rate values themselves up to the breakage parameters. This set of information is then interpreted in connection with milling of the grinding media shapes.

4.2 Determination of selection function values

Basically, a non-linear regression technique was used to find the best combination of fitting parameters to the model by minimizing the sum of squared errors (SSE) between the experimental values $P_{expt}(t)$ and the predicted ones $P_{model}(t)$.

All the runs to carry out a full batch test on a given particle size x were considered for all the grinding time, namely 0, 0.5, 1, 2 and 4 minutes successively.

The first order plots for different feed sizes of quartz ground by balls, Eclipsoids and cubes were plotted using the weight fraction remaining on the top size. Data relative to mono-sized quartz material are in Tables A.1 to A.18 in Appendix A for the three grinding media shapes.

The percentage weight remaining in the top size $w_i(t)$ are given in Tables B.1 to B.3 in Appendix B. Figures 4.1 to 4.3 present these first-order plots.

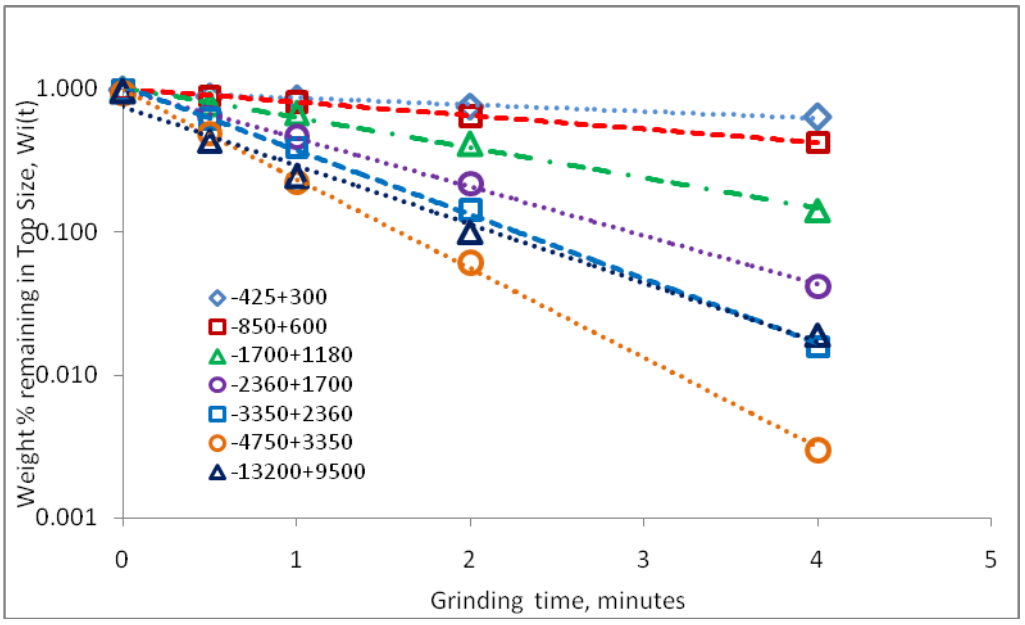

Figure 4.1 First order plots for dry grinding of quartz with 40 mm balls charge.

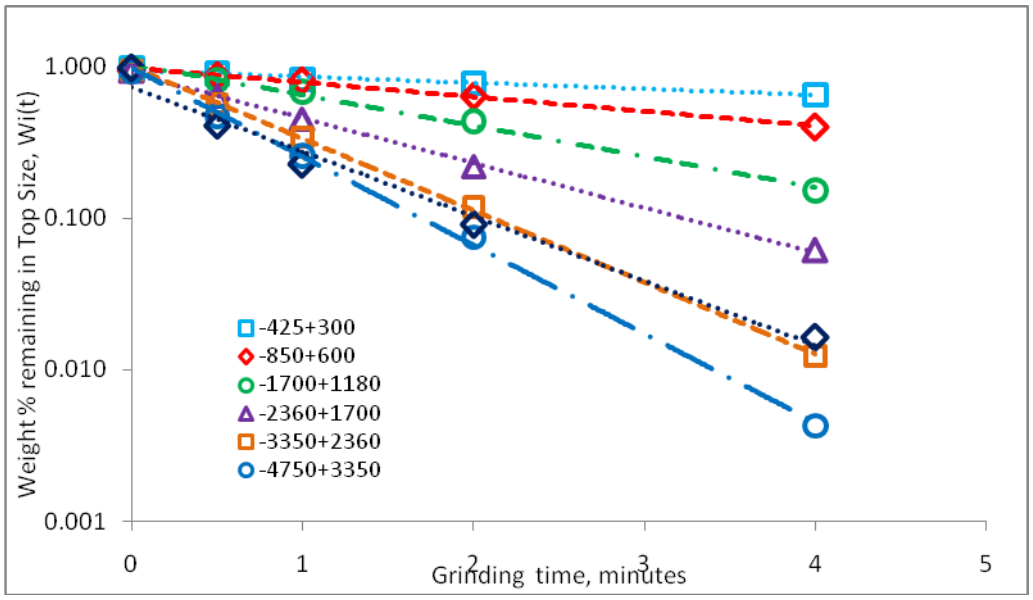

Figure 4.2 First order plots for dry grinding of quartz with 40 mm Eclipsoids charge.

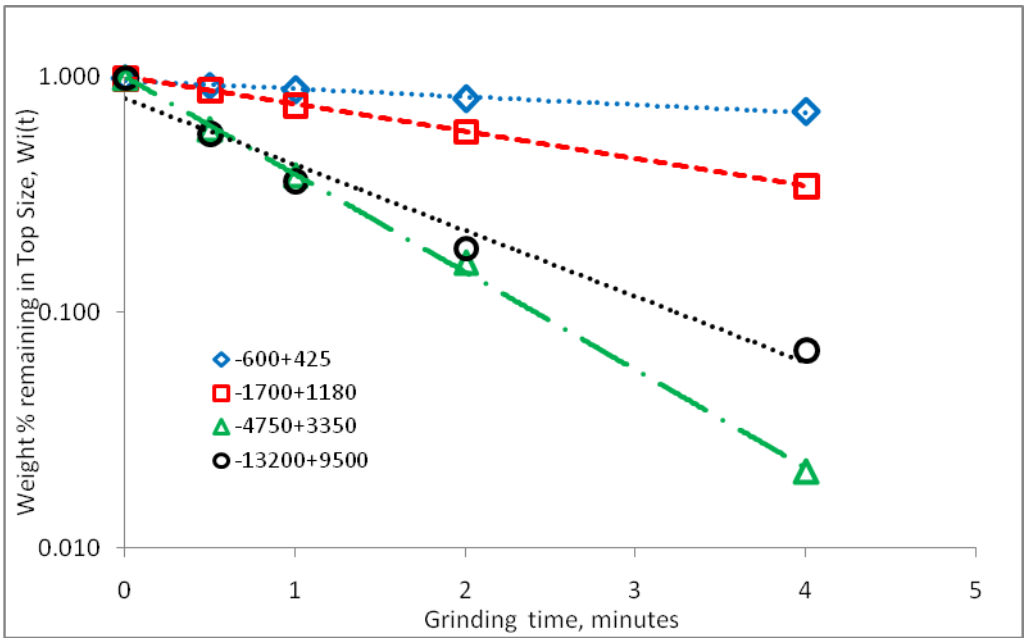

Figure 4.3 First order plots for dry grinding of quartz with 32 mm cubes charge.

All these plots can be described by first-order grinding kinetics with coefficients of determination between 0.972 and 0.999. The incomplete-sieving error was taken into account for the point at zero time. It can be seen that the first-order law is a good approximation for smaller sizes used, but it does not apply for the largest size (-13200+9500 µm). The curves for these largest particles present 3 regions: a rapid breakage region that occurs at first, a more or less first-order breakage region, and finally a slower first-order breakage region. This quartz material exhibits to abnormal breakage (see section 2.3.3) and is assumed to be constituted of two fractions: a fast-breaking fraction and a slow-breaking one. The reason for this abnormal breakage is that all the particles within a size fraction have a distribution of strengths which interacts with distribution of applied forces from the grinding media (Austin *et al.*, 1977).

The variations in the specific rates of breakage at different feed particle sizes for balls, cubes and Eclipsoids are shown in Table 4.1.

Table 4.1 Specific rate of breakage of balls, Eclipsoids and cubes for different particle sizes.

Particle size, x_i (µm)	S_i (min^{-1}) Balls	S_i (min^{-1}) Eclipsoids	S_i (min^{-1}) Cubes
-13200+9500	0.946	0.982	0.644
-9500+6700	-	-	-
-4750+3350	1.437	1.342	0.953
-3350+2360	1.089	1.088	-
-2360+1700	0.714	0.681	-
-1700+1180	0.487	0.469	0.266
-850+600	0.214	0.218	-
-600+425	-	-	0.079
-425+300	0.107	0.094	-
SSE	0.012445	0.009938	0.023280

An analysis of the breakage rate of coarser (-13200+9500 µm), medium (-4750+3350 µm) and finer (-1700+1180 µm) feed size particles revealed that cubes are the least efficient of the three grinding media shapes considered. Spherical balls are the most efficient, but Eclipsoids are breaking the coarser particles faster than balls. Figures 4.4, 4.5 and 4.6 below illustrate this analysis. It can be seen that cubes present the biggest weight % remaining in the top size for the all the size categories of particles considered. On the other hand, Eclipsoids have lesser weight % remaining in the top size than balls only for the coarser particles considered.

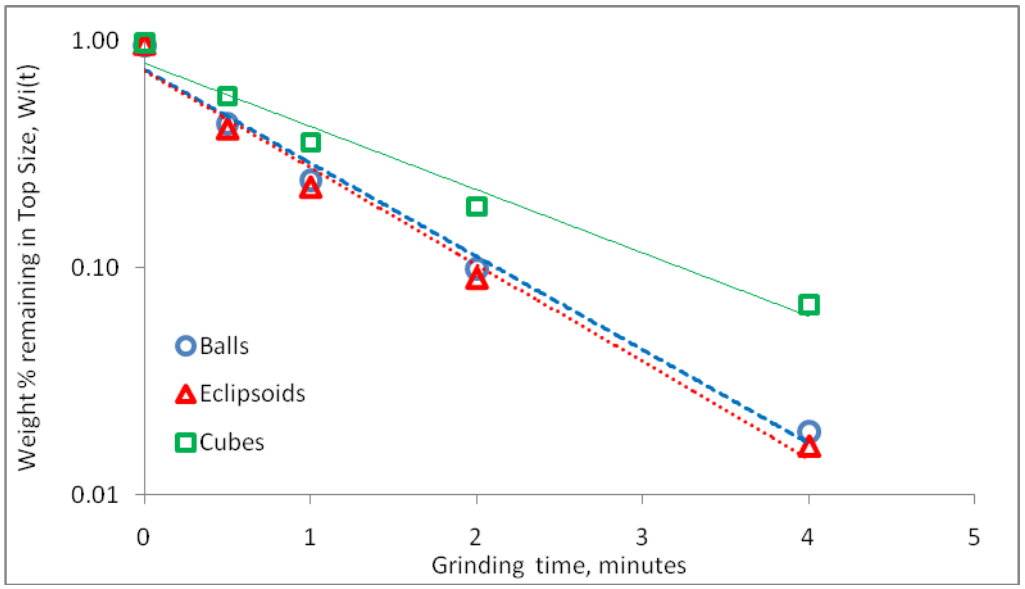

Figure 4.4 First order plots for dry grinding of -13200+9500 µm quartz feed sizes.

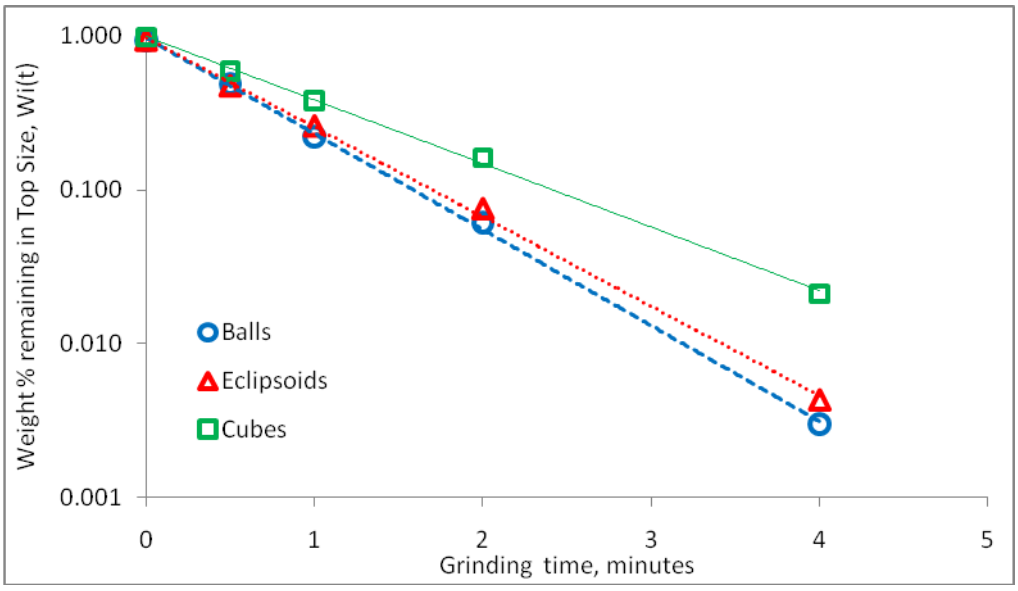

Figure 4.5 First order plots for dry grinding of -4750+3350 µm quartz feed sizes.

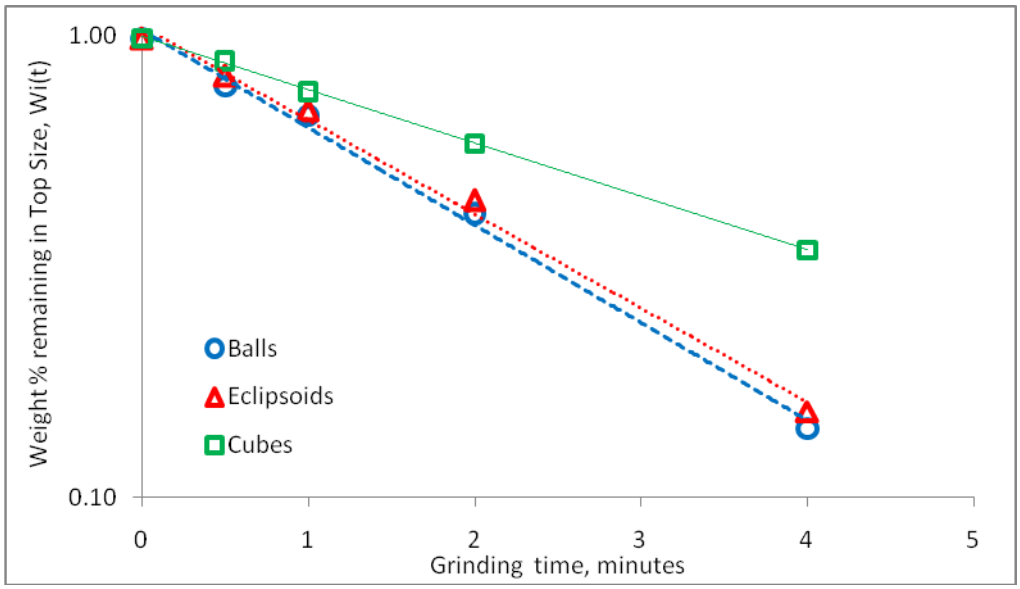

Figure 4.6 First order plots for dry grinding of -1700+1180 µm quartz feed sizes.

Additionally, for the grinding of coarser materials, the cubes results depart the most from the first-order law (see Figure 4.4). Their coefficients of determination R^2 are 0.986, 0.984 and 0.974 for balls, Eclipsoids and cubes respectively.

Undoubtedly, the rate of breakage varies with size. The specific rate of breakage increases up to a maximum feed size and decreases above this size fraction for all grinding charges.

The graphs presenting the variation of the specific rate of breakage are given in Figures B.1, B.2 and B.3, respectively for balls, Eclipsoids and cubes, in Appendix B. The maximum sizes x_m were 7080, 7297 and 7626 µm for balls, Eclipsoids and cubes respectively. Accordingly, the change in the selection function with grinding media shapes is predicted for quartz. Figure 4.7 shows

the specific rate of breakage in function of the particle sizes for grinding of quartz using balls, Eclipsoids and cubes.

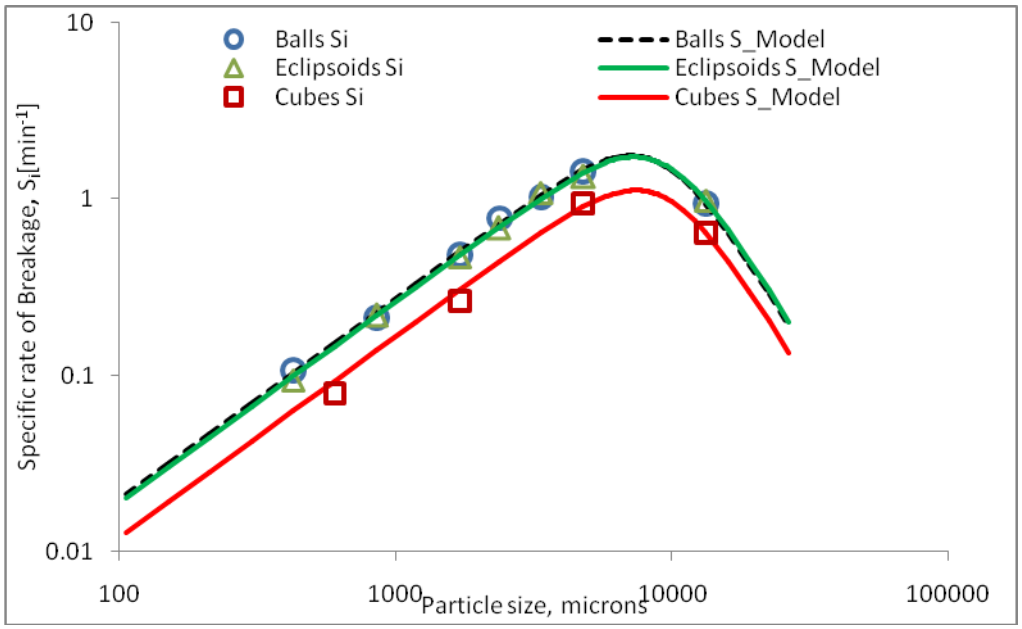

Figure 4.7 Variation of the specific rate of breakage with size for balls, Eclipsoids and cubes as grinding media shapes.

The specific rate of breakage parameters were estimated by using the non-linear regression technique fitting the S_i to Equation (2.5) and are presented in Table 4.2.

Basically, this technique finds the best combination of fitting parameters of a model by minimizing the square of the differences between the experimental values and the predicted ones.

Table 4.2 Breakage rate parameters obtained from the laboratory tests.

Grinding media	*a*	μ	α	Λ
Balls	0.272	8.81	1.14	3.70
Eclipsoids	0.258	9.08	1.14	3.70
Cubes	0.151	9.49	1.14	3.70

The parameter Λ was fixed and kept constant because we do not have enough information to determine it accurately. We used the Austin's value for Λ (Austin *et al.,* 1984).

α which is characteristic of the material was satisfactorily determined using a regression technique and then, kept constant because we utilized the same quartz material for all our batch grinding tests. The parameter α is a positive number normally in the range 0.5 to 1.5. It is characteristic of the material and does not vary with rotational speed, ball load, ball size or mill hold-up over the normal recommended test ranges (Austin and Brame, 1983) for dry milling, but the value of *a* will vary with mill conditions. The value of α that was found to satisfactorily characterize breakage rate is 1.14.

Obviously, the breakage rate study focused mainly on the parameters *a* and μ which vary with the mill conditions.

The values of the parameter *a* were determined, and balls present the highest value while cubes have the lowest one.

The values of x_m at which the breakage is maximum for our material were found to be proportional to the values of μ which are 8.81, 9.08 and 9.49 respectively for balls, Eclipsoids and cubes. These values are inversely proportional to the values of the parameter a of the grinding media shapes investigated.

The coefficient of variation is used as a measurement of the precision of the parameters obtained. The coefficient of variation (CV) is a dimensionless number and it represents the ratio of the standard deviation to the mean.

$$\text{coefficient of variation (CV)} = \frac{\text{standard deviation}}{mean} \tag{4.1}$$

For our investigation, the breakage parameters obtained for balls are considered as our means.

Compared to balls, the coefficients of variation were found to be 3.64 % and 31.46 % for Eclipsoids and cubes respectively, in terms of the parameter a, and 2.17 % and 5.46 % for Eclipsoids and cubes respectively, in terms of the parameter μ.

4.3 Determination of breakage distribution function values

Austin *et al.* (1984) showed that $B_{i,j}$ values can be estimated from size analysis of the product from grinding of size j materials as:

$$B_{i,j} = \frac{\log\left[\left(1-P_i(0)\right)/\left(1-P_i(t)\right)\right]}{\log\left[\left(1-P_{j+1}(0)\right)/\left(1-P_{j+1}\right)\right]} \tag{4.2}$$

where $P_i(t)$ is the weight fraction of the material less than size x_i at time t.

Shorter grinding times resulting in 20 – 30% broken materials out of the top size in order were used to estimate accurately the breakage function parameters. These shorter times are meant to minimize re-breakage, and thereby get more accurate estimates. This method is known as Method B II.

The $B_{i,j}$ values obtained using Equation (4.2) were then fitted to the empirical function given in Equation (2.6) to evaluate the breakage function parameters of the quartz used. This is called Method B III and it requires an estimate of the S values (Austin and Luckie, 1972).

The breakage distribution and the normalized breakage function are given in Tables C.1 to C.18 in Appendix C.

The curves $B_{i,j}$ of the quartz used were found to be falling on top of one another for the values of j. This has proved to be true for all quartz particle size, except for the coarser material. This is referred to as the case of normalized breakage (Austin *et al.*, 1984). Figure 4.8 illustrates this fact for balls. The others figures presenting the normalised breakage for all other grinding media are given in Appendix C (Figures C.1 to C.3).

In addition, the $B_{i,j}$ values are assumed to be normalizable (δ =0). Therefore, the fraction appearing at sizes less than the initial feed size is independent of the initial feed size. The breakage function parameters found for all our grinding media shapes are given in the tables C.30 and C.31 in Appendix C.

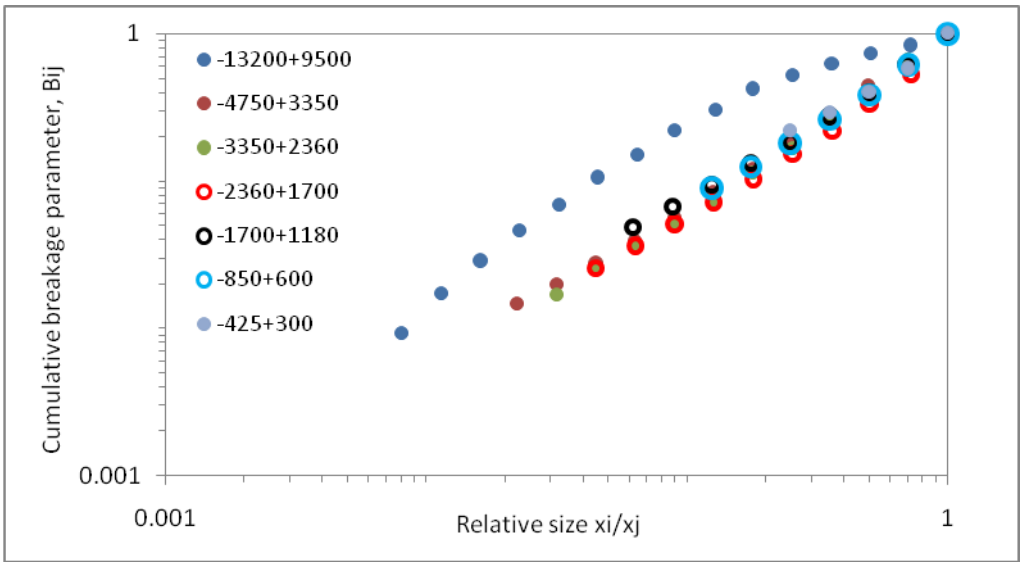

Figure 4.8 Cumulative breakage distribution parameters for different sizes of quartz ground with balls.

The normalised breakage function parameters were found to be: β is constant at 5.80, γ varies from 0.98 to 1.12 and ϕ varies from 0.68 to 0.71. These parameters are presented in Table C.31 in Appendix C.

However, it was found that the B values are insensitive to the precise mill conditions, at least in the normal operating range of milling conditions (Austin, *et al*., 1979). Eventually, it has been decided to consider the average values as the actual breakage function parameters. The grinding is first-order and the $B_{i,j}$ are assumed to be constant with time. In this case, it is assumed that there is no regrowth of particles, smaller or larger, occurring by cold welding. Furthermore, the fracture properties of a given size in the products of breakage are the same as in the raw feed.

Table 4.3 Normalised breakage function parameters for the quartz material used.

Breakage function parameters	β	γ	ϕ
	5.80	1.01	0.71

Austin *et al.* (1984) reported that the product size distribution is sensitive to the value of γ.

The parameters obtained worked for the model used as illustrated in Figures 4.9 for balls, 4.10 for Eclipsoids and 4.11 for cubes.

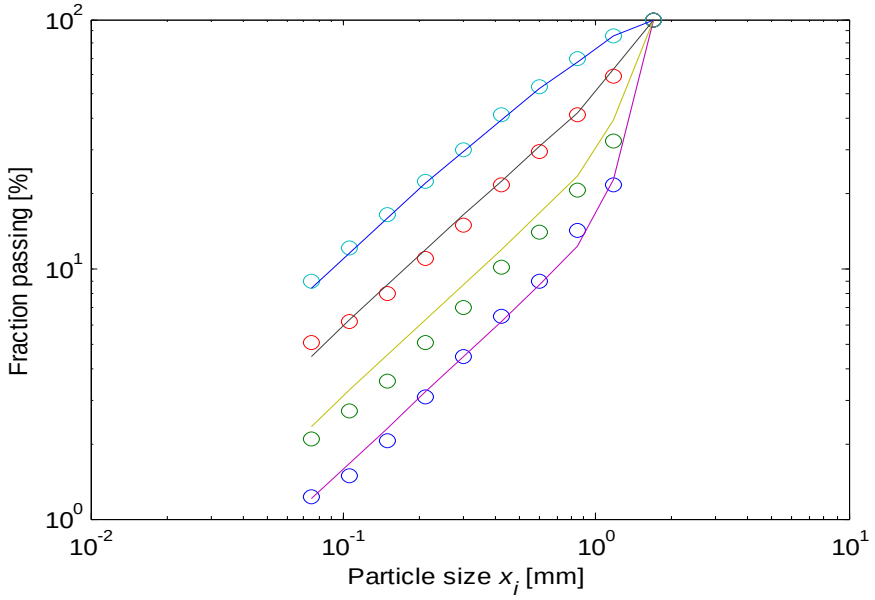

Figure 4.9 Simulated size distributions from batch grinding -1700 +1180 µm feed with balls.

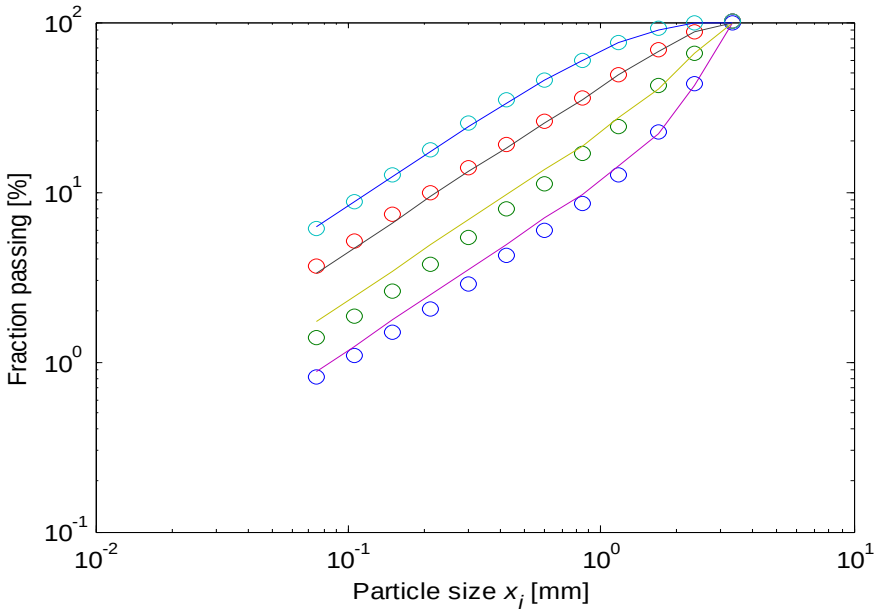

Figure 4.10 Simulated size distributions from batch grinding -3350 + 2360 µm feed with Eclipsoids.

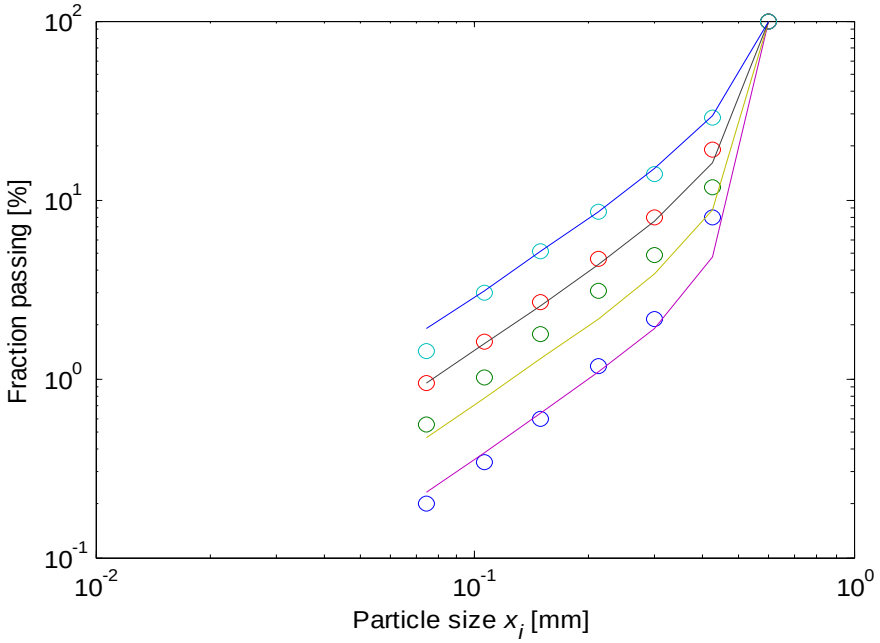

Figure 4.11 Simulated size distributions from batch grinding -600 +425 µm feed with cubes.

4.4 Significance of the results

Comparative batch tests based on the Size-Mass Balance using the three shapes of grinding media of the same mass were conducted with quartz at the same conditions. The fractional rate at which a given size of particle disappears (Selection function) and the primary breakage distribution were then determined and compared for all grinding media.

The values of a and μ which are proportional respectively to the rate of breakage and the degree of cataracting in the mill were used to compare the grinding performances of the grinding media. These values are presented in Figure 4.12 below.

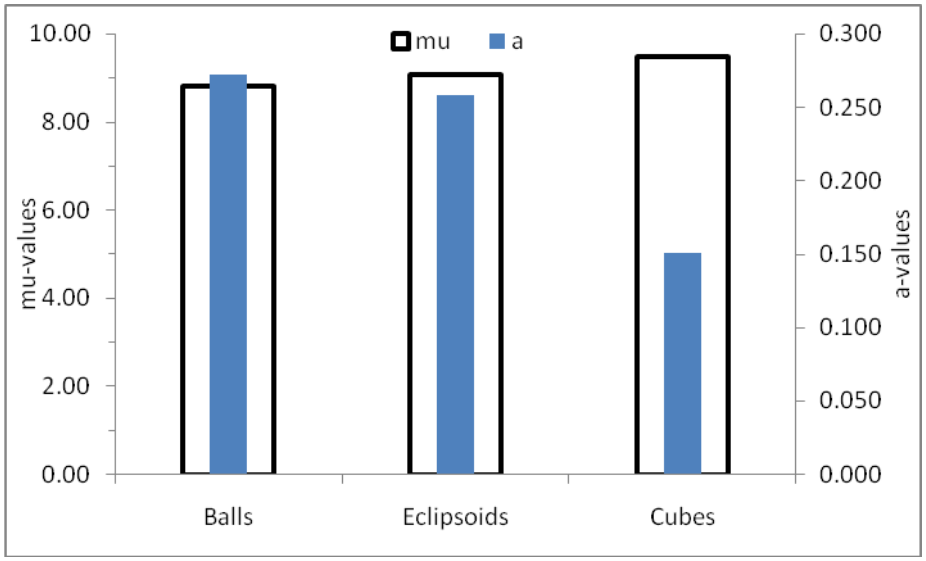

Figure 4.12 a-values and μ-values of balls, Eclipsoids and cubes**.**

Balls present the highest a value, i.e. 0.272 which gives a clear indication of their efficient breakage rate while cubes present the lowest one (0.151). These results show that the grinding media shape have a significant effect on the

breakage rate. This confirms the previous findings by Kelsall et al. (1973) and the fact that balls have the higher rate of breakage compared to Eclipsoids and cubes. In terms of μ, balls have the relative smallest value (8.81) while cubes present the highest one (9.49) with a coefficient of variation of 5.46 %. This might be an indication that cubes cataract more than balls and Eclipsoids, probably because of their geometry. But this higher degree of cataracting does not give a higher breakage rate because the cubes flats facets are not offering sufficient energy impact for particles to be broken. Furthermore, the cataracting effect is also moving particles away from the efficient grinding zone reducing the probability of nipping a particle in a single collision, as well as the probability of grinding a nipped particle by the collision.

The physical properties of these different grinding media are given in Table 3.2. Eclipsoids presents the largest surface area compared to balls and cubes. For the constant mass charge used for our batch grinding tests, the total surface area of Eclipsoids is 1.25 and 1.04 times bigger than the surface area of balls and cubes respectively. Consequently, Eclipsoids should have a reasonably higher breakage rate. In addition, they present point, line and surface contact mechanisms for the grinding action. The advantage of a larger surface area seems to impact on the abnormal region where there are bigger components of chipping and abrasion, leading to lower value of relatively more of the finest quartz material and hence, a lower value of γ. In the abnormal region, i.e. -13200+9500 µm, Eclipsoids have the highest value of S_i (0.982 min^{-1}) compared to balls and cubes. However, the μ value (9.08) indicates a relative higher

degree of cataracting compared to balls which results in moving away particles from the grinding zones.

The sizes at which the specific rate of breakage is maximum are 7080, 7297 and 7626 µm for balls, Eclipsoids and cubes respectively. All these values fall in the -9500+6700 µm class. As a result, all these grinding media are competent to break particles within this class.

Austin (1984) showed that the product size distribution is sensitive to the value of γ. An analysis of the γ values obtained in our investigation and presented in Table C.31 in Appendix C shows that cubes have the highest γ value, i.e. 1.12, while balls and Eclipsoids present more or less the same value (0.99 and 0.98 respectively). Thus, smaller γ values of balls and Eclipsoids indicate higher amount of progeny fines produced from breakage. Undoubtedly, balls and Eclipsoids are more efficient for the grinding process than cubes.

The relatively same values of β and ϕ indicate that balls, Eclipsoids and cubes reduced fractions close to the feed size to a lower size at the same rate.

4.5 Summary

A comparative study is done using balls, Eclipsoids and cubes in order to determine their respective breakage parameters. The concept of size-mass balance or population balance of the mill (Austin et al., 1984) was used to quantify how fast each size breaks, and in what sizes the primary breakage products appears.

As far as the selection function equation is concerned, all the results are in good agreement with the first-order breakage law. It is entirely adequate to describe the specific rate of breakage for balls, cubes and Eclipsoids. Considering the a values, balls proved to have a higher rate of breakage. The μ values give a possible explanation of the lower breakage rate of cubes.

As for the breakage function, it has revealed the material to be acceptably normalizable. More importantly, an analysis of the γ values shows balls and Eclipsoids are efficient for the grinding process, producing more fines from the breakage of the top size material.

This knowledge of the grinding performances of these grinding media shapes lays the foundation of study of the grinding performances of the mixtures made of these different media shapes that will be evaluated in the next chapter.

Chapter 5 Effects of Mixtures of Grinding Media of Different Shapes on Milling Kinetics

This chapter presents the manipulated raw data of the different mixtures made of balls, Eclipsoids and cubes. The selection function is described in terms of a, μ and α, and the breakage function in terms of β, γ, and ϕ.

The different breakage parameters obtained are then used to determine the grinding performances of the different mixtures of grinding media. Eventually, these informations are used to compare their grinding performances to those of the single grinding media shapes and motivate the utilization of mixtures of grinding media of different shapes.

5.1 Introduction

The need to reduce the grinding costs and to increase the grinding and milling efficiency has opened the way to many investigations pertaining to grinding media shapes. As shown in chapter 4, balls were found to be more efficient than other grinding media shapes. But, spherical balls and the alternative grinding media to balls are altered by wear pattern and break during the grinding process. Consequently, the grinding process is thus done with mixtures of grinding media of different sizes and shapes. In addition, very little work has been done on

investigating mixtures of media shapes. That is why it is our intention to investigate mixtures of grinding media of different shapes.

The selection and breakage functions are determined by batch grinding tests performed on single particle sizes for the mixtures of grinding media charge consisting of grinding media of the same total mass.

These breakage parameters are compared to determine the grinding performance of the mixtures of grinding media, and finally compared to the individual grinding media shapes.

5.2 Selection function values of the mixtures of grinding media shape

The first order plots for different feed sizes of quartz ground by the mixture made of 50% balls and 50% Eclipsoids (Mix B-E), the mixture made of 50% balls and 50% cubes (Mix B-C 1) and the mixture made of 75% balls and 25% cubes (Mix B-C 2) were measured and plotted.

The weight fraction remaining on the top size was plotted against different grinding times. Data relative to mono-sized quartz material are in Tables A.19 to A.29 in Appendix A for the different mixtures of grinding media shapes.

The percentage weight remaining in the top size $w_i(t)$ are given in Tables B.4 to B.6 in Appendix B. The first-order plots are presented in Figures 5.1 to 5.3.

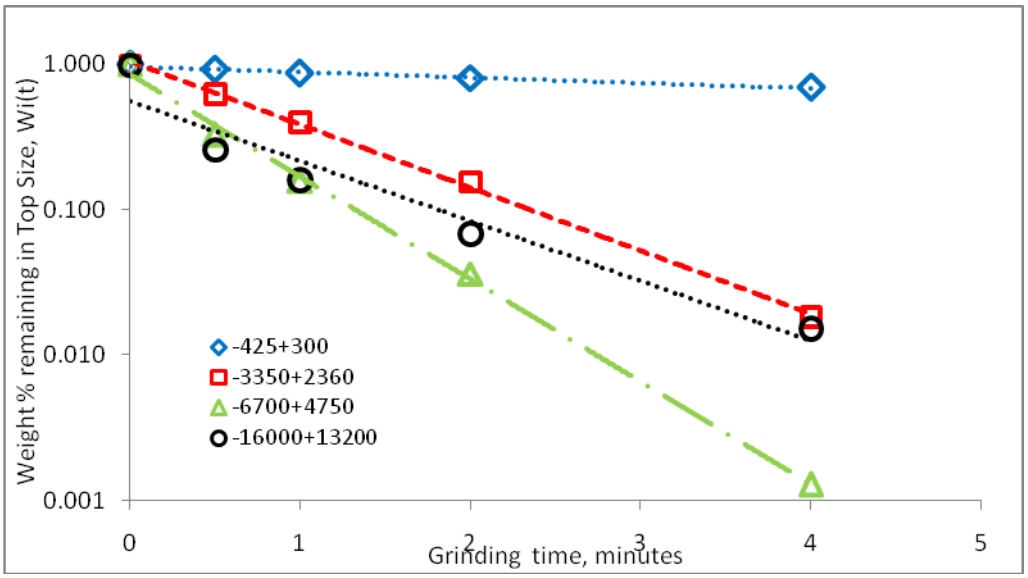

Figure 5.1 First order plots for dry grinding of quartz with the 50-50 mixture of balls and Eclipsoids.

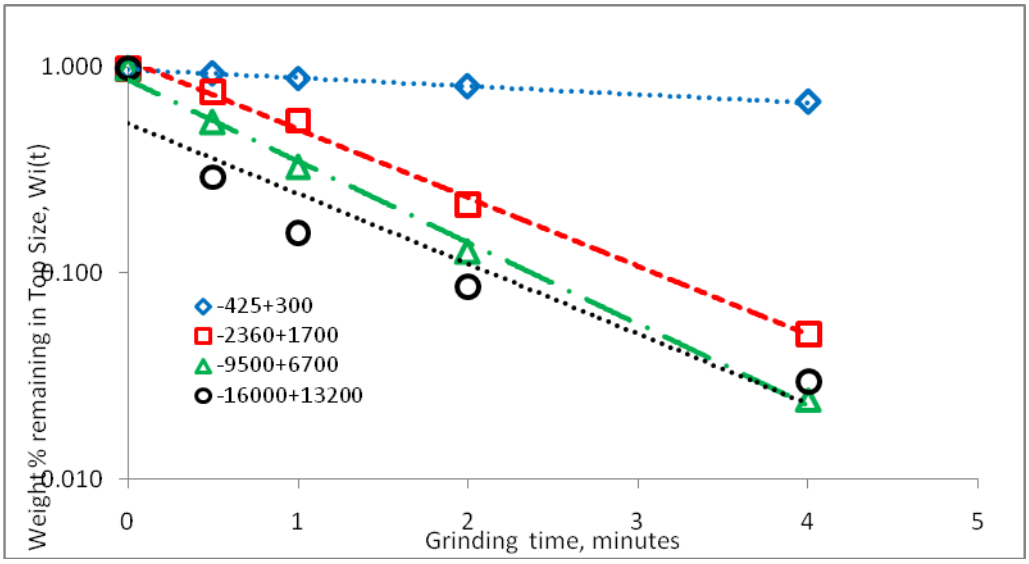

Figure 5.2 First order plots for dry grinding of quartz with the 50-50 mixture of balls and cubes.

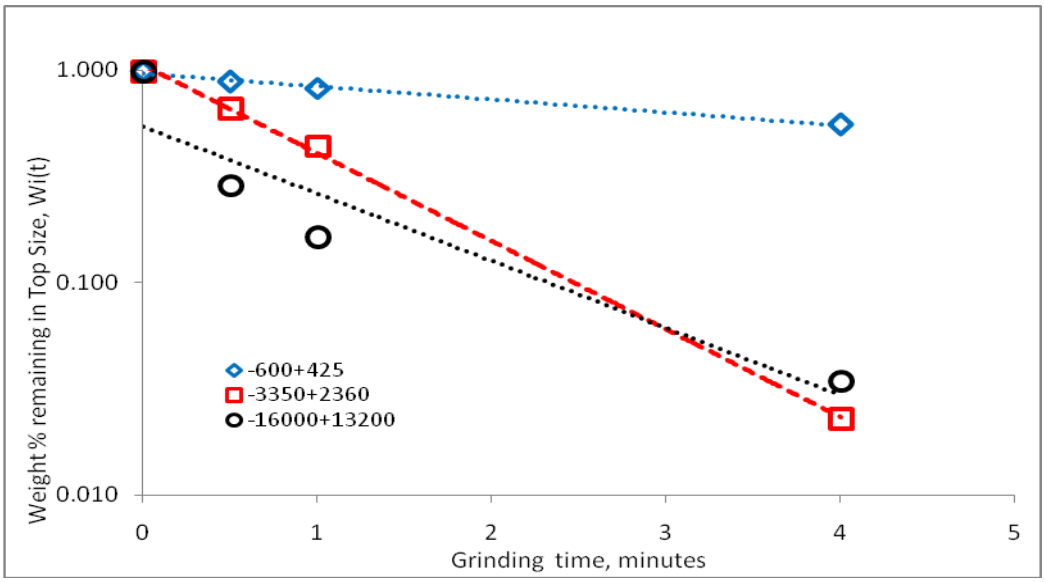

Figure 5.3 First order plots for dry grinding of quartz with the 75-25 mixture of balls and cubes.

It is found that the first-order law is only in agreement with medium and smaller particle sizes, namely particle sizes between -9500+6700 µm and -425+300 µm. These first-order plots are defined with coefficients of determination between 0.991 and 0.999.

Coarser particles (-16000+13200 µm) are subjected to abnormal breakage. The coefficients of determination are 0.940, 0.892 and 0.883 for the 50-50 mixture of balls and Eclipsoids, the 50-50 mixture of balls and cubes and the 75-25 mixture of balls and cubes respectively. All these coefficients are smaller than 0.950 which indicates that the first-order law does not work for these coarser particles.

Similarly, the variations in the specific rates of breakage at different feed particle sizes for these mixtures are shown in Table 5.1.

Table 5.1 Specific rate of breakage of the mixtures of grinding media for different particle sizes.

Particle size, x_i (µm)	S_i (min^{-1}) Mix B-E*	S_i (min^{-1}) Mix B-C1[#]	S_i (min^{-1}) Mix B-C2[$]
-16000+13200	0.950	0.409	0.729
-13200+9500	-	-	-
-9500+6700	-	0.913	-
-6700+4750	1.620	-	-
-4750+3350	-	-	-
-3350+2360	0.999	-	0.954
-2360+1700	-	0.740	-
-1700+1180	-	-	-
-850+600	-	-	-
-600+425	-	-	0.141
-425+300	0.086	0.093	-
SSE	0.011180	0.035727	0.000371

***** Mixture of 50 % balls and 50 % Eclipsoids.

[#] Mixture of 50 % balls and 50 % cubes.

[$] Mixture of 75 % balls and 25 % cubes.

The variations of the specific rate of breakage are given in Figures B.4, B.5 and B.6, respectively for the Mix B-E, the Mix B-C 1 and the Mix B-C 2, in Appendix B.

The sizes where the specific rate of breakage was maximum are 8382, 6115 and 7578 µm for the Mix B-E, the Mix B-C 1 and the Mix B-C 2 respectively. Figure 5.4 shows the specific rate of breakage in function of the particle sizes for all the mixtures used.

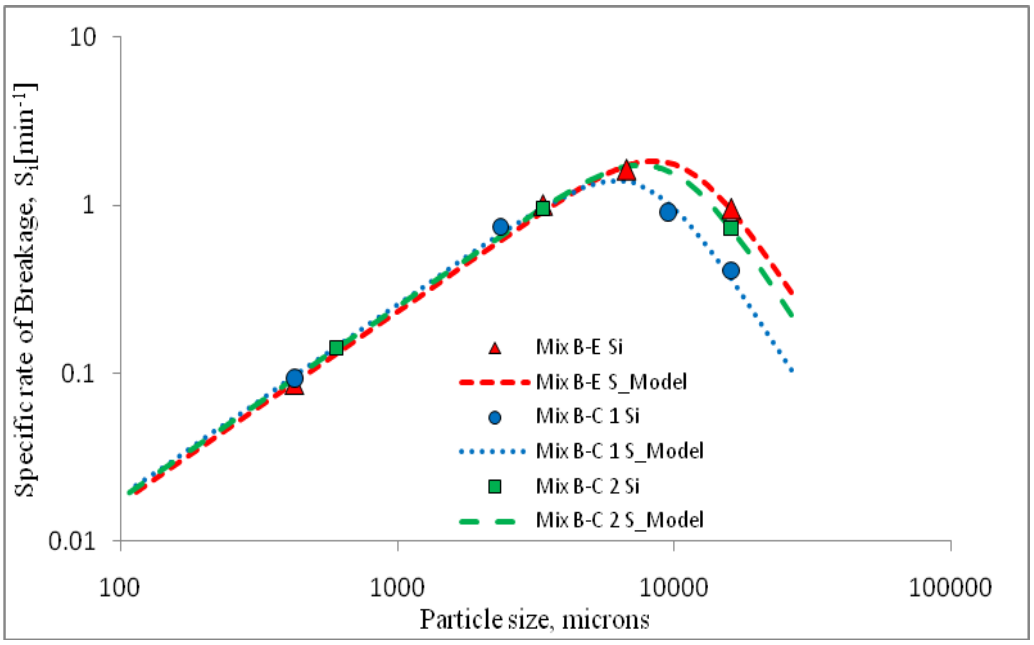

Figure 5.4 Variation of the specific rate of breakage for all the mixtures used as grinding media with size.

These three mixtures have similar breakage rate behaviour in the medium and fine particle size region, but they behave differently in the coarser region.

The breakage rate parameters obtained using these mixtures of grinding media of different shapes are presented in the Table 5.2.

Table 5.2 Breakage rate parameters of the mixtures of grinding media shapes.

Grinding media	*a*	μ	α	Λ
Mix B-E	0.234	10.43	1.14	3.70
Mix B-C 1	0.257	7.61	1.14	3.70
Mix B-C 2	0.249	9.43	1.14	3.70

The values of the parameter a are close for the mixtures considered with a standard deviation of 0.0117 and a coefficient of variation of 4.73 %. Also, they are inversely proportional to the values of μ for the mixture considered. But, the μ values of the mixtures investigated are sensibly different with a coefficient of variation of 15.61 % among them. This indicates different behaviour in terms of grinding.

The values of x_m at which the breakage is maximum for our material were found to be proportional to the values of μ which are 10.43, 7.61 and 9.43 respectively for the Mix B-E, the Mix B-C 1 and the Mix B-C 2.

5.3 Breakage function values of the mixtures of grinding media shape

The $B_{i,j}$ values were obtained using Equation (4.2), and then fitted to the empirical function given in Equation (2.7) to evaluate the breakage function parameters of the quartz used. The breakage distribution and the normalized breakage function are given in Tables C.19 to C.29 in Appendix C. The breakage function parameters were found to be 5.79 and 5.80 for β, they vary from 0.95 to 1.09 for γ and from 0.70 to 0.74 for ϕ.

The quartz material used was assumed to have a normalised breakage (δ=0). The cumulative breakage parameters $B_{i,j}$ were on top of one another for all feed sizes, except for coarser feeds. The cumulative breakage parameters are presented in Figures C.4 to C.5 in Appendix C.

The breakage function parameters found for each of our mixtures are given in the tables C.30 and C.31 in Appendix C. The representative breakage function parameters for the quartz used were found to be: β =5.80, γ =1.01 and ϕ =0.71 (Table 4.3).

The simulated size distributions found are presented in Figure 5.5 for the mixture of 50% balls and 50 % cubes, in Figure 5.6 for the mixture of 50 % balls and 50 % Eclipsoids and in Figure 5.7 for the mixture of 75 % balls and 25 % cubes.

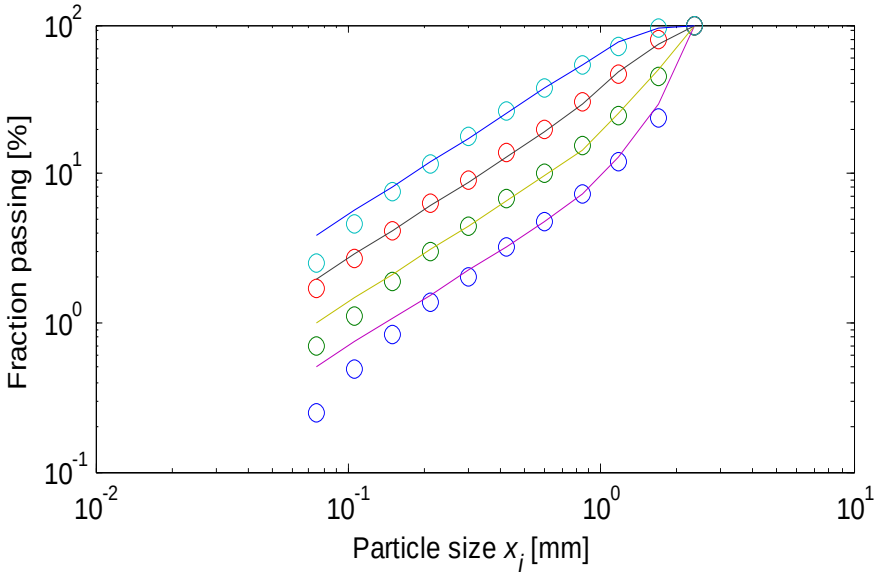

Figure 5.5 Simulated size distributions from batch grinding -2360 + 1700 µm feed with the mixture of 50 % balls and 50 % cubes.

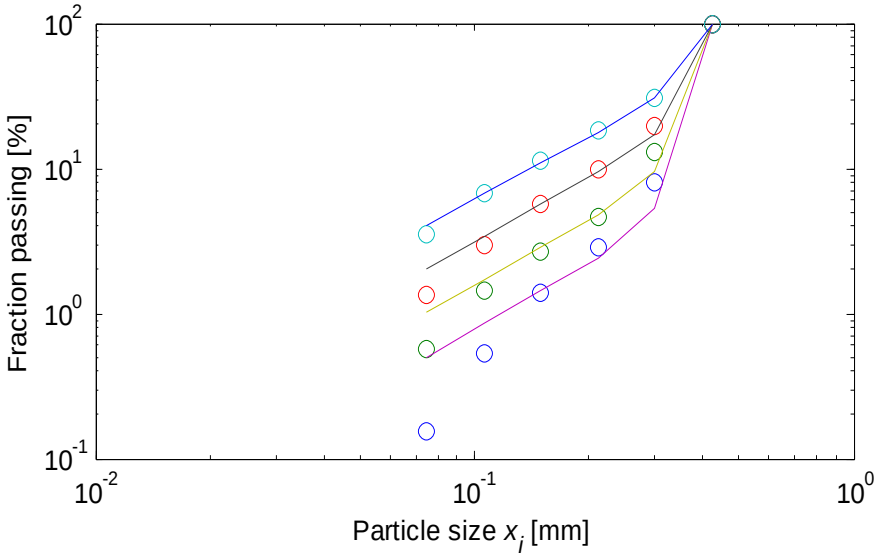

Figure 5.6 Simulated size distributions from batch grinding -425 + 300 µm feed with the mixture of 50 % balls and 50 % Eclipsoids.

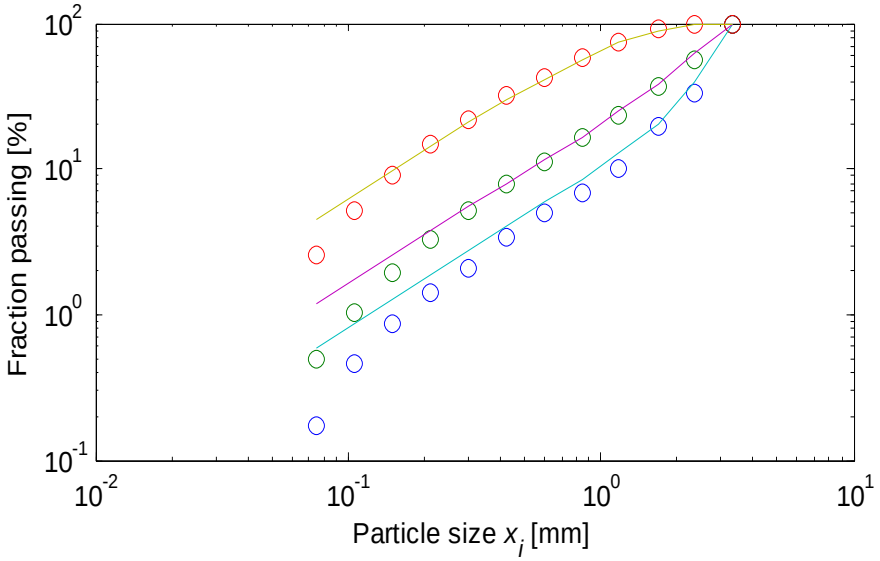

Figure 5.7 Simulated size distributions from batch grinding -3350 +2360 µm feed with the mixture of 75 % balls and 25 % cubes.

The simulated size distributions obtained using mixtures of grinding media are in good agreement with the experimental data down to 150 µm. Below this size,

there is a systematic bending of the experimental data, causing a clear difference between the experimental and simulated data at fines sizes. The experimental particles distributions are less than the ones predicted by the model. This might be the result of the time-dependent and decelerating breakage rate. The production of fines may alter the mechanics of the milling action to give less tumbling. One possible raison of this slowing down may be the fact that air is trapped between particles and the slow movement of air through beds of fine particles might change the mechanics of the breakage action by blowing away particles or by absorbing impact like a hydraulic shock absorber. The accumulation of the fines reduce effective impacts to cause breakage, reducing the contribution of line and area contacts between grinding media. This abnormal breakage behaviour and the slowing-down effect observed are to be investigated.

5.4 Interpretation of the results

Considering the spherical balls the most efficient in terms of grinding performances, different mixtures were constituted adding balls to others grinding media shapes. The mixture of 50 % balls and 50 % Eclipsoids increases the total surface area by 12.50% compared to balls alone and the mixture of 50 % balls and 50 % cubes increases the total surface area by 10.17%. The mixture of 75 % balls and 25 % cubes only increases the total surface area by 5.55%.

The values of a and μ are presented in Figure 5.8 below.

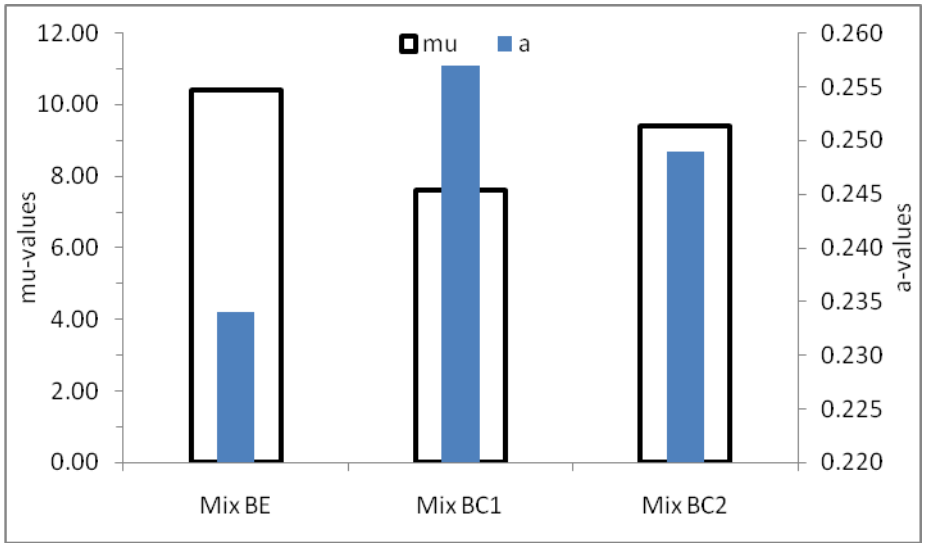

Figure 5.8 *a* -values and μ-values of the mixtures of grinding media used.

The value of *a* of the 50-50 mixture of balls and cubes is the highest among the *a* -values of the mixtures used, meaning it has the higher rate of breakage. The mixture made of 50 % balls and 50 % Eclipsoids presents the biggest μ values (i.e. 10.43) which mean the addition of Eclipsoids to balls has increased the degree of cataracting in the mill (Austin *et al.*, 1984). This cataracting gives higher breakage rates of large sizes in the abnormal region. The highest Si value (0.950 min^{-1}) for this mixture for the -16000+13200 μm support this fact.

The Mix B-C 1 presents less cataracting compared to the Mix B-E, but a relatively higher value of *a* . Consequently, in an attempt to improve the value of *a* , the Mix B-C 2 was constituted, trying to find what would happen to the rate of breakage if the proportion of cubes is decreased in the mixture.

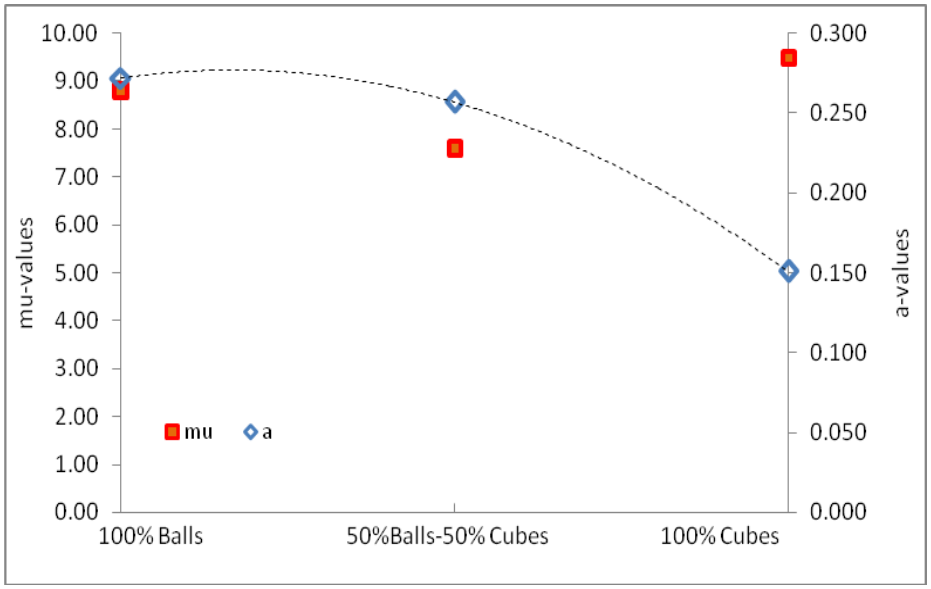

Figure 5.9 Expected evolution of the a-values in terms of percentage of cubes in the mixture.

Contrary to our expectations, the Mix B-C 2 presented a relative low value of a compared to the Mix B-C 1, as shown in Figure 5.10 below. It has decreased from 0.257 to 0.249. These two values are pretty close with a standard deviation of 0.0056. This unexpected behaviour may be attributed to the smaller surface area available for grinding in the Mix B-C 2 compared to the one available in the Mix B-C 1 (see Table 3.2).

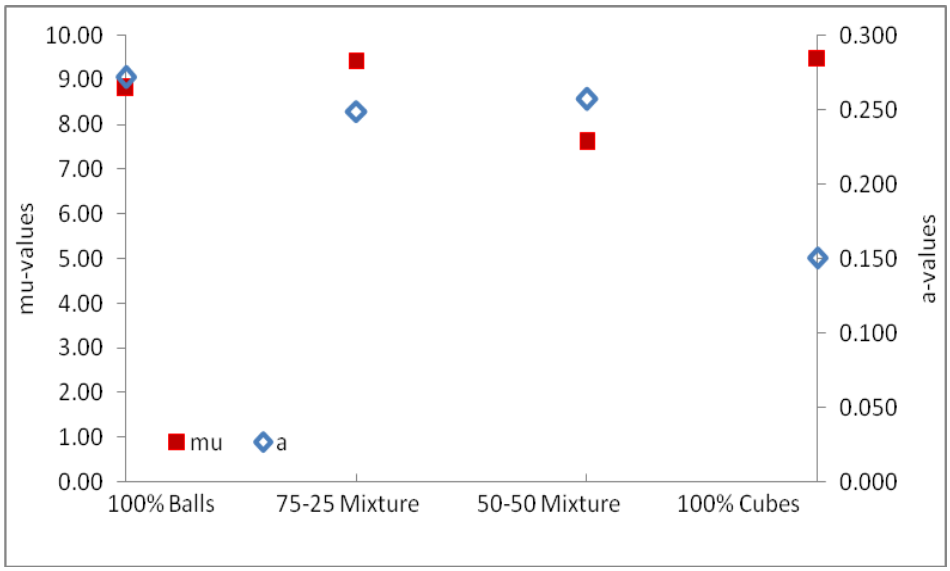

Figure 5.10 Obtained a-values in terms of the percentage of cubes in the mixture.

As shown in Figure 5.4, Mix B-E has a greater breakage rate of large sizes in the abnormal region. This is confirmed by the highest values of μ and x_m.

5.5 Effects of mixtures of grinding media on milling kinetics

Batch grinding tests were performed for balls, Eclipsoids, cubes and their mixture in order to determine the breakage rate and breakage distribution parameters. After establishing the performances of these grinding media shapes, their mixtures were investigated. Our major point of interest is the a and μ parameters.

5.5.1 Mixture of balls and Eclipsoids

The mixture of 50 % balls and 50 % Eclipsoids presented a rate of breakage lower than Eclipsoids alone. On the other hand, the mixture presented an

increase of the degree of cataracting, expressed by the μ value. This makes this mixture capable of higher breakage rate of coarser particles in the abnormal region. In this region, the material is so much weaker in tension than in compression, and the fracture occurs predominantly by cleavage (Spottiswood and Kelly, 1990). Figure 5.11 illustrates this fact.

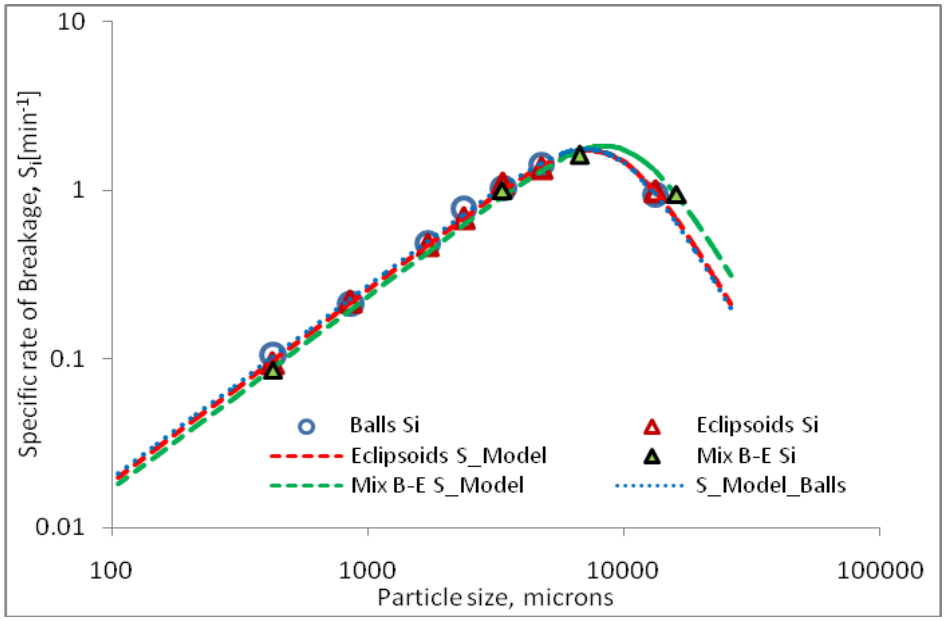

Figure 5.11 Variation of the specific rate of breakage for balls, Eclipsoids and the mixture of balls and Eclipsoids respectively.

Despite the fact that the total surface area was increased by 12.50%, the more surface available for breakage were not expressed in terms of an increase of the breakage rate. Also, the geometry of balls and Eclipsoids in presence offers point, line and area contacts. This causes the feed material to be firstly exposed to coarse grinding which is then used as a new feed for finer grinding (Cuhadaroglu et *al.*, 2008). This causes as well an increase of the cataracting effect, but with lower impact forces to cause breakage. As a result, the load

behaviour is subjected to conflicting behaviour between the different grinding media shapes, though there are more surfaces available for contact mechanisms in grinding action.

Compared to breakage parameters of balls, the values of a present coefficients of variation of 3.64 % and 9.88 % for Eclipsoids and for the mixture of 50 % balls and 50 % Eclipsoids respectively. The coefficients of variation are 2.17 % and 9.88 % for μ respectively for Eclipsoids and for the mixture of 50 % balls and 50 % Eclipsoids. Therefore, Eclispoids can be used as an alternative to balls while the mixture of 50 % balls and 50 % Eclipsoids cannot be recommended. Its coefficients of variations are greater than 5 % in terms of both a and μ.

5.5.2 Mixture of balls and cubes

The mixture of 50 % balls and 50 % cubes has significantly increased the rate of breakage, compared to cubes alone. The value of a has been increased from 0.151 to 0.257, a 41.24% increase. This is a clear indication that the mixture used is more efficient in term of the disappearance of the initial particle size considered for breakage.

The value of μ decreases from 9.49 for cubes alone to 7.61 for the mixture. This indicates that the higher impact forces of cataracting are reduced in this mixture. Hence, cubes seem to have a negative effect on the balls in the mixture in terms of breakage rate.

The coefficients of variation are 31.46 % in terms of a and 5.46 % in terms of μ, compared to balls. Cubes alone are definitely not efficient for grinding.

The mixture of 50 % balls and 50 % cubes presents coefficients of variation of 3.90 % and 9.63 % respectively for a and μ compared to balls. This mixture can be recommended as an alternative to balls. But, there is a need to account for the increase of μ by either the use appropriate lifter designs or the reduction of the rotational speed to decrease the degree of cataracting.

On the other hand, the mixture of 75 % balls and 25 % cubes presents an increase of a from 0.151 to 0.249 and a similar μ (9.43) compared to cubes alone. It presents coefficients of variation of 5.98 % and 4.98 % for a and μ respectively when compared to balls. This mixture need to be investigated more because its coefficients of variation do not allow us to decide on its grinding performances.

Figure 5.12 shows the variation of the specific rate of breakage with size for balls, cubes and for the mixtures of balls and cubes.

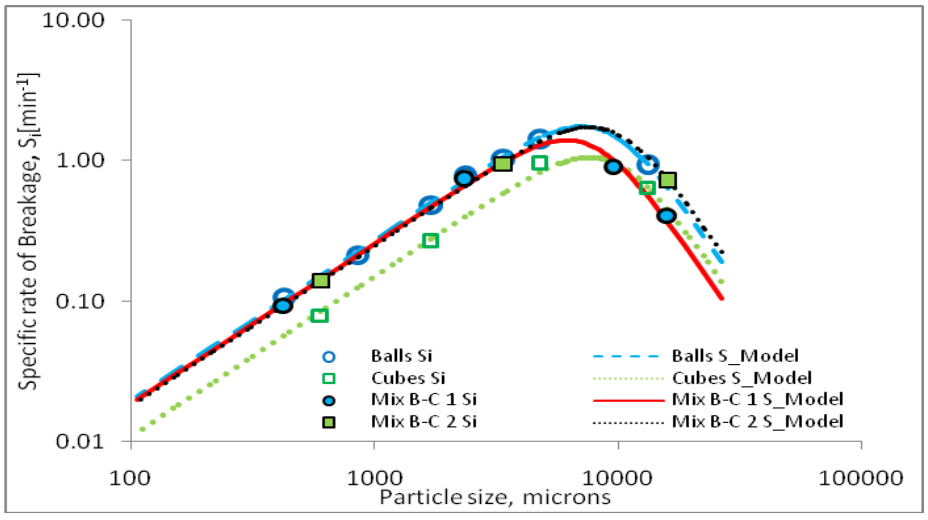

Figure 5.12 Variation of the specific rate of breakage of balls, cubes and the mixtures of balls and cubes.

All the mixtures investigated presents reasonably good breakage rate for medium and fine particle sizes. This means they can as well be used as an alternative to balls for the grinding process.

An overall view of the variation of the specific rate of breakage is illustrated in Figure 5.13.

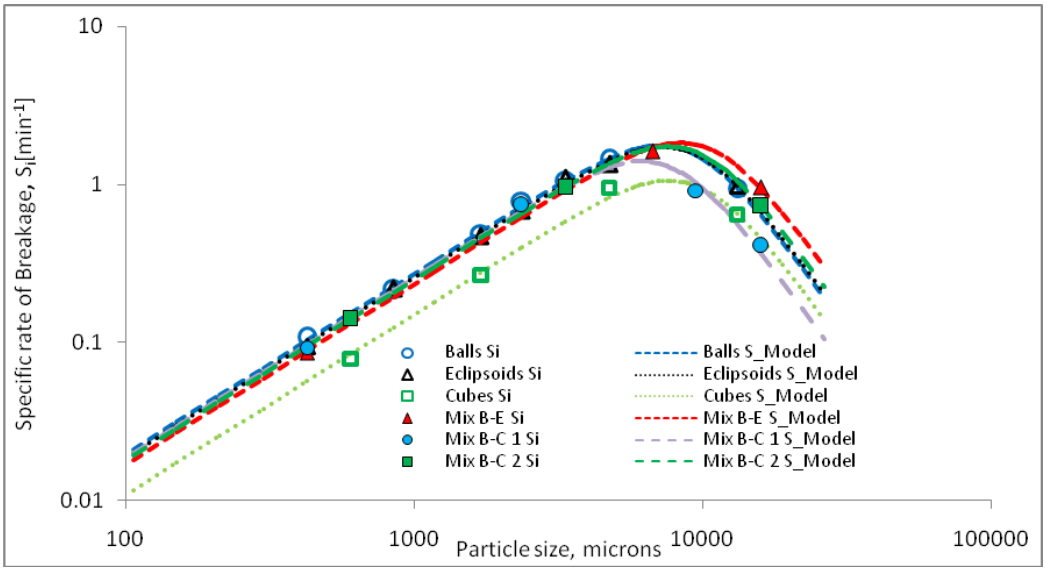

Figure 5.13 Variation of the specific rate of breakage for all the grinding media used.

This Figure shows that the mixtures of grinding media of different shapes break finer and medium particle sizes at similar rate as balls. In the abnormal region, their grinding performances are different. Cubes are the less efficient.

5.6 Power drawn

The specific energy used in all our tests was assumed to be the same, as the mill power drawn by the mill is basically determined by the mass of the charge

(Bond, 1961). Similarly, Lameck (2005) found that the two different grinding media shapes he used drew the same amount of power at all charge levels studied in the speed range within which most mills are operated.

Table 5.3 below presents the values of the average power drawn by the grinding media used. The power drawn is considered the same, their coefficients of variation being smaller than 3.46 %.

Table 5.3 Power drawn by different grinding media shapes.

	Balls	Eclipsoids	Cubes	Mix B-E	Mix B-C 1	Mix B-C 2
Power [Watts]	78.89	80.36	77.66	82.48	78.95	80.01
Coefficient of variation [%]	1.05	0.80	2.59	3.46	0.97	0.36
Mean×(1+2 CV)	80.54	81.64	81.68	88.18	80.48	80.58
Mean×(1-2 CV)	77.24	79.08	73.64	76.78	77.42	79.44

Since the mean power (79.73 W) falls within the range (Mean ± 2 Standard deviations) and the calculated chi-squared χ^2 (0.16941) being smaller than the tabulated χ^2 (1.145), we are 95 % confident that the powers measured for all the loads are identical.

This 'general agreement' that the power drawn is function of the mass of the charge has been confirmed to be true for all shapes, despite the fact that the grinding media shapes investigated are supposed to present different load behaviour during the grinding process due to their geometry.

5.7 Summary

Mixtures of grinding media of different shapes were investigated. It was found that the increase of surface area available for breakage does not necessarily translate into an increase of the breakage rate. In addition, the geometry of the grinding media shapes may lead to conflicting behaviour during the grinding process, nullifying more or less the advantage of several contact mechanisms in grinding action.

The mixtures of grinding media of different shapes present coefficients of variation smaller than 5 % in terms of a and μ when compared to balls and can be recommended as alternative to balls.

The power drawn has been proven to be the same for all the grinding media used. It is function of the mass charge.

Chapter 6 Conclusion

6.1 Introduction

Mixtures of grinding media of different shapes were characterized in the Minerals Processing Laboratory of the University of the Witwatersrand. The main objective was to characterize the material being described in terms of selection and breakage functions. In order to achieve this, a series of laboratory tests was carried out on quartz material.

This chapter summarizes the outcomes of this investigation. The breakage parameters were estimated for mixtures of grinding media of different shapes, and then compared to the parameters for individual grinding media shapes. Their grinding performances were in this way evaluated.

6.2 Summary of findings

The breakage rate parameters were satisfactorily determined. The value for the Λ parameter proposed by Austin *et al.* (1984) was used because we do not have enough information at hand to characterise it correctly. The parameter α was then searched for and the value obtained was used for all the grinding media, α being material dependent. The values of the parameter a were found to be varying from 0.151 for cubes which are the least selective rate function to 0.272 for balls the most selective. All the mixtures present the value for a between these two extremes, but similar with a standard deviation of 0.0056.

The μ parameter was ranging between 8.81 for balls to 10.43 for the mixture made of 50 % of balls and 50 % of Eclipsoids.

The mixture made of 50 % of balls and 50 % of Eclipsoids which presents coefficients of variation greater than 5 % in terms of both breakage rate parameters a and μ is considered not recommendable as an alternative to balls. The mixture made of 50 % of balls and 50 % of cubes is a good alternative to balls and need to be used with lifters designed specifically and at rotational speed that account for the increase of the degree of cataracting. And, the mixture made of 75 % of balls and 25 % of cubes presents parameters a and μ with coefficients of variation of 5.98 % and 4.98 % when compared to balls. This calls for further investigation.

The quartz material utilized was reasonably considered as having a normalizable breakage function. The breakage function parameters were found to be: β =5.80, γ =1.01 and ϕ =0.71.

Our investigation confirms the fact that balls are the most efficient grinding media in terms of breakage rate expressed by the highest a value. It is showed that a mixture of grinding media of different shapes can increase significantly the rate of breakage (up to more than 40 % for the mixture made of 50 % balls and 50 % cubes, compared to cubes alone). In addition, for all the mixtures considered, the increase of a value is inversely proportional to the increase of the μ value. This is a clear indication that grinding media shapes are subjected

to conflicting effect within the mixture. The mixture of balls and Eclipsoids is a good illustration of this fact.

6.3 Overall conclusion

The breakage properties of quartz material were estimated and the effect of mixtures of grinding media of different shapes deduced. This study shows that the breakage rate of the least efficient grinding media shape can be increased when it is used in a mixture of grinding media shape. Obviously, this can be achieved when using an optimal mixture of different grinding media shapes alternatively to 100 % balls in the grinding process. The choice and the proportion of the grinding media shape within the mixture is of great importance in order to take advantage of the contact mechanisms in grinding action and the increase of the surface area available for breakage. Grinding media shapes that are cheaper to manufacture can be mixed with the balls in order to get an efficient mixture in terms of grinding performance per unit media cost.

6.4 Recommendations

Important conclusions were reached through this investigation. But, there is a need to further this study. Other media shapes have to be explored under various mill conditions. The determination of the optimal mixture of grinding media needs to be investigated as well. The load behaviour of the charge has to be studied in order to comprehend the conflicting effects which impact negatively on the performance of mixtures of grinding media of different shapes.

References

Austin, L.G., Luckie, P.T., 1971/72. Methods for determination of breakage distribution parameters, Powder Technology, vol. 5, no. 4, pp 215 – 222.

Austin, L.G., Bhatia, V.K., 1971/72. Experimental methods for grinding studies in laboratory mills, Powder Technology, vol. 5, no. 5, pp 261 – 266.

Austin, L.G., Shoji, K., Everett, M.D., 1973. An explanation of abnormal breakage of large particle sizes in laboratory mills, Powder Technology, vol. 7, no. 1, pp 3 – 7.

Austin, L.G., Shoji, K., Luckie, P.T., 1976. The effect of ball size on mill performance, Powder Technology, vol. 14, no. 1, pp. 71 – 79.

Austin, L.G. and Perez, J.W., 1977. A note on limiting size distribution from closed circuit mills, Powder Technology, vol. 16, pp. 291-293.

Austin, L.G., Trimarchi, T., Weymont, N.P., 1977. An analysis of some cases of non-first-order breakage rates, Powder Technology, vol. 17, no. 1, pp. 109 – 113.

Austin, L.G., Bagga, P., Celik, M., 1981. Breakage properties of some materials in a laboratory ball mills, Powder Technology, vol. 28, pp. 235-243.

Austin, L.G., Shoji, K., Bell, D., 1982. Rate equations for non-linear breakage in mills due to material effects, Powder Technology, vol. 31, no. 1, pp. 127 – 133.

Austin, L.G., Brame, K., 1983. A comparison of Bond method for sizing wet tumbling ball mills with a size-mass balance simulation model, Powder Technology, vol. 34, no. 2, pp. 261 – 274.

Austin, L.G., Klimpel, R.R., Luckie, P.T., 1984. Processing Engineering of Size Reduction: Ball Milling. AIME/ SME, New York, USA.

Austin, L.G., Klimpel, R.R., 1985. Ball wear and ball size distribution in tumbling mills, Powder Technology, vol. 41, no. 3, pp. 279 – 286.

Austin, L.G., Julianelli, K., de Souza, A.S., Schneider, C.L., 2006. Simulation of wet ball milling of iron ore at Carajas – Brazil, International Journal of Mineral Processing, vol. 84, no. 1 – 4, pp. 157 – 171.

Bazin, C., 2005. Data reconciliation for the calibration of a model for batch grinding, Minerals Engineering, vol. 18, no. 10, pp. 1052 – 1056.

Bilgili, E., Scarlett, B., 2005. Population balance of non-linear effects in milling processes. Powder Technology, vol. 153, pp. 59-71.

Bilgili, E., Yepes, J., Scarlett, B., 2005. Formulation of non-liner framework for population balance modelling of batch grinding: Beyond first-order kinetics. Chemical Engineering Science, vol. 61, pp. 33-44.

Bilgili, E., 2007. On the Consequences of non-first-order breakage kinetics in communition processes : Absence of Self-Similar Size Spectra. Particles Particulate Systems Characterization, vol. 24, pp. 12-17.

Bond, F.C., 1960. Crushing and grinding calculations, British Chemical Engineering, vol. 6, pp. 378-391, 543-548.

Cleary, P.W., 2001. Charge behaviour and power consumption in ball mills: sensitivity to mill operating conditions, liner geometry and charge composition, International Journal of Mineral Processing, vol. 63, no. 2, pp. 79 – 114

Cuhadaroglu, D., Samanli, S., Kizgut, S., 2008. The effect of grinding media shape on the specific rate of breakage, Particles Particulate Systems Characterization, vol. 25, pp. 465-473.

Gardner, R.P., Austin, L.G., 1975. The applicability of the first-order grinding law to particles having a distribution of strengths, Powder Technology, vol. 12, no. 1, pp. 65 – 69.

Gupta, A., Yan, D.S., 2006. Mineral Processing Design and Operation: An introduction, Elsevier, ISBN: 978-0-4444-51636-7.

F. Shi, 2004. Comparison of grinding media – Cylpebs versus balls. Minerals Engineering, vol. 17, pp. 1259-1268.

Herbst, J.A., Lo, Y.C., 1989. Grinding efficiency with balls or cones as media. International Journal of Mineral Processing, vol. 26, pp. 141-151.

Hogg, D. and Fuerstaneu, D.W., 1972. Transverse mixing in rotating cylinders, Powder Technology, vol.6, no. 3, pp. 139-148.

Howat, D.D. and Vermeulen, L.A., 1988. Fineness of grind and the consumption and wear rates of metallic grinding media in tumbling mill, Powder Technology, vol. 55, pp. 231-240.

Ipek, H., 2006. The effects of grinding media shapes on breakage rate. Minerals Engineering, 19(1), pp. 91-93.

Ipek, H., 2007. Effects of grinding media shapes on breakage parameters. Particles Particulate Systems Characterization, vol. 24, pp. 229-235.

Kelly, E.G., Spottiswood, D.J., 1982. Introduction to Mineral Processing, John Wiley & Sons, ISBN 0-471-03379-0, USA.

Kelly, E.G., Spottiswood, D.J., 1990. The breakage function; What is it really?, Minerals Engineering, vol. 3, no. 5, pp. 405 – 414.

Kelsall, D.F., Reid, K.J., Restarick, C.J., 1967. Continuous grinding in a small wet ball mill. Part I. A study of the influence of ball diameter, Powder Technology, vol. 1, no. 5, pp. 291 – 300.

Kelsall, D.F., Stewart, P.S.B., Weller, K.R., 1973. Continuous grinding in a small wet ball mill. Part IV. A study of the influence of grinding media load and density, Powder Technology, vol. 7, no. 5, pp. 293 – 301.

King, R.P., 2001. Modeling and Simulation of Mineral Processing Systems, Butterworth-Heinemann, ISBN: 0-7506-4884-8.

Kotake, N., Daibo, K., Yamamoto, T., Kanda, Y., 2004. Experimental investigation on a grinding rate constant of solid materials by a ball mill – effect

of ball diameter and feed size, Powder Technology, vol. 143 – 144, pp. 196 – 203

Kotake, N., Suzuki, K., Asahi, S., Kanda, Y., 2002. Experimental study on the grinding rate constant of solid materials in a ball mill, Powder Technology, vol.122, no. 2 – 3, pp. 101 – 108

Lameck, N.N.S., 2006. Effects of grinding media shapes on ball mill performance, Master of Science Dissertation, University of the Witwatersrand, Johannesburg.

Lameck, N.S., 2006. Effects of grinding media shape on load behavior and mill power in a dry ball mill. Minerals Engineering, vol. 19, pp. 1357-1361.

Makhoka, A.B., Moys, H.M., 2006. Towards optimizing ball-milling capacity: Effect of lifter design. Minerals Engineering, vol. 19, pp. 1439-1445.

Napier-Munn, T.J., Morrell, S., Morrison, R.D., Kojovic, T., 1999. Mineral Comminution Circuits: Their Operation and Optimization. JKMRC, Queensland, Australia.

Nomura, S., Hosoda, K., Tanaka, T., 1991. An analysis of the selection function for mills using balls as grinding media, Powder Technology, vol. 68, no.1, pp. 1 – 12.

Nomura, S., Tanaka, T., Callcott, T.G., 1994. The effect of mill power on the selection function for tumbling and vibration ball mills, Powder Technology, vol. 81, no.2, pp. 101 – 109.

Palm, W.J., 2001. Introduction to Matlab 6 for Engineers, McGraw-Hill, Boston, USA.

Powell, M.S., Morrison, R.D., 2007. The future of comminution modeling, International Journal of Mineral Processing, vol. 84, no. 1 – 4, pp. 228 – 239.

Triola, M.F., 2005. Essentials of Statistics, Second Edition, Pearson Addison-Wesley, ISBN: 0-201-77129-2.

Wills, B.A., 1992. Mineral Processing Technology: An Introduction to the Practical Aspects of Ore Treatment and Mineral Recovery, Fifth Edition. Pergamon.

Yildirim, K., Austin, L.G., 1998. The abrasive wear of cylindrical grinding wear, Wear, vol. 218, no. 1, pp. 15 – 20.

Yildirim, K., Cho, H., Austin, L.G., 1999. The modeling of dry grinding of quartz in tumbling media mills, Powder Technology, vol. 105, no. 1 – 3, pp. 210 – 221.

Appendices

A Particle size analysis of batch grinding tests

This section presents the particle size distributions of the quartz material as obtained after batch grinding tests. They refer to balls, Eclipsoids, cubes, the mixture of 50 % balls and 50 % Eclipsoids (referred as 50-50 mixture of balls and Eclipsoids or Mix B-E), the mixture of 50 % balls and 50 % cubes (referred as 50-50 mixture of balls and cubes or Mix B-C 1) and the mixture of 75 % balls and 25 % cubes (referred as 50-50 mixture of balls and cubes or Mix B-C 2) used as grinding media.

A.1 Batch grinding tests with single grinding media shape

A.1.1 Particle size distributions obtained using balls

Table A.1 Size analysis results for –13200 + 9500 microns quartz ground with balls.

Screen size (μm)	Particle Size distribution									
	Feed		0,5 min		1 min		2 min		4 min	
	%Retained	%Passing	%Retained	%Passing	%Retained	%Passing	%Retained	%Passing	%Retained	%Passing
13200	0.00	100.00	0.00	100.00	0.00	100.00	0.00	100.00	0.00	100.00
9500	96.11	3.89	43.46	56.54	24.37	75.63	9.97	90.03	1.90	98.10
6700	3.89	0.00	19.11	37.43	15.66	59.97	12.98	77.05	1.92	96.18
4750	0.00	0.00	8.71	28.72	10.25	49.72	9.26	67.79	1.94	94.23
3350	0.00	0.00	6.93	21.78	8.96	40.76	8.75	59.04	3.03	91.21
2360	0.00	0.00	5.13	16.66	7.91	32.85	8.49	50.55	4.11	87.10
1700	0.00	0.00	3.80	12.85	6.59	26.26	8.45	42.10	6.14	80.96
1180	0.00	0.00	3.91	8.94	6.94	19.32	7.87	34.23	11.37	69.59
850	0.00	0.00	2.44	6.50	4.74	14.58	7.56	26.67	11.96	57.64
600	0.00	0.00	1.92	4.58	3.95	10.63	7.38	19.29	12.94	44.70
425	0.00	0.00	1.34	3.23	2.77	7.87	5.39	13.90	10.64	34.06
300	0.00	0.00	1.11	2.12	2.38	5.49	4.45	9.45	10.23	23.83
212	0.00	0.00	0.72	1.40	1.86	3.63	3.22	6.24	7.21	16.62
150	0.00	0.00	0.50	0.91	1.17	2.46	2.27	3.97	5.87	10.75
106	0.00	0.00	0.36	0.55	1.01	1.45	1.63	2.34	4.17	6.58
75	0.00	0.00	0.23	0.32	0.68	0.77	1.06	1.28	2.95	3.63
Pan	0.00		0.32		0.77		1.28		3.63	
Total	100.00		100.00		100.00		100.00		100.00	

Table A.2 Size analysis results for – 4750 + 3350 microns quartz ground with balls.

Screen size (µm)	Particle Size distribution									
	Feed		0,5 min		1 min		2 min		4 min	
	%Retained	%Passing	%Retained	%Passing	%Retained	%Passing	%Retained	%Passing	%Retained	%Passing
4750	0.00	100.00	0.00	100.00	0.00	100.00	0.00	100.00	0.00	100.00
3350	94.05	5.95	49.02	50.98	22.30	77.70	6.10	93.90	0.30	99.70
2360	5.95	0.00	21.67	29.30	20.58	57.13	13.40	80.50	1.98	97.72
1700	0.00	0.00	9.70	19.60	15.29	41.84	15.09	65.40	5.64	92.08
1180	0.00	0.00	7.37	12.24	13.74	28.09	18.45	46.95	13.59	78.49
850	0.00	0.00	3.59	8.64	7.46	20.64	11.22	35.74	14.29	64.20
600	0.00	0.00	2.47	6.17	5.64	15.00	9.19	26.55	14.84	49.36
425	0.00	0.00	1.66	4.51	3.95	11.05	6.64	19.91	11.38	37.99
300	0.00	0.00	1.38	3.14	3.36	7.69	5.92	13.99	10.54	27.45
212	0.00	0.00	0.89	2.25	2.23	5.46	4.03	9.96	7.32	20.13
150	0.00	0.00	0.67	1.58	1.65	3.81	2.84	7.12	5.51	14.62
106	0.00	0.00	0.45	1.13	1.05	2.76	1.91	5.21	3.91	10.71
75	0.00	0.00	0.28	0.85	0.63	2.13	1.18	4.03	2.60	8.12
Pan	0.00		0.85		2.13		4.03		8.12	
Total	100.00		100.00		100.00		100.00		100.00	

Table A.3 Size analysis results for – 3350 + 2360 microns quartz ground with balls.

Screen size (µm)	Particle Size distribution									
	Feed		0,5 min		1 min		2 min		4 min	
	%Retained	%Passing	%Retained	%Passing	%Retained	%Passing	%Retained	%Passing	%Retained	%Passing
3350	0.00	100.00	0.00	100.00	0.00	100.00	0.00	100.00	0.00	100.00
2360	98.47	1.53	62.14	37.86	38.99	61.01	14.35	85.65	1.58	98.42
1700	1.53	0.00	14.93	22.93	19.24	41.77	17.23	68.42	5.21	93.22
1180	0.00	0.00	7.95	14.98	15.78	25.98	22.51	45.91	14.04	79.18
850	0.00	0.00	4.23	10.75	7.87	18.11	11.90	34.01	14.97	64.21
600	0.00	0.00	3.08	7.67	5.52	12.59	8.96	25.05	14.86	49.34
425	0.00	0.00	2.00	5.67	3.56	9.03	6.15	18.89	11.87	37.47
300	0.00	0.00	1.66	4.01	2.90	6.13	5.35	13.54	10.88	26.59
212	0.00	0.00	1.11	2.90	1.78	4.35	3.58	9.95	7.25	19.34
150	0.00	0.00	0.78	2.13	1.35	3.00	2.64	7.31	5.33	14.02
106	0.00	0.00	0.48	1.64	0.81	2.19	2.02	5.29	4.10	9.91
75	0.00	0.00	0.26	1.39	0.44	1.75	1.38	3.91	3.16	6.75
Pan	0.00		1.39		1.75		3.91		6.75	
Total	100.00		100.00		100.00		100.00		100.00	

Table A.4 Size analysis results for – 2360 + 1700 microns quartz ground with balls.

Screen size (μm)	Particle Size distribution									
	Feed		0,5 min		1 min		2 min		4 min	
	%Retained	%Passing	%Retained	%Passing	%Retained	%Passing	%Retained	%Passing	%Retained	%Passing
2360	0.00	100.00	0.00	100.00	0.00	100.00	0.00	100.00	0.00	100.00
1700	96.61	3.39	64.87	35.13	46.33	53.67	21.89	78.11	4.17	95.83
1180	3.39	0.00	19.87	15.26	25.14	28.53	26.66	51.44	14.82	81.01
850	0.00	0.00	5.46	9.81	9.71	18.83	14.97	36.48	15.96	65.05
600	0.00	0.00	3.40	6.40	6.15	12.68	10.79	25.68	15.21	49.85
425	0.00	0.00	2.02	4.38	3.79	8.89	6.93	18.75	11.52	38.33
300	0.00	0.00	1.50	2.88	3.07	5.82	5.83	12.92	10.57	27.76
212	0.00	0.00	1.05	1.83	1.92	3.90	4.02	8.90	7.49	20.27
150	0.00	0.00	0.68	1.15	1.30	2.60	2.78	6.12	5.38	14.89
106	0.00	0.00	0.41	0.73	0.83	1.76	1.77	4.35	4.05	10.84
75	0.00	0.00	0.21	0.52	0.48	1.29	1.00	3.35	3.03	7.81
Pan	0.00		0.52		1.29		3.35		7.81	
Total	100.00		100.00		100.00		100.00		100.00	

Table A.5 Size analysis results for – 1700 + 1180 microns quartz ground with balls.

Screen size (μm)	Particle Size distribution									
	Feed		0,5 min		1 min		2 min		4 min	
	%Retained	%Passing	%Retained	%Passing	%Retained	%Passing	%Retained	%Passing	%Retained	%Passing
1700	0.00	100.00	0.00	100.00	0.00	100.00	0.00	100.00	0.00	100.00
1180	98.96	1.04	78.18	21.82	67.35	32.65	41.32	58.68	14.15	85.85
850	1.04	0.00	7.52	14.30	11.84	20.80	17.11	41.57	15.91	69.94
600	0.00	0.00	5.33	8.97	6.66	14.15	12.25	29.32	16.16	53.79
425	0.00	0.00	2.48	6.49	3.96	10.19	7.74	21.58	12.38	41.41
300	0.00	0.00	2.02	4.47	3.19	7.00	6.58	15.00	11.41	29.99
212	0.00	0.00	1.39	3.08	1.95	5.05	4.05	10.95	7.50	22.50
150	0.00	0.00	1.01	2.07	1.47	3.58	2.93	8.03	5.95	16.55
106	0.00	0.00	0.58	1.49	0.87	2.72	1.85	6.17	4.38	12.18
75	0.00	0.00	0.26	1.23	0.62	2.09	1.10	5.07	3.21	8.96
Pan	0.00		1.23		2.09		5.07		8.96	
Total	100.00		100.00		100.00		100.00		100.00	

Table A.6 Size analysis results for – 850 + 600 microns quartz ground with balls.

Screen size (µm)	Particle Size distribution									
	Feed		0,5 min		1 min		2 min		4 min	
	%Retained	%Passing	%Retained	%Passing	%Retained	%Passing	%Retained	%Passing	%Retained	%Passing
850	0.00	100.00	0.00	100.00	0.00	100.00	0.00	100.00	0.00	100.00
600	99.30	0.70	89.27	10.73	81.32	18.68	65.20	34.80	42.26	57.74
425	0.70	0.00	4.18	6.55	7.03	11.65	12.15	22.65	16.86	40.88
300	0.00	0.00	2.25	4.30	4.19	7.46	7.83	14.82	12.80	28.08
212	0.00	0.00	1.09	3.21	2.27	5.19	4.60	10.22	7.97	20.11
150	0.00	0.00	0.96	2.25	1.47	3.72	3.11	7.11	5.79	14.32
106	0.00	0.00	0.76	1.49	0.89	2.83	1.93	5.18	4.15	10.17
75	0.00	0.00	0.51	0.98	0.53	2.30	1.08	4.09	2.81	7.36
Pan	0.00		0.98		2.30		4.09		7.36	
Total	100.00		100.00		100.00		100.00		100.00	

Table A.7 Size analysis for – 425 + 300 microns quartz ground with balls.

Screen size (µm)	Particle Size distribution									
	Feed		0,5 min		1 min		2 min		4 min	
	%Retained	%Passing	%Retained	%Passing	%Retained	%Passing	%Retained	%Passing	%Retained	%Passing
425	0.00	100.00	0.00	100.00	0.00	100.00	0.00	100.00	0.00	100.00
300	98.36	1.64	89.57	10.43	85.50	14.50	75.79	24.21	63.17	36.83
212	1.64	0.00	7.02	3.41	8.81	5.69	11.82	12.40	14.24	22.59
150	0.00	0.00	0.92	2.49	1.62	4.07	3.83	8.57	6.49	16.11
106	0.00	0.00	0.62	1.87	1.08	2.99	2.32	6.25	4.05	12.05
75	0.00	0.00	0.39	1.47	0.72	2.27	1.58	4.67	2.79	9.26
Pan	0.00		1.47		2.27		4.67		9.26	
Total	100.00		100.00		100.00		100.00		100.00	

A.1.2 Particle size distributions obtained using Eclipsoids

Table A.8 Size analysis results for – 13200 + 9500 microns quartz ground with Eclipsoids.

Screen size (μm)	Particle Size distribution									
	Feed		0,5 min		1 min		2 min		4 min	
	%Retained	%Passing	%Retained	%Passing	%Retained	%Passing	%Retained	%Passing	%Retained	%Passing
13200	0.00	100.00	0.00	100.00	0.00	100.00	0.00	100.00	0.00	100.00
9500	97.69	2.31	41.23	58.77	22.82	77.18	9.05	90.95	1.64	98.36
6700	2.31	0.00	19.46	39.31	17.62	59.56	10.79	80.15	3.35	95.00
4750	0.00	0.00	10.13	29.18	10.64	48.92	7.86	72.30	2.64	92.36
3350	0.00	0.00	6.71	22.47	9.21	39.71	8.39	63.90	3.19	89.17
2360	0.00	0.00	5.35	17.13	7.86	31.85	8.99	54.91	4.78	84.39
1700	0.00	0.00	3.89	13.24	6.02	25.83	8.30	46.61	6.59	77.80
1180	0.00	0.00	3.84	9.40	6.27	19.56	9.38	37.23	10.60	67.20
850	0.00	0.00	2.35	7.05	4.49	15.07	7.69	29.54	10.79	56.42
600	0.00	0.00	1.94	5.11	3.98	11.09	7.30	22.24	11.86	44.55
425	0.00	0.00	1.31	3.80	3.81	7.28	5.47	16.77	9.83	34.72
300	0.00	0.00	1.12	2.68	2.33	4.95	4.92	11.85	9.50	25.22
212	0.00	0.00	0.74	1.94	1.55	3.41	3.36	8.49	6.64	18.58
150	0.00	0.00	0.52	1.42	1.03	2.38	2.47	6.02	5.48	13.09
106	0.00	0.00	0.37	1.05	0.49	1.89	1.75	4.27	3.62	9.47
75	0.00	0.00	0.26	0.79	0.49	1.40	1.27	2.99	2.38	7.09
Pan	0.00		0.79		1.40		2.99		7.09	
Total	100.00		100.00		100.00		100.00		100.00	

Table A.9 Size analysis results for – 4750 + 3350 microns quartz ground with Eclipsoids.

Screen size (μm)	Particle Size distribution									
	Feed		0,5 min		1 min		2 min		4 min	
	%Retained	%Passing	%Retained	%Passing	%Retained	%Passing	%Retained	%Passing	%Retained	%Passing
4750	0.00	100.00	0.00	100.00	0.00	100.00	0.00	100.00	0.00	100.00
3350	94.57	5.43	47.65	52.35	26.14	73.86	7.56	92.44	0.43	99.57
2360	5.43	0.00	24.11	28.24	23.68	50.18	15.69	76.75	2.62	96.95
1700	0.00	0.00	9.96	18.29	14.82	35.36	16.40	60.35	6.94	90.01
1180	0.00	0.00	7.18	11.11	13.35	22.01	17.02	43.33	14.73	75.28
850	0.00	0.00	3.37	7.74	6.37	15.64	10.85	32.48	13.78	61.51
600	0.00	0.00	2.31	5.43	4.42	11.22	8.47	24.01	13.30	48.21
425	0.00	0.00	1.47	3.96	2.94	8.28	6.05	17.96	10.99	37.21
300	0.00	0.00	1.20	2.76	2.50	5.78	5.20	12.76	10.16	27.06
212	0.00	0.00	0.79	1.97	1.60	4.18	3.50	9.26	6.76	20.30
150	0.00	0.00	0.56	1.41	1.22	2.96	2.59	6.67	5.20	15.09
106	0.00	0.00	0.40	1.01	0.83	2.13	1.67	5.00	3.42	11.67
75	0.00	0.00	0.28	0.73	0.61	1.52	1.01	3.99	2.09	9.58
Pan	0.00		0.73		1.52		3.99		9.58	
Total	100.00		100.00		100.00		100.00		100.00	

Table A.10 Size analysis results for – 3350 + 2360 microns quartz ground with Eclipsoids.

Screen size	Particle Size distribution									
	Feed		0,5 min		1 min		2 min		4 min	
(µm)	%Retained	%Passing	%Retained	%Passing	%Retained	%Passing	%Retained	%Passing	%Retained	%Passing
3350	0.00	100.00	0.00	100.00	0.00	100.00	0.00	100.00	0.00	100.00
2360	95.30	4.70	57.16	42.84	34.63	65.37	11.88	88.12	1.24	98.76
1700	4.70	0.00	20.06	22.78	23.21	42.16	19.53	68.59	5.91	92.85
1180	0.00	0.00	10.15	12.63	17.68	24.48	20.22	48.37	17.42	75.43
850	0.00	0.00	4.14	8.48	7.81	16.67	12.82	35.55	15.66	59.77
600	0.00	0.00	2.61	5.88	5.39	11.28	9.69	25.86	14.03	45.73
425	0.00	0.00	1.69	4.19	3.27	8.01	6.66	19.20	10.56	35.17
300	0.00	0.00	1.31	2.88	2.64	5.37	5.49	13.72	9.51	25.66
212	0.00	0.00	0.83	2.05	1.64	3.73	3.74	9.97	8.15	17.52
150	0.00	0.00	0.55	1.50	1.10	2.63	2.65	7.33	5.05	12.47
106	0.00	0.00	0.40	1.10	0.77	1.86	2.20	5.13	3.70	8.77
75	0.00	0.00	0.28	0.82	0.47	1.40	1.46	3.67	2.64	6.13
Pan	0.00		0.82		1.40		3.67		6.13	
Total	100.00		100.00		100.00		100.00		100.00	

Table A.11 Size analysis results for – 2360 + 1700 microns quartz ground with Eclipsoids.

Screen size	Particle Size distribution									
	Feed		0,5 min		1 min		2 min		4 min	
(µm)	%Retained	%Passing	%Retained	%Passing	%Retained	%Passing	%Retained	%Passing	%Retained	%Passing
2360	0.00	100.00	0.00	100.00	0.00	100.00	0.00	100.00	0.00	100.00
1700	94.21	5.79	64.58	35.42	45.33	54.67	22.06	77.94	6.15	93.85
1180	5.79	0.00	18.77	16.65	25.58	29.09	27.63	50.31	20.27	73.58
850	0.00	0.00	6.50	10.16	10.12	18.96	16.22	34.09	14.74	58.84
600	0.00	0.00	3.43	6.73	6.45	12.51	9.86	24.23	12.68	46.16
425	0.00	0.00	2.05	4.67	3.82	8.69	6.48	17.75	11.47	34.70
300	0.00	0.00	1.46	3.21	2.92	5.78	4.43	13.32	9.81	24.89
212	0.00	0.00	0.96	2.26	1.70	4.08	3.25	10.07	6.64	18.24
150	0.00	0.00	0.64	1.61	1.18	2.90	2.70	7.36	4.94	13.31
106	0.00	0.00	0.36	1.25	0.71	2.19	2.10	5.27	3.69	9.61
75	0.00	0.00	0.24	1.01	0.53	1.66	1.37	3.90	2.79	6.83
Pan	0.00		1.01		1.66		3.90		6.83	
Total	100.00		100.00		100.00		100.00		100.00	

Table A.12 Size analysis results for – 1700 + 1180 microns quartz ground with Eclipsoids.

Screen size	Particle Size distribution									
	Feed		0,5 min		1 min		2 min		4 min	
(µm)	%Retained	%Passing	%Retained	%Passing	%Retained	%Passing	%Retained	%Passing	%Retained	%Passing
1700	0.00	100.00	0.00	100.00	0.00	100.00	0.00	100.00	0.00	100.00
1180	98.73	1.27	81.91	18.09	69.03	30.97	44.13	55.87	15.36	84.64
850	1.27	0.00	7.47	10.62	12.19	18.78	20.30	35.57	19.08	65.57
600	0.00	0.00	3.85	6.78	6.40	12.38	12.30	23.27	17.89	47.67
425	0.00	0.00	2.10	4.67	3.64	8.74	7.16	16.11	12.60	35.08
300	0.00	0.00	1.58	3.09	2.98	5.77	5.62	10.49	10.95	24.13
212	0.00	0.00	0.91	2.18	1.77	4.00	3.46	7.04	7.25	16.88
150	0.00	0.00	0.88	1.30	1.55	2.44	2.33	4.70	5.28	11.61
106	0.00	0.00	0.45	0.85	0.85	1.60	1.49	3.21	3.78	7.82
75	0.00	0.00	0.29	0.56	0.50	1.10	0.83	2.38	2.71	5.12
Pan	0.00		0.56		1.10		2.38		5.12	
Total	100.00		100.00		100.00		100.00		100.00	

Table A.13 Size analysis results for – 850 + 600 microns quartz ground with Eclipsoids.

Screen size	Particle Size distribution									
	Feed		0,5 min		1 min		2 min		4 min	
(µm)	%Retained	%Passing	%Retained	%Passing	%Retained	%Passing	%Retained	%Passing	%Retained	%Passing
850	0.00	100.00	0.00	100.00	0.00	100.00	0.00	100.00	0.00	100.00
600	94.89	5.11	87.61	12.39	80.51	19.49	64.26	35.74	40.25	59.75
425	5.11	0.00	4.55	7.85	7.43	12.06	12.51	23.23	17.03	42.72
300	0.00	0.00	2.67	5.18	4.42	7.64	7.88	15.35	13.23	29.48
212	0.00	0.00	1.51	3.67	2.34	5.30	4.69	10.66	8.22	21.26
150	0.00	0.00	1.00	2.67	1.47	3.83	3.40	7.26	5.95	15.32
106	0.00	0.00	0.73	1.95	1.00	2.83	1.96	5.30	4.22	11.10
75	0.00	0.00	0.52	1.43	0.75	2.08	1.33	3.97	2.99	8.11
Pan	0.00		1.43		2.08		3.97		8.11	
Total	100.00		100.00		100.00		100.00		100.00	

Table A.14 Size analysis results for – 425 + 300 microns quartz ground with Eclipsoids.

Screen size	Particle Size distribution									
	Feed		0,5 min		1 min		2 min		4 min	
(µm)	%Retained	%Passing	%Retained	%Passing	%Retained	%Passing	%Retained	%Passing	%Retained	%Passing
425	0.00	100.00	0.00	100.00	0.00	100.00	0.00	100.00	0.00	100.00
300	97.41	2.59	90.31	9.69	82.86	17.14	78.20	21.80	65.77	34.23
212	2.59	0.00	6.82	2.87	11.20	5.94	10.82	10.98	14.18	20.05
150	0.00	0.00	0.90	1.97	1.36	4.57	3.55	7.43	6.55	13.50
106	0.00	0.00	0.48	1.49	1.06	3.52	2.05	5.38	3.83	9.67
75	0.00	0.00	0.30	1.20	0.78	2.74	1.33	4.05	2.67	7.00
Pan	0.00		1.20		2.74		4.05		7.00	
Total	100.00		100.00		100.00		100.00		100.00	

A.1.3 Particle size distributions obtained using cubes

Table A.15 Size analysis results for –13200 + 9500 microns quartz ground with cubes.

Screen size	Particle Size distribution									
	Feed		0,5 min		1 min		2 min		4 min	
(μm)	%Retained	%Passing	%Retained	%Passing	%Retained	%Passing	%Retained	%Passing	%Retained	%Passing
13200	0.00	100.00	0.00	100.00	0.00	100.00	0.00	100.00	0.00	100.00
9500	99.21	0.79	57.69	42.31	36.14	63.86	18.78	81.22	6.92	93.08
6700	0.79	0.00	17.50	24.81	20.63	43.24	15.92	65.29	7.08	86.00
4750	0.00	0.00	7.96	16.85	11.71	31.53	11.02	54.27	6.43	79.58
3350	0.00	0.00	4.53	12.32	7.86	23.67	9.99	44.28	7.53	72.05
2360	0.00	0.00	3.33	8.99	5.68	17.99	8.99	35.29	9.25	62.80
1700	0.00	0.00	2.21	6.78	4.12	13.87	6.92	28.37	9.16	53.64
1180	0.00	0.00	2.11	4.67	3.78	10.09	6.70	21.67	10.81	42.83
850	0.00	0.00	1.22	3.46	2.65	7.44	5.12	16.55	9.25	33.58
600	0.00	0.00	1.01	2.45	2.18	5.26	4.50	12.05	7.88	25.70
425	0.00	0.00	0.70	1.75	1.47	3.79	3.30	8.76	6.55	19.14
300	0.00	0.00	0.59	1.16	1.22	2.57	2.82	5.94	6.05	13.09
212	0.00	0.00	0.36	0.80	0.85	1.72	1.82	4.12	4.11	8.99
150	0.00	0.00	0.30	0.50	0.64	1.08	1.42	2.69	3.17	5.82
106	0.00	0.00	0.23	0.26	0.48	0.60	0.99	1.71	2.13	3.68
75	0.00	0.00	0.16	0.10	0.34	0.27	0.72	0.99	1.59	2.10
Pan	0.00		0.10		0.27		0.99		2.10	
Total	100.00		100.00		100.00		100.00		100.00	

Table A.16 Size analysis results for –4750 + 3350 microns quartz ground with cubes.

Screen size	Particle Size distribution									
	Feed		0,5 min		1 min		2 min		4 min	
(μm)	%Retained	%Passing	%Retained	%Passing	%Retained	%Passing	%Retained	%Passing	%Retained	%Passing
4750	0.00	100.00	0.00	100.00	0.00	100.00	0.00	100.00	0.00	100.00
3350	98.76	1.24	59.60	40.40	38.05	61.95	16.27	83.73	2.11	97.89
2360	1.24	0.00	22.03	18.37	27.98	33.97	25.40	58.32	10.33	87.56
1700	0.00	0.00	7.28	11.09	12.41	21.57	17.97	40.36	16.95	70.61
1180	0.00	0.00	4.40	6.69	8.36	13.21	14.62	25.74	20.44	50.16
850	0.00	0.00	2.42	4.28	4.09	9.12	7.78	17.95	12.29	37.87
600	0.00	0.00	1.38	2.90	2.87	6.25	4.77	13.19	9.23	28.64
425	0.00	0.00	1.01	1.89	1.87	4.38	3.76	9.42	7.40	21.24
300	0.00	0.00	0.71	1.18	1.57	2.81	3.10	6.33	6.46	14.78
212	0.00	0.00	0.44	0.74	0.98	1.83	1.91	4.42	4.06	10.72
150	0.00	0.00	0.27	0.46	0.63	1.20	1.54	2.88	3.19	7.53
106	0.00	0.00	0.22	0.25	0.49	0.70	1.02	1.87	2.53	5.00
75	0.00	0.00	0.19	0.06	0.40	0.30	0.67	1.20	1.67	3.33
Pan	0.00		0.06		0.30		1.20		3.33	
Total	100.00		100.00		100.00		100.00		100.00	

Table A.17 Size analysis results for –1700 + 1180 microns quartz ground with cubes.

Screen size (µm)	Particle Size distribution									
	Feed		0,5 min		1 min		2 min		4 min	
	%Retained	%Passing	%Retained	%Passing	%Retained	%Passing	%Retained	%Passing	%Retained	%Passing
1700	0.00	100.00	0.00	100.00	0.00	100.00	0.00	100.00	0.00	100.00
1180	98.88	1.12	88.51	11.49	75.87	24.13	58.59	41.41	34.43	65.57
850	1.12	0.00	5.71	5.77	10.29	13.84	16.74	24.67	22.54	43.03
600	0.00	0.00	2.44	3.34	4.73	9.11	9.39	15.28	13.95	29.08
425	0.00	0.00	1.24	2.10	2.77	6.34	4.74	10.54	9.12	19.96
300	0.00	0.00	0.79	1.31	1.87	4.47	3.51	7.03	6.94	13.03
212	0.00	0.00	0.48	0.83	1.09	3.37	2.00	5.03	4.38	8.64
150	0.00	0.00	0.07	0.76	1.07	2.31	1.63	3.39	3.12	5.52
106	0.00	0.00	0.22	0.54	0.59	1.72	1.05	2.34	2.15	3.38
75	0.00	0.00	0.24	0.30	0.41	1.31	0.72	1.62	1.51	1.86
Pan	0.00		0.30		1.31		1.62		1.86	
Total	100.00		100.00		100.00		100.00		100.00	

Table A.18 Size analysis results for –600 + 425 microns quartz ground with cubes.

Screen size (µm)	Particle Size distribution									
	Feed		0,5 min		1 min		2 min		4 min	
	%Retained	%Passing	%Retained	%Passing	%Retained	%Passing	%Retained	%Passing	%Retained	%Passing
600	0.00	100.00	0.00	100.00	0.00	100.00	0.00	100.00	0.00	100.00
425	99.37	0.63	92.14	7.86	88.25	11.75	81.09	18.91	71.57	28.43
300	0.63	0.00	5.74	2.12	6.81	4.94	11.02	7.89	14.45	13.98
212	0.00	0.00	0.95	1.17	1.84	3.09	3.18	4.71	5.42	8.56
150	0.00	0.00	0.57	0.60	1.31	1.79	2.04	2.67	3.43	5.13
106	0.00	0.00	0.26	0.34	0.77	1.01	1.08	1.59	2.14	2.98
75	0.00	0.00	0.14	0.20	0.46	0.55	0.65	0.93	1.57	1.41
Pan	0.00		0.20		0.55		0.93		1.41	
Total	100.00		100.00		100.00		100.00		100.00	

A.2 Batch grinding tests with mixtures of grinding media shape

A.2.1 Particle size distributions obtained using a 50-50 mixture of balls and Eclipsoids.

Table A.19 Size analysis results for –16000 + 13200 microns quartz ground with a 50-50 mixture of balls and Eclipsoids.

Screen size	Particle Size distribution									
	Feed		0,5 min		1 min		2 min		4 min	
(µm)	%Retained	%Passing	%Retained	%Passing	%Retained	%Passing	%Retained	%Passing	%Retained	%Passing
16000	0.00	100.00	0.00	100.00	0.00	100.00	0.00	100.00	0.00	100.00
13200	98.58	1.42	25.87	74.13	16.11	83.89	6.87	93.13	1.53	98.47
9500	1.42	0.00	30.28	43.85	22.52	61.37	13.37	79.76	3.69	94.77
6700	0.00	0.00	12.63	31.22	12.33	49.05	8.63	71.13	3.72	91.06
4750	0.00	0.00	7.20	24.02	8.74	40.31	6.74	64.39	2.84	88.22
3350	0.00	0.00	5.38	18.65	7.29	33.02	7.06	57.33	3.37	84.85
2360	0.00	0.00	4.21	14.44	5.99	27.03	7.69	49.64	4.55	80.29
1700	0.00	0.00	3.21	11.23	5.00	22.03	7.28	42.35	6.44	73.85
1180	0.00	0.00	2.99	8.24	5.46	16.57	9.91	32.44	10.69	63.16
850	0.00	0.00	2.15	6.10	4.01	12.56	7.23	25.21	10.41	52.75
600	0.00	0.00	1.85	4.24	3.50	9.06	6.43	18.78	11.70	41.05
425	0.00	0.00	1.28	2.96	2.58	6.48	5.22	13.56	9.45	31.60
300	0.00	0.00	1.08	1.88	2.26	4.22	4.67	8.89	9.67	21.93
212	0.00	0.00	0.69	1.19	1.43	2.79	2.84	6.05	7.03	14.90
150	0.00	0.00	0.50	0.69	1.13	1.66	2.56	3.49	5.49	9.41
106	0.00	0.00	0.36	0.33	0.83	0.84	1.80	1.70	3.89	5.52
75	0.00	0.00	0.25	0.09	0.58	0.25	1.18	0.52	2.74	2.78
Pan	0.00		0.09		0.25		0.52		2.78	
Total	100.00		100.00		100.00		100.00		100.00	

Table A.20 Size analysis results for –6700 + 4750 microns quartz ground with a 50-50 mixture of balls and Eclipsoids.

Screen size	Particle Size distribution									
	Feed		0,5 min		1 min		2 min		4 min	
(μm)	%Retained	%Passing	%Retained	%Passing	%Retained	%Passing	%Retained	%Passing	%Retained	%Passing
6700	0.00	100.00	0.00	100.00	0.00	100.00	0.00	100.00	0.00	100.00
4750	98.75	1.25	32.47	67.53	15.72	84.28	3.62	96.38	0.13	99.87
3350	1.25	0.00	31.83	35.70	25.16	59.12	10.95	85.42	1.18	98.69
2360	0.00	0.00	13.69	22.01	17.92	41.19	15.53	69.89	3.82	94.86
1700	0.00	0.00	6.78	15.23	11.40	29.79	14.18	55.71	7.78	87.08
1180	0.00	0.00	5.61	9.62	10.66	19.13	16.62	39.09	14.68	72.40
850	0.00	0.00	2.76	6.86	5.48	13.65	9.99	29.10	13.85	58.55
600	0.00	0.00	2.11	4.75	4.10	9.55	8.27	20.84	13.99	44.56
425	0.00	0.00	1.36	3.39	2.87	6.68	5.77	15.07	11.73	32.83
300	0.00	0.00	1.13	2.27	2.37	4.31	4.98	10.09	10.30	22.53
212	0.00	0.00	0.81	1.46	1.49	2.82	3.63	6.46	7.01	15.52
150	0.00	0.00	0.54	0.92	1.10	1.73	2.34	4.12	5.70	9.82
106	0.00	0.00	0.43	0.49	0.79	0.94	1.61	2.52	4.39	5.43
75	0.00	0.00	0.27	0.22	0.53	0.40	1.07	1.45	2.80	2.63
Pan	0.00		0.22		0.40		1.45		2.63	
Total	100.00		100.00		100.00		100.00		100.00	

Table A.21 Size analysis results for –3350 + 2360 microns quartz ground with a 50-50 mixture of balls and Eclipsoids.

Screen size	Particle Size distribution									
	Feed		0,5 min		1 min		2 min		4 min	
(μm)	%Retained	%Passing	%Retained	%Passing	%Retained	%Passing	%Retained	%Passing	%Retained	%Passing
3350	0.00	100.00	0.00	100.00	0.00	100.00	0.00	100.00	0.00	100.00
2360	98.66	1.34	62.58	37.42	40.10	59.90	15.51	84.49	1.83	98.17
1700	1.34	0.00	15.56	21.87	20.78	39.12	17.52	66.97	7.23	90.94
1180	0.00	0.00	8.89	12.98	14.80	24.33	19.19	47.78	13.95	76.98
850	0.00	0.00	3.96	9.02	7.35	16.97	12.10	35.68	15.66	61.33
600	0.00	0.00	3.06	5.95	5.16	11.81	9.87	25.81	15.24	46.08
425	0.00	0.00	2.08	3.87	3.67	8.14	7.15	18.66	11.87	34.21
300	0.00	0.00	1.42	2.45	2.92	5.22	6.10	12.56	10.88	23.33
212	0.00	0.00	0.89	1.57	1.77	3.44	4.13	8.43	7.43	15.90
150	0.00	0.00	0.71	0.86	1.42	2.02	3.22	5.22	6.03	9.87
106	0.00	0.00	0.48	0.38	0.93	1.10	2.19	3.03	4.20	5.67
75	0.00	0.00	0.31	0.07	0.68	0.42	1.69	1.34	3.33	2.34
Pan	0.00		0.07		0.42		1.34		2.34	
Total	100.00		100.00		100.00		100.00		100.00	

Table A.22 Size analysis results for –425 + 300 microns quartz ground with a 50-50 mixture of balls and Eclipsoids.

Screen size	Particle Size distribution									
	Feed		0,5 min		1 min		2 min		4 min	
(μm)	%Retained	%Passing	%Retained	%Passing	%Retained	%Passing	%Retained	%Passing	%Retained	%Passing
425	0.00	100.00	0.00	100.00	0.00	100.00	0.00	100.00	0.00	100.00
300	99.02	0.98	92.11	7.89	86.85	13.15	80.43	19.57	69.14	30.86
212	0.98	0.00	5.08	2.81	8.49	4.66	9.77	9.80	12.86	18.00
150	0.00	0.00	1.42	1.40	1.97	2.69	4.13	5.67	6.77	11.23
106	0.00	0.00	0.86	0.53	1.25	1.44	2.73	2.94	4.56	6.67
75	0.00	0.00	0.38	0.15	0.86	0.57	1.61	1.32	3.17	3.50
Pan	0.00		0.15		0.57		1.32		3.50	
Total	100.00		100.00		100.00		100.00		100.00	

A.2.2 Particle size distributions obtained using a 50-50 mixture of balls and cubes

Table A.23 Size analysis results for –16000 + 13200 microns quartz ground with a 50-50 mixture of balls and cubes.

Screen size	Particle Size distribution									
	Feed		0,5 min		1 min		2 min		4 min	
(μm)	%Retained	%Passing	%Retained	%Passing	%Retained	%Passing	%Retained	%Passing	%Retained	%Passing
16000	0.00	100.00	0.00	100.00	0.00	100.00	0.00	100.00	0.00	100.00
13200	99.36	0.64	29.38	70.62	15.79	84.21	8.65	91.35	2.99	97.01
9500	0.64	0.00	32.41	38.21	24.24	59.97	14.66	76.69	6.13	90.89
6700	0.00	0.00	12.23	25.98	14.44	45.53	10.45	66.24	4.73	86.15
4750	0.00	0.00	6.07	19.92	8.23	37.30	8.29	57.96	3.31	82.85
3350	0.00	0.00	4.00	15.91	6.39	30.91	6.66	51.30	4.38	78.47
2360	0.00	0.00	3.61	12.30	5.87	25.04	7.23	44.07	5.50	72.97
1700	0.00	0.00	2.71	9.59	4.69	20.35	6.69	37.38	6.72	66.25
1180	0.00	0.00	2.68	6.92	5.22	15.13	6.95	30.43	9.52	56.73
850	0.00	0.00	1.86	5.05	3.69	11.44	6.34	24.08	9.39	47.34
600	0.00	0.00	1.51	3.55	3.31	8.13	6.32	17.76	10.14	37.20
425	0.00	0.00	1.09	2.45	2.31	5.81	4.66	13.10	8.56	28.64
300	0.00	0.00	0.91	1.54	2.08	3.73	4.26	8.84	8.43	20.20
212	0.00	0.00	0.55	0.99	1.30	2.43	2.84	6.00	6.29	13.91
150	0.00	0.00	0.41	0.58	0.96	1.47	2.26	3.74	5.06	8.85
106	0.00	0.00	0.32	0.26	0.72	0.75	1.60	2.14	3.85	5.00
75	0.00	0.00	0.16	0.10	0.51	0.24	1.18	0.97	2.89	2.11
Pan	0.00		0.10		0.24		0.97		2.11	
Total	100.00		100.00		100.00		100.00		100.00	

Table A.24 Size analysis results for –9500 + 6700 microns quartz ground with a 50-50 mixture of balls and cubes.

Screen size	Particle Size distribution									
	Feed		0,5 min		1 min		2 min		4 min	
(µm)	%Retained	%Passing	%Retained	%Passing	%Retained	%Passing	%Retained	%Passing	%Retained	%Passing
9500	0.00	100.00	0.00	100.00	0.00	100.00	0.00	100.00	0.00	100.00
6700	98.73	1.27	54.20	45.80	32.74	67.26	12.74	87.26	2.43	97.57
4750	1.27	0.00	15.79	30.01	17.74	49.52	12.77	74.50	2.50	95.07
3350	0.00	0.00	9.31	20.70	12.14	37.38	12.02	62.48	4.75	90.32
2360	0.00	0.00	6.26	14.44	9.64	27.75	11.86	50.63	7.28	83.03
1700	0.00	0.00	3.67	10.77	6.40	21.34	9.66	40.97	9.34	73.70
1180	0.00	0.00	3.27	7.50	5.56	15.78	10.55	30.41	20.11	53.59
850	0.00	0.00	2.03	5.47	3.89	11.89	7.35	23.06	12.40	41.19
600	0.00	0.00	1.67	3.80	3.21	8.68	6.37	16.68	10.37	30.82
425	0.00	0.00	1.12	2.68	2.42	6.26	4.63	12.05	8.43	22.39
300	0.00	0.00	0.93	1.75	2.14	4.11	3.99	8.07	7.42	14.97
212	0.00	0.00	0.71	1.04	1.53	2.58	2.69	5.38	4.46	10.51
150	0.00	0.00	0.44	0.60	1.04	1.54	2.10	3.28	4.03	6.48
106	0.00	0.00	0.31	0.30	0.77	0.77	1.47	1.81	2.95	3.53
75	0.00	0.00	0.22	0.08	0.53	0.24	1.10	0.71	2.03	1.50
Pan	0.00		0.08		0.24		0.71		1.50	
Total	100.00		100.00		100.00		100.00		100.00	

Table A.25 Size analysis results for –2360 + 1700 microns quartz ground with a 50-50 mixture of balls and cubes.

Screen size	Particle Size distribution									
	Feed		0,5 min		1 min		2 min		4 min	
(µm)	%Retained	%Passing	%Retained	%Passing	%Retained	%Passing	%Retained	%Passing	%Retained	%Passing
2360	0.00	100.00	0.00	100.00	0.00	100.00	0.00	100.00	0.00	100.00
1700	99.05	0.95	76.26	23.74	55.24	44.76	21.64	78.36	5.05	94.95
1180	0.95	0.00	11.71	12.04	20.12	24.64	32.31	46.05	22.59	72.36
850	0.00	0.00	4.66	7.38	9.17	15.47	16.10	29.95	18.75	53.61
600	0.00	0.00	2.65	4.73	5.51	9.96	9.91	20.03	16.38	37.23
425	0.00	0.00	1.53	3.19	3.11	6.85	6.10	13.94	10.92	26.31
300	0.00	0.00	1.15	2.04	2.43	4.42	4.76	9.18	8.65	17.66
212	0.00	0.00	0.68	1.36	1.41	3.01	2.87	6.30	5.95	11.71
150	0.00	0.00	0.55	0.82	1.15	1.86	2.16	4.14	4.13	7.58
106	0.00	0.00	0.33	0.49	0.74	1.12	1.45	2.69	3.06	4.52
75	0.00	0.00	0.24	0.25	0.41	0.70	0.97	1.72	2.01	2.50
Pan	0.00		0.25		0.70		1.72		2.50	
Total	100.00		100.00		100.00		100.00		100.00	

Table A.26 Size analysis results for –425 + 300 microns quartz ground with a 50-50 mixture of balls and cubes.

Screen size (µm)	Particle Size distribution									
	Feed		0,5 min		1 min		2 min		4 min	
	%Retained	%Passing	%Retained	%Passing	%Retained	%Passing	%Retained	%Passing	%Retained	%Passing
425	0.00	100.00	0.00	100.00	0.00	100.00	0.00	100.00	0.00	100.00
300	99.15	0.85	93.43	6.57	88.72	11.28	80.61	19.39	67.98	32.02
212	0.85	0.00	4.20	2.38	6.01	5.27	11.29	8.10	15.20	16.81
150	0.00	0.00	1.03	1.34	2.17	3.10	3.56	4.54	7.49	9.32
106	0.00	0.00	0.62	0.72	1.33	1.77	2.24	2.30	4.41	4.91
75	0.00	0.00	0.39	0.32	1.00	0.77	1.46	0.83	3.00	1.91
Pan	0.00		0.32		0.77		0.83		1.91	
Total	100.00		100.00		100.00		100.00		100.00	

A.2.3 Particle size distributions obtained using a 75-25 mixture of balls and cubes

Table A.27 Size analysis results for –16000 + 13200 microns quartz ground with a 75-25 mixture of balls and cubes.

Screen size (µm)	Particle Size distribution							
	Feed		0,5 min		1 min		4 min	
	% Retained	% Passing	% Retained	% Passing	% Retained	% Passing	% Retained	% Passing
16000	0.00	100.00	0.00	100.00	0.00	100.00	0.00	100.00
13200	99.10	0.90	28.68	71.32	16.34	83.66	3.44	96.56
9500	0.90	0.00	30.43	40.89	24.46	59.20	5.15	91.40
6700	0.00	0.00	11.75	29.14	13.06	46.13	3.21	88.19
4750	0.00	0.00	7.41	21.74	8.43	37.70	2.91	85.28
3350	0.00	0.00	5.13	16.61	6.91	30.79	3.43	81.85
2360	0.00	0.00	3.65	12.96	6.02	24.77	5.09	76.76
1700	0.00	0.00	2.86	10.10	4.64	20.13	6.36	70.40
1180	0.00	0.00	2.74	7.36	5.07	15.06	11.07	59.33
850	0.00	0.00	1.84	5.53	3.64	11.42	10.45	48.88
600	0.00	0.00	1.65	3.88	3.24	8.18	11.66	37.22
425	0.00	0.00	1.11	2.77	2.36	5.82	9.06	28.16
300	0.00	0.00	0.95	1.82	2.02	3.80	8.38	19.78
212	0.00	0.00	0.65	1.18	1.48	2.32	6.53	13.24
150	0.00	0.00	0.60	0.58	1.06	1.26	4.89	8.36
106	0.00	0.00	0.33	0.24	0.70	0.56	3.53	4.83
75	0.00	0.00	0.21	0.03	0.39	0.17	2.36	2.47
Pan	0.00		0.03		0.17		2.47	
Total	100.00		100.00		100.00		100.00	

Table A.28 Size analysis results for –3350 + 2360 microns quartz ground with a 75-25 mixture of balls and cubes.

Screen size (µm)	Particle Size distribution							
	Feed		0,5 min		1 min		4 min	
	% Retained	% Passing	% Retained	% Passing	% Retained	% Passing	% Retained	% Passing
3350	0.00	100.00	0.00	100.00	0.00	100.00	0.00	100.00
2360	99.02	0.98	66.34	33.66	44.02	55.98	2.28	97.72
1700	0.98	0.00	14.08	19.58	19.32	36.66	7.36	90.36
1180	0.00	0.00	9.47	10.11	13.36	23.30	16.94	73.42
850	0.00	0.00	3.22	6.89	6.62	16.68	15.76	57.66
600	0.00	0.00	1.92	4.96	5.34	11.34	14.89	42.78
425	0.00	0.00	1.56	3.40	3.54	7.80	11.03	31.75
300	0.00	0.00	1.34	2.06	2.64	5.16	9.80	21.95
212	0.00	0.00	0.66	1.40	1.84	3.31	7.32	14.63
150	0.00	0.00	0.53	0.87	1.39	1.92	5.50	9.14
106	0.00	0.00	0.41	0.46	0.90	1.02	3.97	5.16
75	0.00	0.00	0.28	0.18	0.53	0.49	2.63	2.53
Pan	0.00		0.18		0.49		2.53	
Total	100.00		100.00		100.00		100.00	

Table A.29 Size analysis results for –425 + 300 microns quartz ground with a 75-25 mixture of balls and cubes.

Screen size (µm)	Particle Size distribution							
	Feed		0,5 min		1 min		4 min	
	% Retained	% Passing	% Retained	% Passing	% Retained	% Passing	% Retained	% Passing
600	0.00	100.00	0.00	100.00	0.00	100.00	0.00	100.00
425	99.54	0.46	87.99	12.01	82.43	17.57	55.25	44.75
300	0.46	0.00	7.83	4.18	8.97	8.60	19.12	25.63
212	0.00	0.00	1.35	2.83	2.65	5.95	9.43	16.21
150	0.00	0.00	0.88	1.95	1.82	4.13	5.82	10.38
106	0.00	0.00	0.62	1.33	1.21	2.92	3.92	6.46
75	0.00	0.00	0.49	0.84	0.78	2.14	2.56	3.90
Pan	0.00		0.84		2.14		3.90	
Total	100.00		100.00		100.00		100.00	

B Selection functions for all batch grinding tests

B.1. Weight percentage remaining in the top size $w_i(t)$

Table B.1 Weight percentage remaining in the top size $w_i(t)$ for balls.

Grinding time (min)	-425+300	-850+600	-1700+1180	-2360+1700	-3350+2360	-4750+3350	-13200+9500
0	0.9836	0.9930	0.9896	0.9661	0.9847	0.9405	0.9611
0.5	0.8957	0.8927	0.7818	0.6487	0.6214	0.4902	0.4346
1	0.8550	0.8132	0.6735	0.4633	0.3899	0.2230	0.2437
2	0.7579	0.6520	0.4132	0.2189	0.1435	0.0610	0.0997
4	0.6317	0.4226	0.1415	0.0417	0.0158	0.0030	0.0190
First order equation	$0.958e^{-0.107x}$	$0.997e^{-0.214x}$	$1.033e^{-0.487x}$	$0.988e^{-0.783x}$	$1.052e^{-1.037x}$	$0.979e^{-1.437x}$	$0.747e^{-0.946x}$
R^2=	0.987	0.999	0.995	0.998	0.998	0.999	0.986

Table B.2 Weight percentage remaining in the top size $w_i(t)$ for Eclipsoids.

Grinding time (min)	-425+300	-850+600	-1700+1180	-2360+1700	-3350+2360	-4750+3350	-13200+9500
0	0.9741	0.9489	0.9873	0.9421	0.9530	0.9457	0.9769
0.5	0.9031	0.8761	0.8191	0.6458	0.5716	0.4765	0.4123
1	0.8286	0.8051	0.6903	0.4533	0.3463	0.2614	0.2282
2	0.7820	0.6426	0.4413	0.2206	0.1188	0.0756	0.0905
4	0.6577	0.4025	0.1536	0.0615	0.0124	0.0043	0.0164
First order equation	$0.945e^{-0.094x}$	$0.976e^{-0.218x}$	$1.049e^{-0.469x}$	$0.907e^{-0.681x}$	$0.994e^{-1.088x}$	$0.978e^{-1.342x}$	$0.735e^{-0.982x}$
R^2=	0.972	0.995	0.993	0.998	0.999	0.998	0.984

Table B.3 Weight percentage remaining in the top size $w_i(t)$ for cubes.

Grinding time (min)	-600+425	-1700+1180	-4750+3350	-13200+9500
0	0.9937	0.9888	0.9876	0.9921
0.5	0.9214	0.8851	0.5960	0.5769
1	0.8825	0.7587	0.3805	0.3614
2	0.8109	0.5859	0.1627	0.1878
4	0.7157	0.3443	0.0211	0.0692
First order equation	$0.967e^{-0.079x}$	$0.996e^{-0.266x}$	$0.996e^{-0.953x}$	$0.804e^{-0.644x}$
R^2=	0.976	0.999	0.998	0.973

Table B.4 Weight percentage remaining in the top size $w_i(t)$ for a 50-50 mixture of balls and Eclipsoids.

Grinding time (min)	-425+300	-3350+2360	-6700+4750	-16000+13200
0	0.9902	0.9866	0.9875	0.9858
0.5	0.9211	0.6258	0.3247	0.2587
1	0.8685	0.4010	0.1572	0.1611
2	0.8043	0.1551	0.0362	0.0687
4	0.6914	0.0183	0.0013	0.0153
First order equation	$0.966e^{-0.086x}$	$1.047e^{-0.999x}$	$0.852e^{-1.620x}$	$0.557e^{-0.950x}$
R^2=	0.983	0.998	0.997	0.940

Table B.5 Weight percentage remaining in the top size $w_i(t)$ for a 50-50 mixture of balls and cubes.

Grinding time (min)	-425+300	-2360+1700	-9500+6700	-16000+13200
0	0.9915	0.9905	0.9873	0.9936
0.5	0.9343	0.7626	0.5420	0.2938
1	0.8872	0.5524	0.3274	0.1579
2	0.8061	0.2164	0.1274	0.0865
4	0.6798	0.0505	0.0243	0.0299
First order equation	$0.980e^{-0.093x}$	$1.071e^{-0.76x}$	$0.874e^{-0.913x}$	$0.532e^{-0.784x}$
R^2=	0.996	0.996	0.995	0.892

Table B.6 Weight percentage remaining in the top size $w_i(t)$ for a 75-25 mixture of balls and cubes.

Grinding time (min)	-600+425	-3350+2360	-16000+13200
0	0.9954	0.9902	0.9910
0.5	0.8799	0.6634	0.2868
1	0.8243	0.4402	0.1634
4	0.5525	0.0228	0.0344
First order equation	$0.965e^{-0.141x}$	$1.058e^{-0.954x}$	$0.545e^{-0.729x}$
R^2=	0.991	0.999	0.883

B.2 Variation of the specific rate of breakage with size

B.2.1 Variation of the specific rate of breakage for balls, cubes and Eclipsoids.

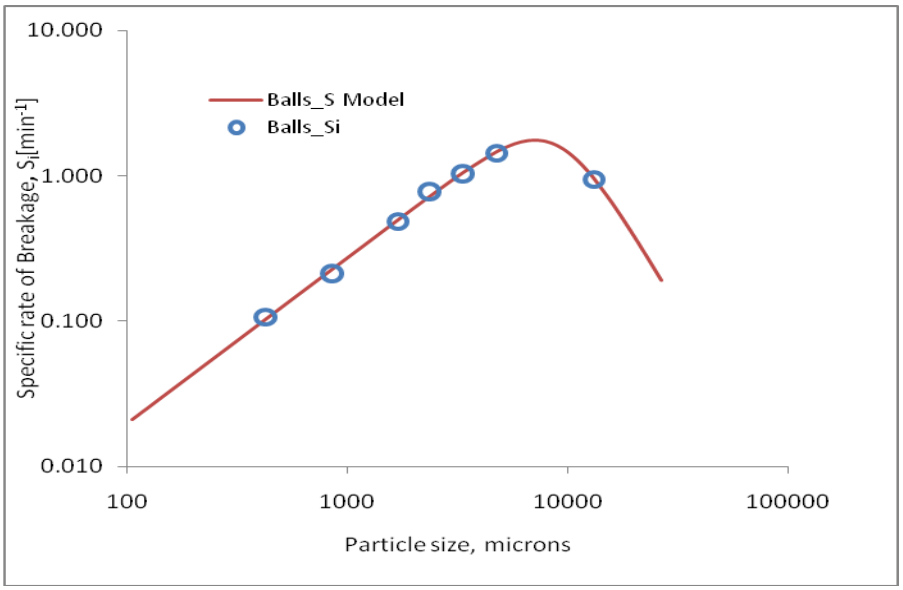

Figure B.1 Variation of the specific rate of breakage with size for balls.

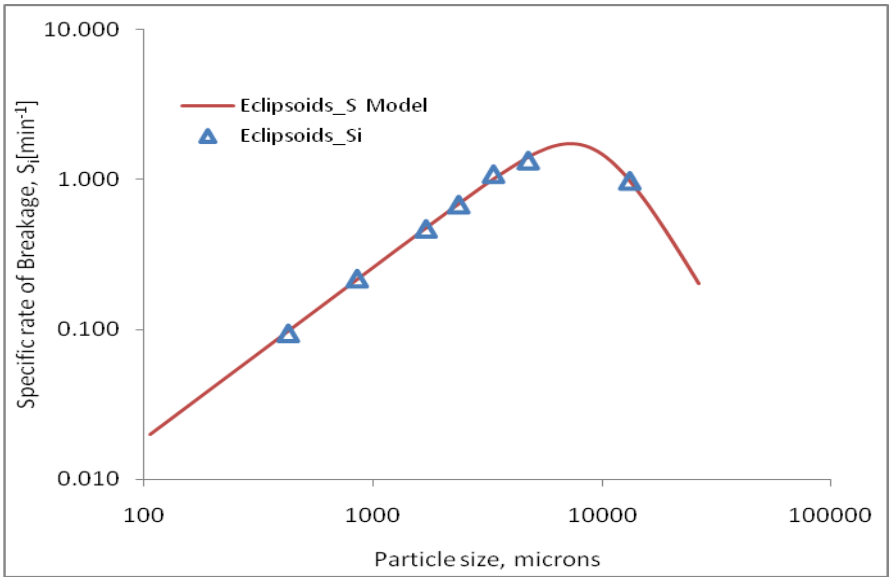

Figure B.2 Variation of the specific rate of breakage with size for Eclipsoids.

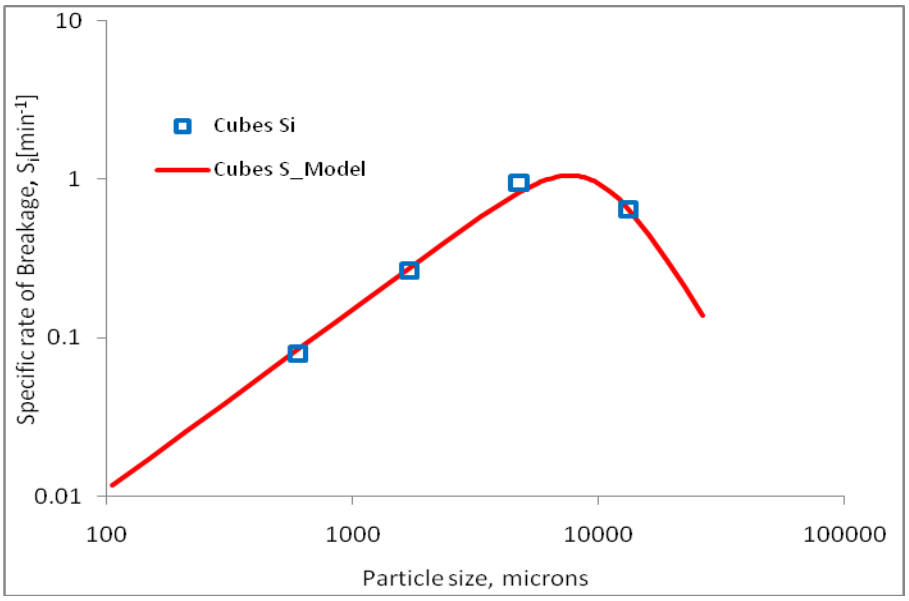

Figure B.3 Variation of the specific rate of breakage with size for cubes.

B.2.2 Variation of the specific rate of breakage for the different mixtures of grinding media shapes used

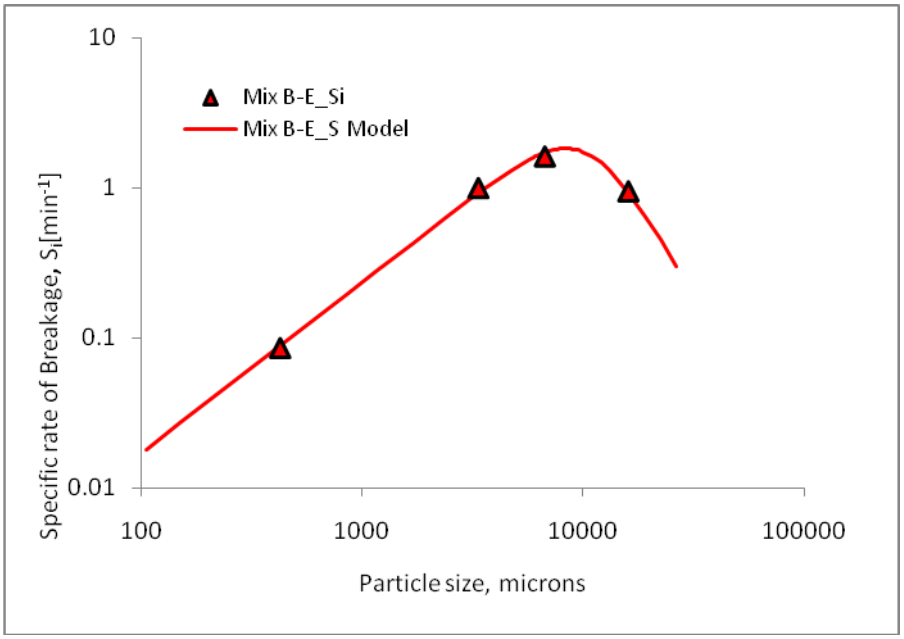

Figure B.4 Variation of the specific rate of breakage with size for a 50-50 mixture of balls and Eclipsoids.

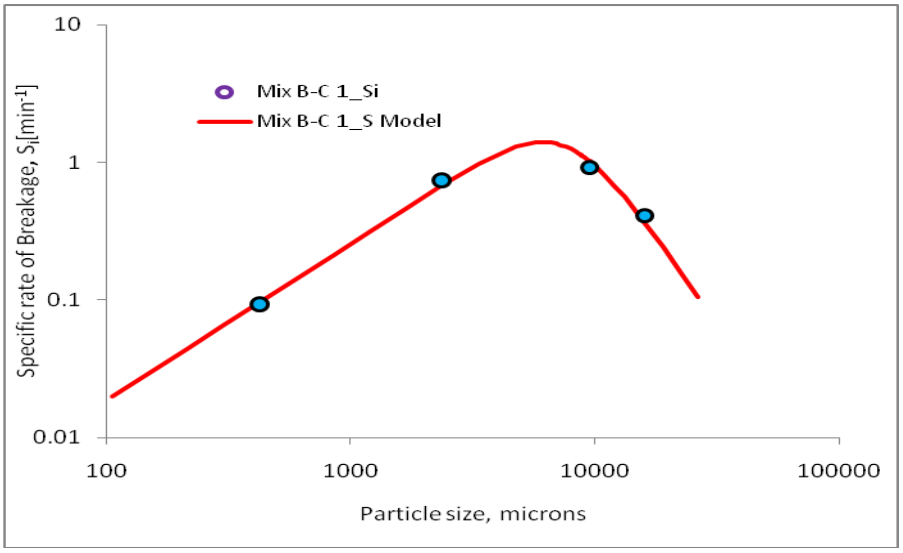

Figure B.5 Variation of the specific rate of breakage with size for a 50-50 mixture of balls and cubes.

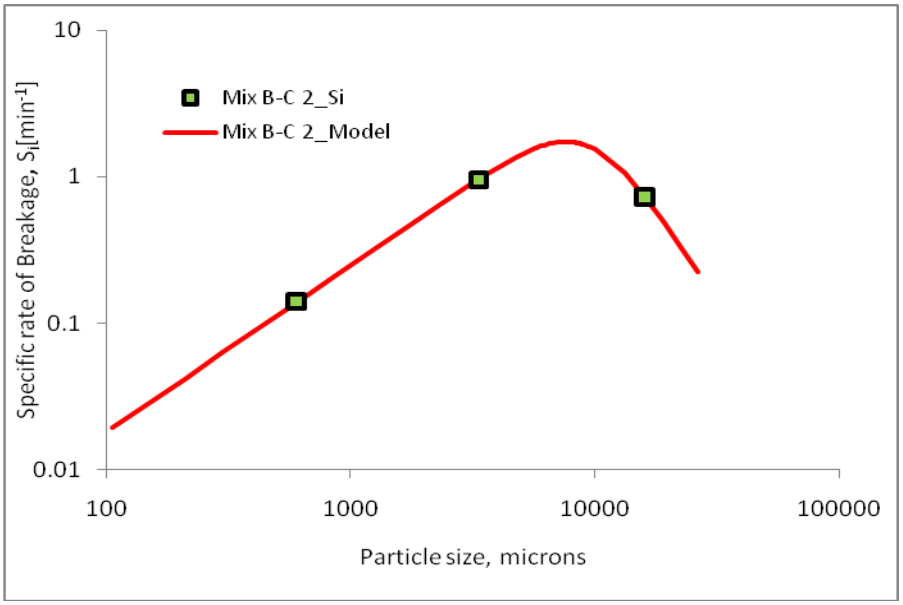

Figure B.6 Variation of the specific rate of breakage with size for a 75-25 mixture of balls and cubes.

B.2.3 Comparison of the different variations of the specific rate of breakage

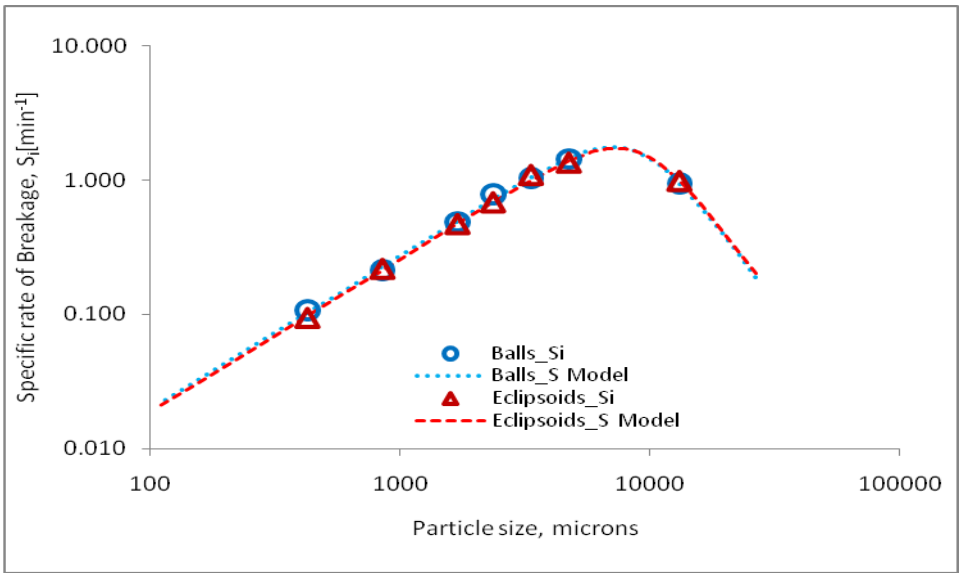

Figure B.7 Variation of the specific rate of breakage with size for balls and Eclipsoids.

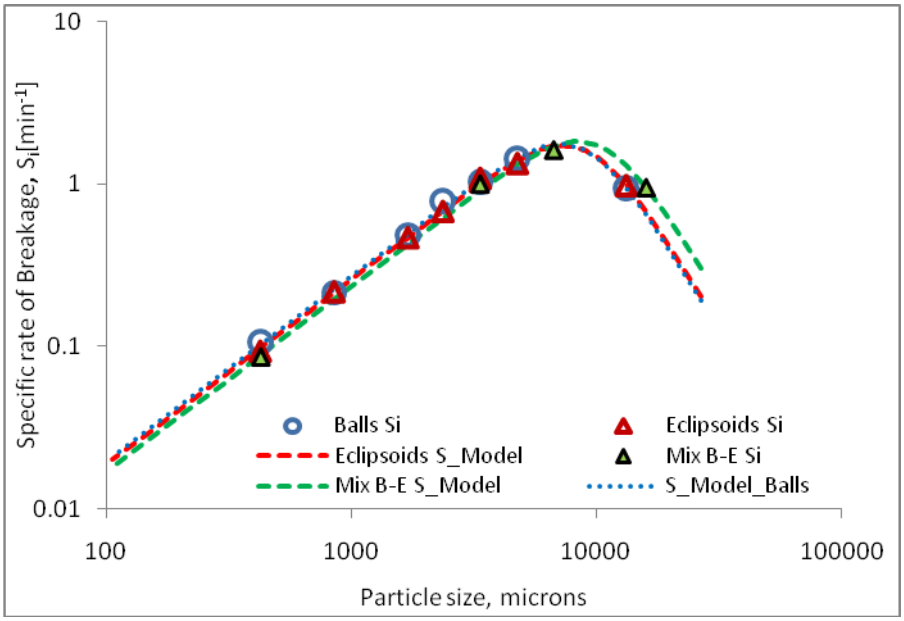

Figure B.8 Variation of the specific rate of breakage with size for balls, Eclipsoids and a 50-50 mixture of balls and Eclipsoids.

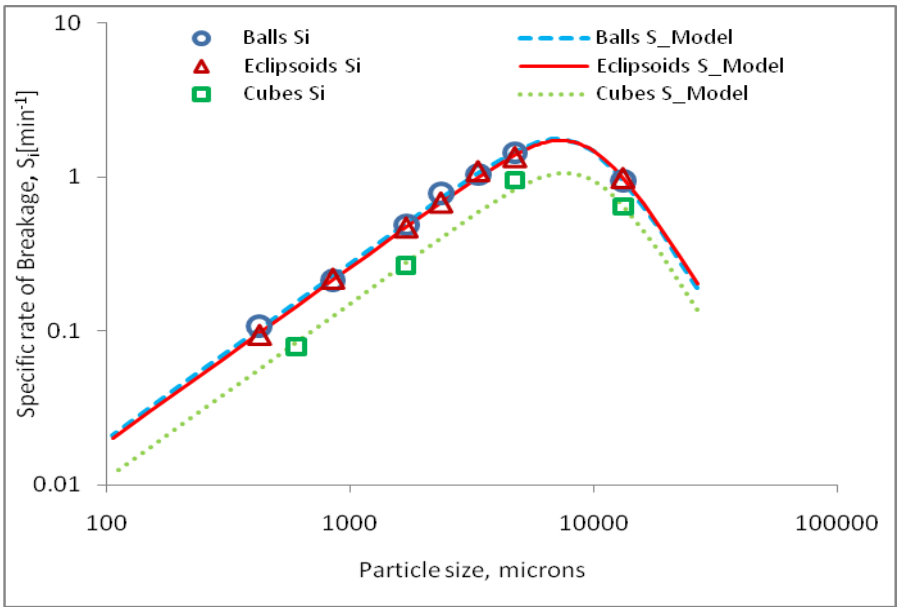

Figure B.9 Variation of the specific rate of breakage with size for the three shapes used: balls, Eclipsoids and cubes as grinding media shapes.

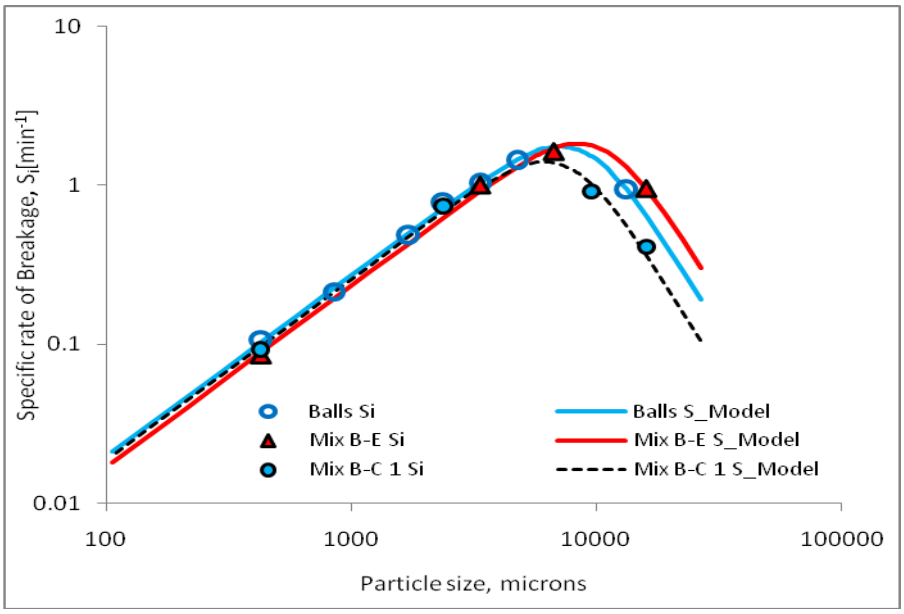

Figure B.10 Variation of the specific rate of breakage with size for balls, a 50-50 mixture of balls and Eclipsoids and a 50-50 mixture of balls and cubes.

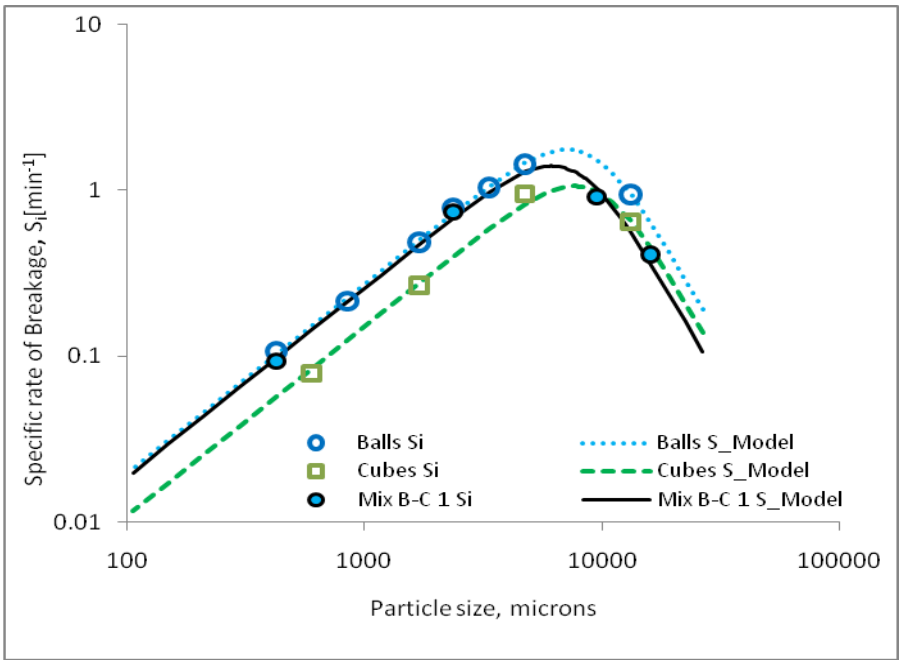

Figure B.11 Variation of the specific rate of breakage with size for balls, cubes and a 50-50 mixture of balls and cubes.

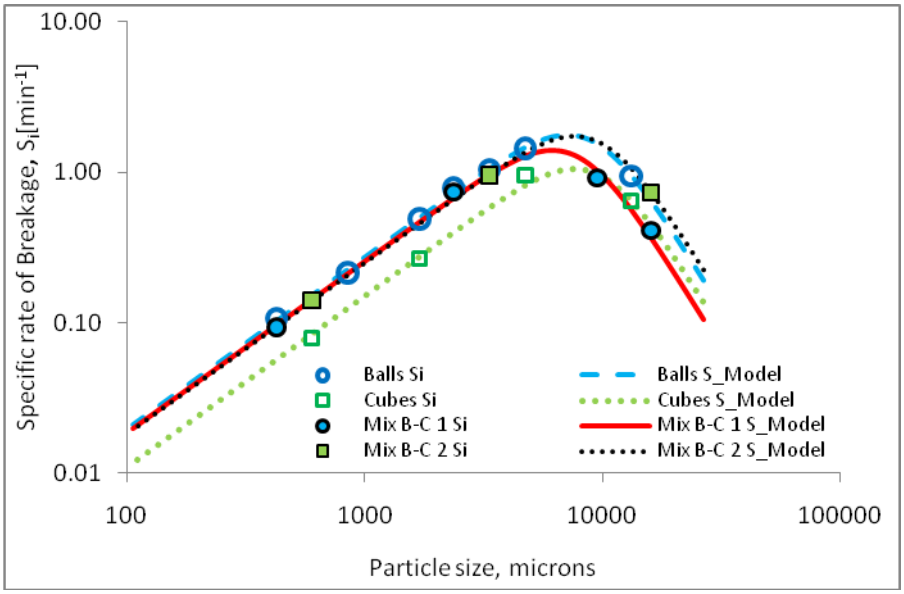

Figure B.12 Variation of the specific rate of breakage with size for balls, cubes, a 50-50 mixture and a 75-25 mixture of balls and cubes.

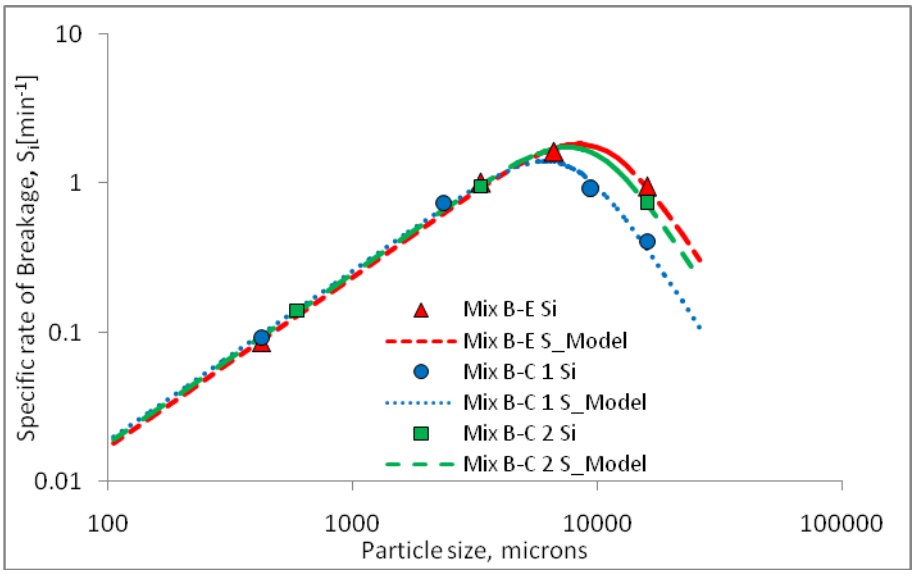

Figure B.13 Variation of the specific rate of breakage with size for the different mixtures used.

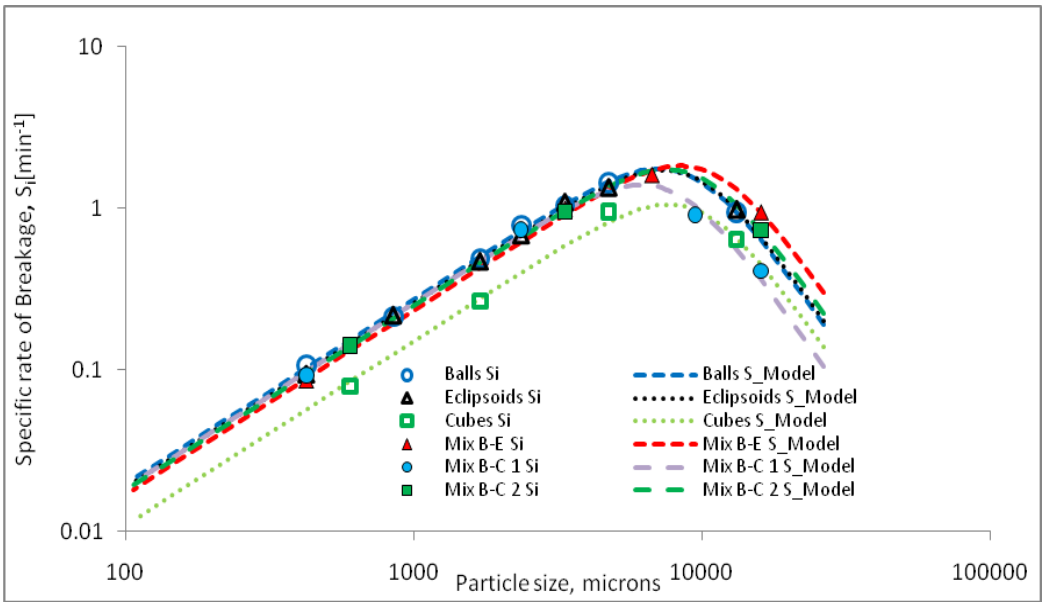

Figure B.14 Variation of the specific rate of breakage with size for all the grinding media shapes.

C Breakage function tables and curves

This section presents the tables and graphs of the reduced breakage functions plotted. The B-II method (Austin *et al.*, 1984) was used to get estimates of the different values of B_{ij} corresponding first to the tests carried out with different grinding media shapes, then with the mixtures of grinding media of different shapes. These calculations were done using short grinding times, i.e. 0.5 min.

C.1 Breakage function obtained for the different grinding media shapes

C.1.1 Breakage function obtained for balls

Table C.1 Breakage function for –13200 + 9500 microns quartz ground with balls.

13200 microns		Feed		Product		Bij
		%Retained	%Passing	%Retained	%Passing	
16000	13200	0.00	100.00	0.00	100.00	
13200	9500	96.11	3.89	43.46	56.54	1.000000
9500	6700	3.89	0.00	19.11	37.43	0.590842
6700	4750	0.00	0.00	8.71	28.72	0.426605
4750	3350	0.00	0.00	6.93	21.78	0.309620
3350	2360	0.00	0.00	5.13	16.66	0.229596
2360	1700	0.00	0.00	3.80	12.85	0.173383
1700	1180	0.00	0.00	3.91	8.94	0.118042
1180	850	0.00	0.00	2.44	6.50	0.084705
850	600	0.00	0.00	1.92	4.58	0.059031
600	425	0.00	0.00	1.34	3.23	0.041437
425	300	0.00	0.00	1.11	2.12	0.027012
300	212	0.00	0.00	0.72	1.40	0.017826
212	150	0.00	0.00	0.50	0.91	0.011498
150	106	0.00	0.00	0.36	0.55	0.006989
106	75	0.00	0.00	0.23	0.32	0.004016
75	0	0.00		0.32		

Normalized Breakage function	
Size	Bij
1.000000	1.000000
0.719697	0.590842
0.507576	0.426605
0.359848	0.309620
0.253788	0.229596
0.178788	0.173383
0.128788	0.118042
0.089394	0.084705
0.064394	0.059031
0.045455	0.041437
0.032197	0.027012
0.022727	0.017826
0.016061	0.011498
0.011364	0.006989
0.008030	0.004016

Table C.2 Breakage function for –4750 + 3350 microns quartz ground with balls.

4750 microns		Feed		Product		Bij
		%Retained	%Passing	%Retained	%Passing	
6700	4750	0.00	100.00	0.00	100.00	
4750	3350	94.05	5.95	49.02	50.98	1.000000
3350	2360	5.95	0.00	21.67	29.30	0.532276
2360	1700	0.00	0.00	9.70	19.60	0.334906
1700	1180	0.00	0.00	7.37	12.24	0.200359
1180	850	0.00	0.00	3.59	8.64	0.138751
850	600	0.00	0.00	2.47	6.17	0.097781
600	425	0.00	0.00	1.66	4.51	0.070865
425	300	0.00	0.00	1.38	3.14	0.048896
300	212	0.00	0.00	0.89	2.25	0.034897
212	150	0.00	0.00	0.67	1.58	0.024432
150	106	0.00	0.00	0.45	1.13	0.017495
106	75	0.00	0.00	0.28	0.85	0.013127
75	0	0.00		0.85		

Normalized Breakage function	
Size	Bij
1.000000	1.000000
0.705263	0.532276
0.496842	0.334906
0.357895	0.200359
0.248421	0.138751
0.178947	0.097781
0.126316	0.070865
0.089474	0.048896
0.063158	0.034897
0.044632	0.024432
0.031579	0.017495
0.022316	0.013127

Table C.3 Breakage function for –3350 + 2360 microns quartz ground with balls.

3350 microns		Feed		Product		Bij
		%Retained	%Passing	%Retained	%Passing	
4750	3350	0.00	100.00	0.00	100.00	
3350	2360	98.47	1.53	62.14	37.86	1.000000
2360	1700	1.53	0.00	14.93	22.93	0.565846
1700	1180	0.00	0.00	7.95	14.98	0.352639
1180	850	0.00	0.00	4.23	10.75	0.247157
850	600	0.00	0.00	3.08	7.67	0.173478
600	425	0.00	0.00	2.00	5.67	0.126874
425	300	0.00	0.00	1.66	4.01	0.088962
300	212	0.00	0.00	1.11	2.90	0.064051
212	150	0.00	0.00	0.78	2.13	0.046744
150	106	0.00	0.00	0.48	1.64	0.036013
106	75	0.00	0.00	0.26	1.39	0.030363
75	0	0.00		1.39		

Normalized Breakage function	
Size	Bij
1.000000	1.000000
0.704478	0.565846
0.507463	0.352639
0.352239	0.247157
0.253731	0.173478
0.179104	0.126874
0.126866	0.088962
0.089552	0.064051
0.063284	0.046744
0.044776	0.036013
0.031642	0.030363

Table C.4 Breakage function for –2360 + 1700 microns quartz ground with balls.

2360 microns		Feed		Product		Bij
		%Retained	%Passing	%Retained	%Passing	
3350	2360	0.00	100.00	0.00	100.00	
2360	1700	96.61	3.39	64.87	35.13	1.000000
1700	1180	3.39	0.00	19.87	15.26	0.415682
1180	850	0.00	0.00	5.46	9.81	0.259045
850	600	0.00	0.00	3.40	6.40	0.166058
600	425	0.00	0.00	2.02	4.38	0.112381
425	300	0.00	0.00	1.50	2.88	0.073324
300	212	0.00	0.00	1.05	1.83	0.046248
212	150	0.00	0.00	0.68	1.15	0.028956
150	106	0.00	0.00	0.41	0.73	0.018486
106	75	0.00	0.00	0.21	0.52	0.013187
75	0	0.00		0.52		

Normalized Breakage function	
Size	Bij
1.000000	1.000000
0.720339	0.415682
0.500000	0.259045
0.360169	0.166058
0.254237	0.112381
0.180085	0.073324
0.127119	0.046248
0.089831	0.028956
0.063559	0.018486
0.044915	0.013187

Table C.5 Breakage function for –1700 + 1180 microns quartz ground with balls.

1700 microns		Feed		Product		Bij
		%Retained	%Passing	%Retained	%Passing	
2360	1700	0.00	100.00	0.00	100.00	
1700	1180	98.96	1.04	78.18	21.82	1.000000
1180	850	1.04	0.00	7.52	14.30	0.654472
850	600	0.00	0.00	5.33	8.97	0.398651
600	425	0.00	0.00	2.48	6.49	0.284760
425	300	0.00	0.00	2.02	4.47	0.193891
300	212	0.00	0.00	1.39	3.08	0.132559
212	150	0.00	0.00	1.01	2.07	0.088727
150	106	0.00	0.00	0.58	1.49	0.063813
106	75	0.00	0.00	0.26	1.23	0.052625
75	0	0.00		1.23		

Normalized Breakage function	
Size	Bij
1.000000	1.000000
0.694118	0.654472
0.500000	0.398651
0.352941	0.284760
0.250000	0.193891
0.176471	0.132559
0.124706	0.088727
0.088235	0.063813
0.062353	0.052625

Table C.6 Breakage function for –850 + 600 microns quartz ground with balls.

850 microns		Feed		Product		Bij
		%Retained	%Passing	%Retained	%Passing	
1180	850	0.00	100.00	0.00	100.00	
850	600	99.30	0.70	89.27	10.73	1.000000
600	425	0.70	0.00	4.18	6.55	0.636167
425	300	0.00	0.00	2.25	4.30	0.412934
300	212	0.00	0.00	1.09	3.21	0.306250
212	150	0.00	0.00	0.96	2.25	0.213518
150	106	0.00	0.00	0.76	1.49	0.141155
106	75	0.00	0.00	0.51	0.98	0.092575
75	0	0.00		0.98		

Normalized Breakage function	
Size	Bij
1.000000	1.000000
0.705882	0.636167
0.500000	0.412934
0.352941	0.306250
0.249412	0.213518
0.176471	0.141155
0.124706	0.092575

Table C.7 Breakage function for –425 + 300 microns quartz ground with balls.

425 microns		Feed		Product		Bij
		%Retained	%Passing	%Retained	%Passing	
600	425	0.00	100.00	0.00	100.00	
425	300	98.36	1.64	89.57	10.43	1.000000
300	212	1.64	0.00	7.02	3.41	0.370727
212	150	0.00	0.00	0.92	2.49	0.269543
150	106	0.00	0.00	0.62	1.87	0.201737
106	75	0.00	0.00	0.39	1.47	0.158810
75	0	0.00		1.47		

Normalized Breakage function	
Size	Bij
1.000000	1.000000
0.705882	0.370727
0.498824	0.269543
0.352941	0.201737
0.249412	0.158810

C.1.2 Breakage function obtained for Eclipsoids

Table C.8 Breakage function for –13200 + 9500 microns quartz ground with Eclipsoids.

13200 microns		Feed		Product		Bij
		%Retained	%Passing	%Retained	%Passing	
16000	13200	0.00	100.00	0.00	100.00	
13200	9500	97.69	2.31	41.23	58.77	1.000000
9500	6700	2.31	0.00	19.46	39.31	0.578873
6700	4750	0.00	0.00	10.13	29.18	0.399990
4750	3350	0.00	0.00	6.71	22.47	0.295064
3350	2360	0.00	0.00	5.35	17.13	0.217733
2360	1700	0.00	0.00	3.89	13.24	0.164568
1700	1180	0.00	0.00	3.84	9.40	0.114419
1180	850	0.00	0.00	2.35	7.05	0.084789
850	600	0.00	0.00	1.94	5.11	0.060798
600	425	0.00	0.00	1.31	3.80	0.044885
425	300	0.00	0.00	1.12	2.68	0.031507
300	212	0.00	0.00	0.74	1.94	0.022753
212	150	0.00	0.00	0.52	1.42	0.016593
150	106	0.00	0.00	0.37	1.05	0.012193
106	75	0.00	0.00	0.26	0.79	0.009168
75	0	0.00		0.79		

Normalized Breakage function	
Size	Bij
1.000000	1.000000
0.719697	0.578873
0.507576	0.399990
0.359848	0.295064
0.253788	0.217733
0.178788	0.164568
0.128788	0.114419
0.089394	0.084789
0.064394	0.060798
0.045455	0.044885
0.032197	0.031507
0.022727	0.022753
0.016061	0.016593
0.011364	0.012193
0.008030	0.009168

Table C.9 Breakage function for –4750 + 3350 microns quartz ground with Eclipsoids.

4750 microns		Feed		Product		Bij
		%Retained	%Passing	%Retained	%Passing	
6700	4750	0.00	100.00	0.00	100.00	
4750	3350	94.57	5.43	47.65	52.35	1.000000
3350	2360	5.43	0.00	24.11	28.24	0.484134
2360	1700	0.00	0.00	9.96	18.29	0.294568
1700	1180	0.00	0.00	7.18	11.11	0.171708
1180	850	0.00	0.00	3.37	7.74	0.117469
850	600	0.00	0.00	2.31	5.43	0.081411
600	425	0.00	0.00	1.47	3.96	0.058863
425	300	0.00	0.00	1.20	2.76	0.040791
300	212	0.00	0.00	0.79	1.97	0.029003
212	150	0.00	0.00	0.56	1.41	0.020695
150	106	0.00	0.00	0.40	1.01	0.014786
106	75	0.00	0.00	0.28	0.73	0.010702
75	0	0.00		0.73		

Normalized Breakage function	
Size	Bij
1.000000	1.000000
0.705263	0.484134
0.496842	0.294568
0.357895	0.171708
0.248421	0.117469
0.178947	0.081411
0.126316	0.058863
0.089474	0.040791
0.063158	0.029003
0.044632	0.020695
0.031579	0.014786
0.022316	0.010702

Table C.10 Breakage function for –3350 + 2360 microns quartz ground with Eclipsoids.

3350 microns		Feed		Product		Bij
		%Retained	%Passing	%Retained	%Passing	
4750	3350	0.00	100.00	0.00	100.00	
3350	2360	95.30	4.70	57.16	42.84	1.000000
2360	1700	4.70	0.00	20.06	22.78	0.505721
1700	1180	0.00	0.00	10.15	12.63	0.264064
1180	850	0.00	0.00	4.14	8.48	0.173434
850	600	0.00	0.00	2.61	5.88	0.118472
600	425	0.00	0.00	1.69	4.19	0.083687
425	300	0.00	0.00	1.31	2.88	0.057148
300	212	0.00	0.00	0.83	2.05	0.040544
212	150	0.00	0.00	0.55	1.50	0.029616
150	106	0.00	0.00	0.40	1.10	0.021662
106	75	0.00	0.00	0.28	0.82	0.016109
75	0	0.00		0.82		

Normalized Breakage function	
Size	Bij
1.000000	1.000000
0.704478	0.505721
0.507463	0.264064
0.352239	0.173434
0.253731	0.118472
0.179104	0.083687
0.126866	0.057148
0.089552	0.040544
0.063284	0.029616
0.044776	0.021662
0.031642	0.016109

Table C.11 Breakage function for –2360 + 1700 microns quartz ground with Eclipsoids.

2360 microns		Feed		Product		Bij
		%Retained	%Passing	%Retained	%Passing	
3350	2360	0.00	100.00	0.00	100.00	
2360	1700	94.21	5.79	64.58	35.42	1.000000
1700	1180	5.79	0.00	18.77	16.65	0.482207
1180	850	0.00	0.00	6.50	10.16	0.283533
850	600	0.00	0.00	3.43	6.73	0.184363
600	425	0.00	0.00	2.05	4.67	0.126678
425	300	0.00	0.00	1.46	3.21	0.086506
300	212	0.00	0.00	0.96	2.26	0.060428
212	150	0.00	0.00	0.64	1.61	0.043083
150	106	0.00	0.00	0.36	1.25	0.033300
106	75	0.00	0.00	0.24	1.01	0.026786
75	0	0.00		1.01		

Normalized Breakage function	
Size	Bij
1.000000	1.000000
0.720339	0.482207
0.500000	0.283533
0.360169	0.184363
0.254237	0.126678
0.180085	0.086506
0.127119	0.060428
0.089831	0.043083
0.063559	0.033300
0.044915	0.026786

Table C.12 Breakage function for –1700 + 1180 microns quartz ground with Eclipsoids.

1700 microns		Feed		Product		Bij
		%Retained	%Passing	%Retained	%Passing	
2360	1700	0.00	100.00	0.00	100.00	
1700	1180	98.73	1.27	81.91	18.09	1.000000
1180	850	1.27	0.00	7.47	10.62	0.601336
850	600	0.00	0.00	3.85	6.78	0.375777
600	425	0.00	0.00	2.10	4.67	0.256310
425	300	0.00	0.00	1.58	3.09	0.168133
300	212	0.00	0.00	0.91	2.18	0.117892
212	150	0.00	0.00	0.88	1.30	0.069847
150	106	0.00	0.00	0.45	0.85	0.045698
106	75	0.00	0.00	0.29	0.56	0.030232
75	0	0.00		0.56		

Normalized Breakage function	
Size	Bij
1.000000	1.000000
0.694118	0.601336
0.500000	0.375777
0.352941	0.256310
0.250000	0.168133
0.176471	0.117892
0.124706	0.069847
0.088235	0.045698
0.062353	0.030232

Table C.13 Breakage function for –850 + 600 microns quartz ground with Eclipsoids.

850 microns		Feed		Product		Bij
		%Retained	%Passing	%Retained	%Passing	
1180	850	0.00	100.00	0.00	100.00	
850	600	94.89	5.11	87.61	12.39	1.000000
600	425	5.11	0.00	4.55	7.85	1.022562
425	300	0.00	0.00	2.67	5.18	0.665658
300	212	0.00	0.00	1.51	3.67	0.467915
212	150	0.00	0.00	1.00	2.67	0.339247
150	106	0.00	0.00	0.73	1.95	0.246299
106	75	0.00	0.00	0.52	1.43	0.179715
75	0	0.00		1.43		

Normalized Breakage function	
Size	Bij
1.000000	1.000000
0.705882	1.022562
0.500000	0.665658
0.352941	0.467915
0.249412	0.339247
0.176471	0.246299
0.124706	0.179715

Table C.14 Breakage function for –425 + 300 microns quartz ground with Eclipsoids.

425 microns		Feed		Product		Bij
		%Retained	%Passing	%Retained	%Passing	
600	425	0.00	100.00	0.00	100.00	
425	300	97.41	2.59	90.31	9.69	1.000000
300	212	2.59	0.00	6.82	2.87	0.385332
212	150	0.00	0.00	0.90	1.97	0.263166
150	106	0.00	0.00	0.48	1.49	0.198756
106	75	0.00	0.00	0.30	1.20	0.159192
75	0	0.00		1.20		

Normalized Breakage function	
Size	Bij
1.000000	1.000000
0.705882	0.385332
0.498824	0.263166
0.352941	0.198756
0.249412	0.159192

C.1.3 Breakage function obtained for cubes

Table C.15 Breakage function for –13200 + 9500 microns quartz ground with cubes.

13200 microns		Feed		Product		Bij
		%Retained	%Passing	%Retained	%Passing	
16000	13200	0.00	100.00	0.00	100.00	
13200	9500	99.21	0.79	57.69	42.31	1.000000
9500	6700	0.79	0.00	17.50	24.81	0.525975
6700	4750	0.00	0.00	7.96	16.85	0.340304
4750	3350	0.00	0.00	4.53	12.32	0.242559
3350	2360	0.00	0.00	3.33	8.99	0.173737
2360	1700	0.00	0.00	2.21	6.78	0.129569
1700	1180	0.00	0.00	2.11	4.67	0.088247
1180	850	0.00	0.00	1.22	3.46	0.064885
850	600	0.00	0.00	1.01	2.45	0.045747
600	425	0.00	0.00	0.70	1.75	0.032528
425	300	0.00	0.00	0.59	1.16	0.021550
300	212	0.00	0.00	0.36	0.80	0.014810
212	150	0.00	0.00	0.30	0.50	0.009208
150	106	0.00	0.00	0.23	0.26	0.004871
106	75	0.00	0.00	0.16	0.10	0.001875
75	0	0.00		0.10		

Normalized Breakage function	
Size	Bij
1.000000	1.000000
0.719697	0.525975
0.507576	0.340304
0.359848	0.242559
0.253788	0.173737
0.178788	0.129569
0.128788	0.088247
0.089394	0.064885
0.064394	0.045747
0.045455	0.032528
0.032197	0.021550
0.022727	0.014810
0.016061	0.009208
0.011364	0.004871
0.008030	0.001875

Table C.16 Breakage function for –4750 + 3550 microns quartz ground with cubes.

4750 microns		Feed		Product		Bij
		%Retained	%Passing	%Retained	%Passing	
6700	4750	0.00	100.00	0.00	100.00	
4750	3350	98.76	1.24	59.60	40.40	1.000000
3350	2360	1.24	0.00	22.03	18.37	0.401878
2360	1700	0.00	0.00	7.28	11.09	0.232771
1700	1180	0.00	0.00	4.40	6.69	0.137206
1180	850	0.00	0.00	2.42	4.28	0.086595
850	600	0.00	0.00	1.38	2.90	0.058250
600	425	0.00	0.00	1.01	1.89	0.037764
425	300	0.00	0.00	0.71	1.18	0.023412
300	212	0.00	0.00	0.44	0.74	0.014613
212	150	0.00	0.00	0.27	0.46	0.009205
150	106	0.00	0.00	0.22	0.25	0.004893
106	75	0.00	0.00	0.19	0.06	0.001181
75	0	0.00		0.06		

Normalized Breakage function	
Size	Bij
1.000000	1.000000
0.705263	0.401878
0.496842	0.232771
0.357895	0.137206
0.248421	0.086595
0.178947	0.058250
0.126316	0.037764
0.089474	0.023412
0.063158	0.014613
0.044632	0.009205
0.031579	0.004893
0.022316	0.001181

Table C.17 Breakage function for –1700 + 1180 microns quartz ground with cubes.

1700 microns		Feed		Product		Bij
		%Retained	%Passing	%Retained	%Passing	
2360	1700	0.00	100.00	0.00	100.00	
1700	1180	98.88	1.12	88.51	11.49	1.000000
1180	850	1.12	0.00	5.71	5.77	0.536756
850	600	0.00	0.00	2.44	3.34	0.306396
600	425	0.00	0.00	1.24	2.10	0.191440
425	300	0.00	0.00	0.79	1.31	0.118692
300	212	0.00	0.00	0.48	0.83	0.074862
212	150	0.00	0.00	0.07	0.76	0.068728
150	106	0.00	0.00	0.22	0.54	0.048819
106	75	0.00	0.00	0.24	0.30	0.027428
75	0	0.00		0.30		

Normalized Breakage function	
Size	Bij
1.000000	1.000000
0.694118	0.536756
0.500000	0.306396
0.352941	0.191440
0.250000	0.118692
0.176471	0.074862
0.124706	0.068728
0.088235	0.048819
0.062353	0.027428

Table C.18 Breakage function for –600 + 425 microns quartz ground with cubes.

600 microns		Feed		Product		Bij
		%Retained	%Passing	%Retained	%Passing	
850	600	0.00	100.00	0.00	100.00	
600	425	99.37	0.63	92.14	7.86	1.000000
425	300	0.63	0.00	5.74	2.12	0.283939
300	212	0.00	0.00	0.95	1.17	0.156248
212	150	0.00	0.00	0.57	0.60	0.079556
150	106	0.00	0.00	0.26	0.34	0.045244
106	75	0.00	0.00	0.14	0.20	0.026465
75	0	0.00		0.20		

Normalized Breakage function	
Size	Bij
1.000000	1.000000
0.708333	0.283939
0.500000	0.156248
0.353333	0.079556
0.250000	0.045244
0.176667	0.026465

C.2 Breakage function obtained for the mixtures of grinding media of different shapes

C.2.1 Breakage function obtained for a 50-50 mixture of balls and Eclipsoids

Table C.19 Breakage function for –16000 + 13200 microns quartz ground with a 50-50 mixture of balls and Eclipsoids.

16000 microns		Feed		Product		Bij
		%Retained	%Passing	%Retained	%Passing	
19000	16000	0.00	100.00	0.00	100.00	
16000	13200	98.58	1.42	25.87	74.13	1.000000
13200	9500	1.42	0.00	30.28	43.85	0.431421
9500	6700	0.00	0.00	12.63	31.22	0.279732
6700	4750	0.00	0.00	7.20	24.02	0.205366
4750	3350	0.00	0.00	5.38	18.65	0.154269
3350	2360	0.00	0.00	4.21	14.44	0.116575
2360	1700	0.00	0.00	3.21	11.23	0.089068
1700	1180	0.00	0.00	2.99	8.24	0.064290
1180	850	0.00	0.00	2.15	6.10	0.047007
850	600	0.00	0.00	1.85	4.24	0.032416
600	425	0.00	0.00	1.28	2.96	0.022453
425	300	0.00	0.00	1.08	1.88	0.014172
300	212	0.00	0.00	0.69	1.19	0.008943
212	150	0.00	0.00	0.50	0.69	0.005166
150	106	0.00	0.00	0.36	0.33	0.002499
106	75	0.00	0.00	0.25	0.09	0.000640
75	0	0.00		0.09		

Normalized Breakage function	
Size	Bij
1.000000	1.000000
0.825000	0.431421
0.593750	0.279732
0.418750	0.205366
0.296875	0.154269
0.209375	0.116575
0.147500	0.089068
0.106250	0.064290
0.073750	0.047007
0.053125	0.032416
0.037500	0.022453
0.026563	0.014172
0.018750	0.008943
0.013250	0.005166
0.009375	0.002499
0.006625	0.000640

Table C.20 Breakage function for –6700 + 4750 microns quartz ground with a 50-50 mixture of balls and Eclipsoids.

6700 microns		Feed		Product		Bij
		%Retained	%Passing	%Retained	%Passing	
9500	6700	0.00	100.00	0.00	100.00	
6700	4750	98.75	1.25	32.47	67.53	1.000000
4750	3350	1.25	0.00	31.83	35.70	0.397006
3350	2360	0.00	0.00	13.69	22.01	0.223452
2360	1700	0.00	0.00	6.78	15.23	0.148567
1700	1180	0.00	0.00	5.61	9.62	0.090936
1180	850	0.00	0.00	2.76	6.86	0.063870
850	600	0.00	0.00	2.11	4.75	0.043775
600	425	0.00	0.00	1.36	3.39	0.031033
425	300	0.00	0.00	1.13	2.27	0.020607
300	212	0.00	0.00	0.81	1.46	0.013205
212	150	0.00	0.00	0.54	0.92	0.008312
150	106	0.00	0.00	0.43	0.49	0.004422
106	75	0.00	0.00	0.27	0.22	0.001971
75	0	0.00		0.22		

Normalized Breakage function	
Size	Bij
1.000000	1.000000
0.708955	0.397006
0.500000	0.223452
0.352239	0.148567
0.253731	0.090936
0.176119	0.063870
0.126866	0.043775
0.089552	0.031033
0.063433	0.020607
0.044776	0.013205
0.031642	0.008312
0.022388	0.004422
0.015821	0.001971

Table C.21 Breakage function for –3350 + 2360 microns quartz ground with a 50-50 mixture of balls and Eclipsoids.

3350 microns		Feed		Product		Bij
		%Retained	%Passing	%Retained	%Passing	
4750	3350	0.00	100.00	0.00	100.00	
3350	2360	98.66	1.34	62.58	37.42	1.000000
2360	1700	1.34	0.00	15.56	21.87	0.542022
1700	1180	0.00	0.00	8.89	12.98	0.305360
1180	850	0.00	0.00	3.96	9.02	0.207547
850	600	0.00	0.00	3.06	5.95	0.134859
600	425	0.00	0.00	2.08	3.87	0.086807
425	300	0.00	0.00	1.42	2.45	0.054552
300	212	0.00	0.00	0.89	1.57	0.034704
212	150	0.00	0.00	0.71	0.86	0.018917
150	106	0.00	0.00	0.48	0.38	0.008383
106	75	0.00	0.00	0.31	0.07	0.001534
75	0	0.00		0.07		

Normalized Breakage function	
Size	Bij
1.000000	1.000000
0.704478	0.542022
0.507463	0.305360
0.352239	0.207547
0.253731	0.134859
0.179104	0.086807
0.126866	0.054552
0.089552	0.034704
0.063284	0.018917
0.044776	0.008383
0.031642	0.001534

Table C.22 Breakage function for –425 + 300 microns quartz ground with a 50-50 mixture of balls and Eclipsoids.

425 microns		Feed		Product		Bij
		%Retained	%Passing	%Retained	%Passing	
600	425	0.00	100.00	0.00	100.00	
425	300	99.02	0.98	92.11	7.89	1.000000
300	212	0.98	0.00	5.08	2.81	0.394371
212	150	0.00	0.00	1.42	1.40	0.194532
150	106	0.00	0.00	0.86	0.53	0.074020
106	75	0.00	0.00	0.38	0.15	0.020932
75	0	0.00		0.15		

Normalized Breakage function	
Size	Bij
1.000000	1.000000
0.705882	0.394371
0.498824	0.194532
0.352941	0.074020
0.249412	0.020932

C.2.2 Breakage function obtained for a 50-50 mixture of balls and cubes

Table C.23 Breakage function for –16000 + 13200 microns quartz ground with a 50-50 mixture of balls and cubes.

16000 microns		Feed		Product		Bij
		%Retained	%Passing	%Retained	%Passing	
19000	16000	0.00	100.00	0.00	100.00	
16000	13200	99.36	0.64	29.38	70.62	1.000000
13200	9500	0.64	0.00	32.41	38.21	0.395116
9500	6700	0.00	0.00	12.23	25.98	0.246906
6700	4750	0.00	0.00	6.07	19.92	0.182266
4750	3350	0.00	0.00	4.00	15.91	0.142256
3350	2360	0.00	0.00	3.61	12.30	0.107738
2360	1700	0.00	0.00	2.71	9.59	0.082782
1700	1180	0.00	0.00	2.68	6.92	0.058814
1180	850	0.00	0.00	1.86	5.05	0.042546
850	600	0.00	0.00	1.51	3.55	0.029632
600	425	0.00	0.00	1.09	2.45	0.020372
425	300	0.00	0.00	0.91	1.54	0.012738
300	212	0.00	0.00	0.55	0.99	0.008152
212	150	0.00	0.00	0.41	0.58	0.004758
150	106	0.00	0.00	0.32	0.26	0.002151
106	75	0.00	0.00	0.16	0.10	0.000838
75	0	0.00		0.10		

Normalized Breakage function	
Size	Bij
1.000000	1.000000
0.825000	0.395116
0.593750	0.246906
0.418750	0.182266
0.296875	0.142256
0.209375	0.107738
0.147500	0.082782
0.106250	0.058814
0.073750	0.042546
0.053125	0.029632
0.037500	0.020372
0.026563	0.012738
0.018750	0.008152
0.013250	0.004758
0.009375	0.002151
0.006625	0.000838

Table C.24 Breakage function for –9500 + 6700 microns quartz ground with a 50-50 mixture of balls and cubes.

9500 microns		Feed		Product		Bij
		%Retained	%Passing	%Retained	%Passing	
13200	9500	0.00	100.00	0.00	100.00	
9500	6700	98.73	1.27	54.20	45.80	1.000000
6700	4750	1.27	0.00	15.79	30.01	0.594932
4750	3350	0.00	0.00	9.31	20.70	0.386634
3350	2360	0.00	0.00	6.26	14.44	0.259992
2360	1700	0.00	0.00	3.67	10.77	0.190054
1700	1180	0.00	0.00	3.27	7.50	0.129951
1180	850	0.00	0.00	2.03	5.47	0.093758
850	600	0.00	0.00	1.67	3.80	0.064581
600	425	0.00	0.00	1.12	2.68	0.045245
425	300	0.00	0.00	0.93	1.75	0.029469
300	212	0.00	0.00	0.71	1.04	0.017415
212	150	0.00	0.00	0.44	0.60	0.010069
150	106	0.00	0.00	0.31	0.30	0.004950
106	75	0.00	0.00	0.22	0.08	0.001352
75	0	0.00		0.08		

Normalized Breakage function	
Size	Bij
1.000000	1.000000
0.705263	0.594932
0.500000	0.386634
0.352632	0.259992
0.248421	0.190054
0.178947	0.129951
0.124211	0.093758
0.089474	0.064581
0.063158	0.045245
0.044737	0.029469
0.031579	0.017415
0.022316	0.010069
0.015789	0.004950
0.011158	0.001352

Table C.25 Breakage function for –2360 + 1700 microns quartz ground with a 50-50 mixture of balls and cubes.

2360 microns		Feed		Product		Bij
		%Retained	%Passing	%Retained	%Passing	
3350	2360	0.00	100.00	0.00	100.00	
2360	1700	99.05	0.95	76.26	23.74	1.000000
1700	1180	0.95	0.00	11.71	12.04	0.490374
1180	850	0.00	0.00	4.66	7.38	0.292881
850	600	0.00	0.00	2.65	4.73	0.185078
600	425	0.00	0.00	1.53	3.19	0.124110
425	300	0.00	0.00	1.15	2.04	0.078770
300	212	0.00	0.00	0.68	1.36	0.052467
212	150	0.00	0.00	0.55	0.82	0.031394
150	106	0.00	0.00	0.33	0.49	0.018661
106	75	0.00	0.00	0.24	0.25	0.009638
75	0	0.00		0.25		

Normalized Breakage function	
Size	Bij
1.000000	1.000000
0.720339	0.490374
0.500000	0.292881
0.360169	0.185078
0.254237	0.124110
0.180085	0.078770
0.127119	0.052467
0.089831	0.031394
0.063559	0.018661
0.044915	0.009638

Table C.26 Breakage function for –425 + 300 microns quartz ground with a 50-50 mixture of balls and cubes.

425 microns		Feed		Product		Bij
		%Retained	%Passing	%Retained	%Passing	
600	425	0.00	100.00	0.00	100.00	
425	300	99.15	0.85	93.43	6.57	1.000000
300	212	0.85	0.00	4.20	2.38	0.404082
212	150	0.00	0.00	1.03	1.34	0.227024
150	106	0.00	0.00	0.62	0.72	0.121143
106	75	0.00	0.00	0.39	0.32	0.054473
75	0	0.00		0.32		

Normalized Breakage function	
Size	Bij
1.000000	1.000000
0.705882	0.404082
0.498824	0.227024
0.352941	0.121143
0.249412	0.054473

C.2.3 Breakage function obtained for a 75-25 mixture of balls and cubes

Table C.27 Breakage function for –16000 + 13200 microns quartz ground with a 75-25 mixture of balls and cubes.

16000 microns		Feed		Product		Bij
		%Retained	%Passing	%Retained	%Passing	
19000	16000	0.00	100.00	0.00	100.00	
16000	13200	99.10	0.90	28.68	71.32	1.000000
13200	9500	0.90	0.00	30.43	40.89	0.423986
9500	6700	0.00	0.00	11.75	29.14	0.277821
6700	4750	0.00	0.00	7.41	21.74	0.197641
4750	3350	0.00	0.00	5.13	16.61	0.146471
3350	2360	0.00	0.00	3.65	12.96	0.111925
2360	1700	0.00	0.00	2.86	10.10	0.085879
1700	1180	0.00	0.00	2.74	7.36	0.061675
1180	850	0.00	0.00	1.84	5.53	0.045850
850	600	0.00	0.00	1.65	3.88	0.031904
600	425	0.00	0.00	1.11	2.77	0.022685
425	300	0.00	0.00	0.95	1.82	0.014835
300	212	0.00	0.00	0.65	1.18	0.009547
212	150	0.00	0.00	0.60	0.58	0.004653
150	106	0.00	0.00	0.33	0.24	0.001955
106	75	0.00	0.00	0.21	0.03	0.000280
75	0	0.00		0.03		

Normalized Breakage function	
Size	Bij
1.000000	1.000000
0.825000	0.423986
0.593750	0.277821
0.418750	0.197641
0.296875	0.146471
0.209375	0.111925
0.147500	0.085879
0.106250	0.061675
0.073750	0.045850
0.053125	0.031904
0.037500	0.022685
0.026563	0.014835
0.018750	0.009547
0.013250	0.004653
0.009375	0.001955
0.006625	0.000280

Table C.28 Breakage function for –3350 + 2360 microns quartz ground with a 75-25 mixture of balls and cubes.

3350 microns		Feed		Product		Bij
		%Retained	%Passing	%Retained	%Passing	
4750	3350	0.00	100.00	0.00	100.00	
3350	2360	99.02	0.98	66.34	33.66	1.000000
2360	1700	0.98	0.00	14.08	19.58	0.543949
1700	1180	0.00	0.00	9.47	10.11	0.266090
1180	850	0.00	0.00	3.22	6.89	0.178153
850	600	0.00	0.00	1.92	4.96	0.127092
600	425	0.00	0.00	1.56	3.40	0.086464
425	300	0.00	0.00	1.34	2.06	0.051954
300	212	0.00	0.00	0.66	1.40	0.035114
212	150	0.00	0.00	0.53	0.87	0.021744
150	106	0.00	0.00	0.41	0.46	0.011423
106	75	0.00	0.00	0.28	0.18	0.004375
75	0	0.00		0.18		

Normalized Breakage function	
Size	Bij
1.000000	1.000000
0.704478	0.543949
0.507463	0.266090
0.352239	0.178153
0.253731	0.127092
0.179104	0.086464
0.126866	0.051954
0.089552	0.035114
0.063284	0.021744
0.044776	0.011423
0.031642	0.004375

Table C.29 Breakage function for –600 + 425 microns quartz ground with a 75-25 mixture of balls and cubes.

600 microns		Feed		Product		Bij
		%Retained	%Passing	%Retained	%Passing	
850	600	0.00	100.00	0.00	100.00	
600	425	99.54	0.46	87.99	12.01	1.000000
425	300	0.46	0.00	7.83	4.18	0.346156
300	212	0.00	0.00	1.35	2.83	0.232617
212	150	0.00	0.00	0.88	1.95	0.159530
150	106	0.00	0.00	0.62	1.33	0.108586
106	75	0.00	0.00	0.49	0.84	0.068231
75	0	0.00		0.84		

Normalized Breakage function	
Size	Bij
1.000000	1.000000
0.708333	0.346156
0.500000	0.232617
0.353333	0.159530
0.250000	0.108586
0.176667	0.068231

C.3 Breakage function parameters obtained for the grinding media shapes

The $B_{i,j}$ values were obtained using the equation below:

$$B_{i,j} = \frac{\log\left[\left(1-P_i(0)\right)/\left(1-P_i(t)\right)\right]}{\log\left[\left(1-P_{j+1}(0)\right)/\left(1-P_{j+1}\right)\right]} \qquad \text{(C.1)}$$

Then, these $B_{i,j}$ values were fitted to the empirical function given by Austin (1984) to evaluate the breakage function parameters of the quartz used.

$$B_{i,j} = \phi_j\left[\frac{x_{i-1}}{x_j}\right]^{\gamma} + (1-\phi_j)\left[\frac{x_{i-1}}{x_j}\right]^{\beta} \qquad \text{(C.2)}$$

The breakage function parameters for all our grinding media shapes were found to be:

Table C.30: Breakage function parameters obtained with the grinding media shapes used.

	Balls	Eclipsoids	Cubes	Mix B-E*	Mix B-C 1#	Mix B-C 2$
Beta	5.80	5.80	5.80	5.79	5.78	5.80
Gamma	1.00	1.06	1.14	1.11	0.99	0.99
Phi	0.75	0.72	0.71	0.76	0.75	0.78
Delta	0.05	0.02	0.01	0.01	0.02	0.05

***** Mixture of 50 % balls and 50 % Eclipsoids.

[#] Mixture of 50 % balls and 50 % cubes.

[$] Mixture of 75 % balls and 25 % cubes.

The values of the parameter δ were all found very closed to zero.

The total deviation (from the mean) of the particular point (x,y) is the vertical distance $y - \bar{y}$, which is the distance between the point (x, y) and the horizontal line passing through the sample mean $\bar{y}$ (Triola, 2005).The total deviation was found to be 0.006,i.e. 0.6%.

The quartz material used was then assumed to be normalizable (δ=0). Therefore, the fractions appearing at sizes less than the initial feed size were assumed independent of the initial feed size.

As a result, another parameter search was implemented with δ=0. The breakage function parameters considered for all our grinding media shapes were finally found to be:

Table C.31: Normalised breakage function parameters obtained with the grinding media shapes used.

	Balls	Eclipsoids	Cubes	Mix B-E*	Mix B-C 1#	Mix B-C 2$
Beta	5.80	5.80	5.79	5.79	5.79	5.80
Gamma	0.98	0.99	1.12	1.09	0.95	0.96
Phi	0.68	0.69	0.71	0.74	0.74	0.70
Delta	0.00	0.00	0.00	0.00	0.00	0.00

The standard variation values were found to be 0.0055, 0.0718 and 0.0253 for parameters β, γ and ϕ respectively. Eventually, it has been decided to consider the average values as the actual breakage function parameters.

Table C.32: Breakage function parameters obtained for the quartz material used.

Breakage function parameters	β	γ	ϕ
	5.80	1.01	0.71

C.2.4 Cumulative breakage distribution parameters $B_{i,j}$

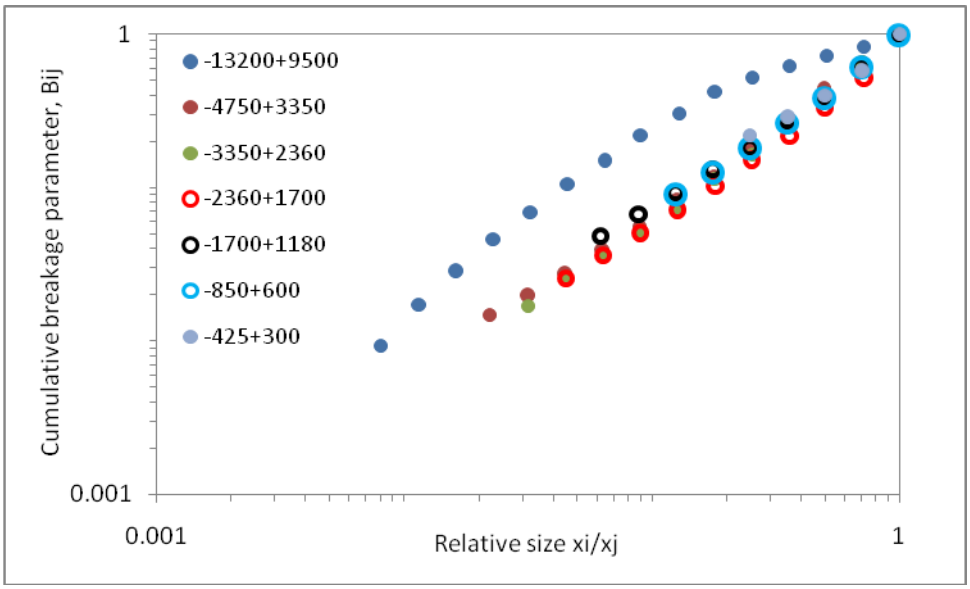

Figure C.1 Cumulative breakage distribution parameters for different sizes of quartz ground with balls.

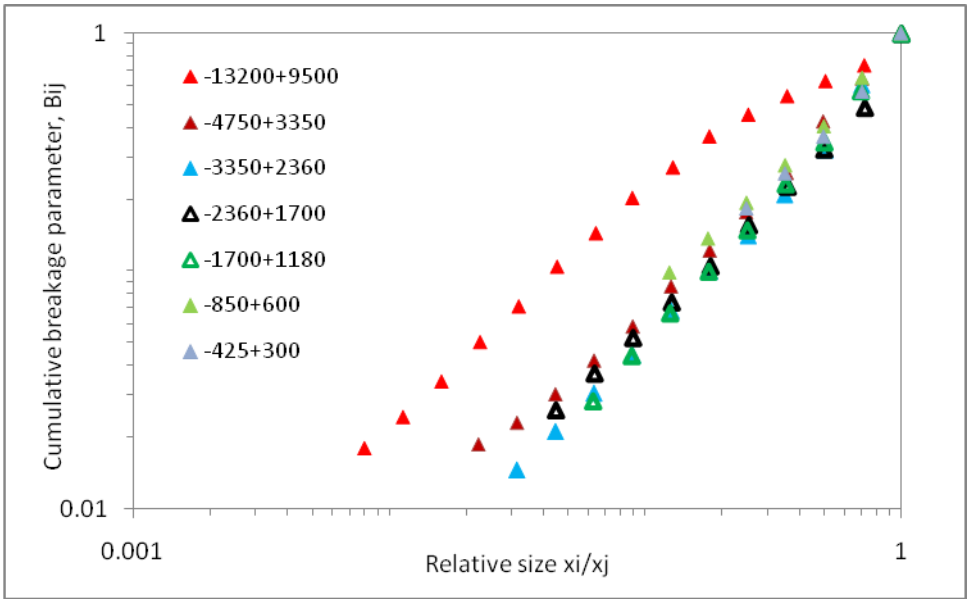

Figure C.2 Cumulative breakage distribution parameters for different sizes of quartz ground with Eclipsoids.

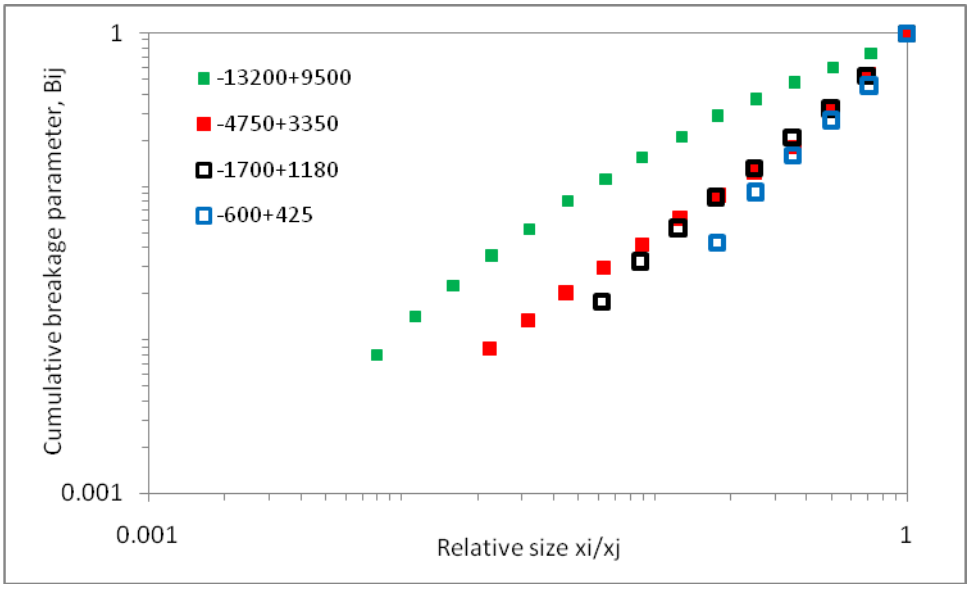

Figure C.3 Cumulative breakage distribution parameters for different sizes of quartz ground with cubes.

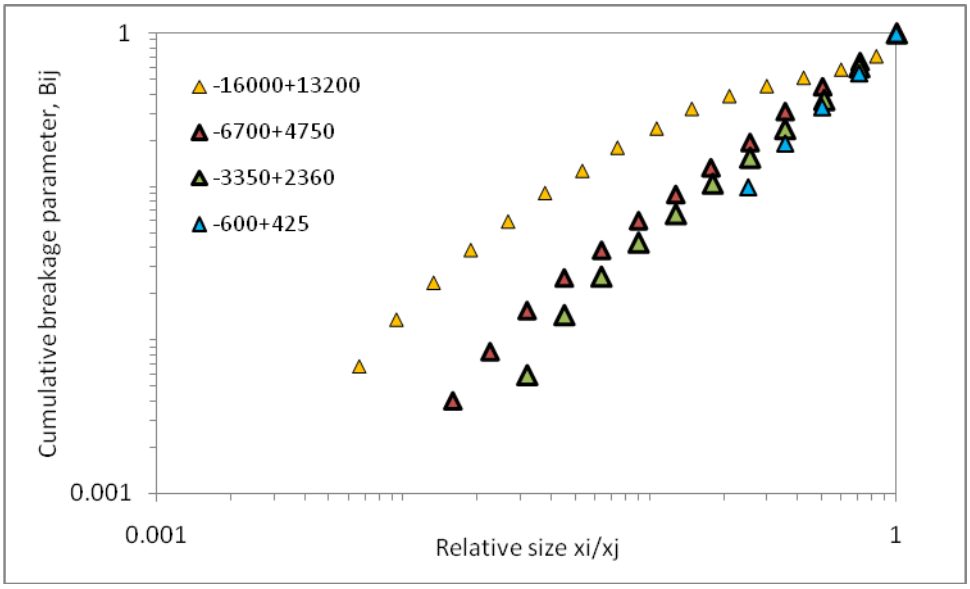

Figure C.4 Cumulative breakage distribution parameters for different sizes of quartz ground with mixture of 50 % balls and 50 % Eclipsoids.

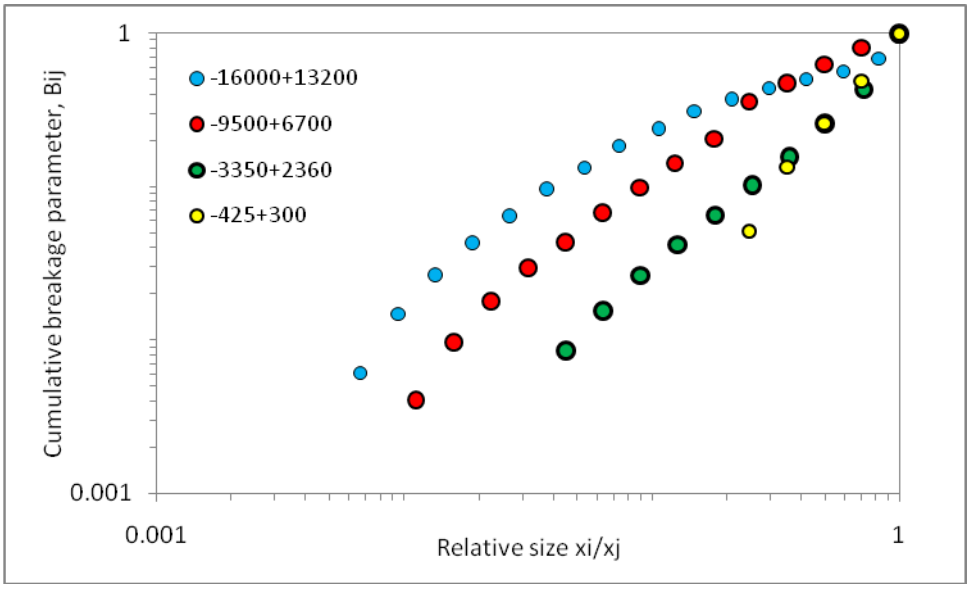

Figure C.5 Cumulative breakage distribution parameters for different sizes of quartz ground with mixture of 50 % balls and 50 % cubes.

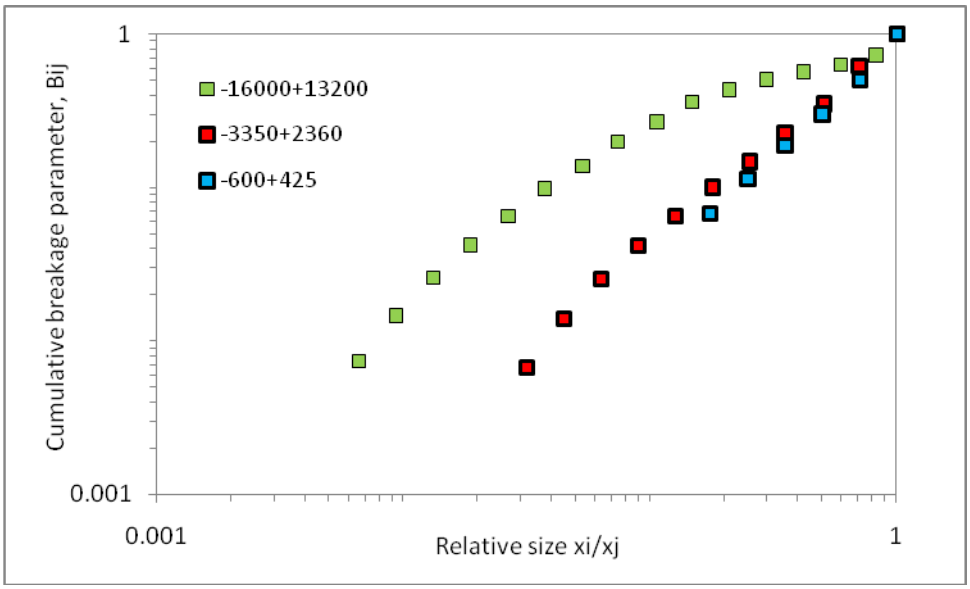

Figure C.6 Cumulative breakage distribution parameters for different sizes of quartz ground with mixture of 75 % balls and 25 % cubes.

D Non-linear regression technique

A non-linear regression technique was implemented on the data collected from the batch grinding tests performed. Basically, the goal of this technique is to find the best-fit values of the model (Motulsky and Christopoulos, 2003). More precisely, it aims at finding the best combination of fitting parameters of a model by minimizing the square of the differences between the experimental values $P_{expt}(t)$ and the predicted ones $P_{model}(t)$. The first order breakage law was used as our model to estimate the selection function. Consequently, the parameters that are likely to be correct are those that minimize the sum of squares. This objective function is defined as

$$SSE = \sum_{r=1}^{R} \left[P_{expt}(t) - P_{model}(t) \right]^2 \qquad \text{(D.1)}$$

where R is the number of runs considered to carry out a full batch test on a given particle size x.

$P_{expt}(t)$ retained experimental mass fraction on the top size screen x at grinding time t

$P_{model}(t)$ predicted mass fraction retained on size screen x_{i+1} after grinding of single-sized quartz material of initial size x_i for a total grinding time t.

Knowing that the average amount of scatter is not the same all the way at all values of X, a weighting scheme need to be applied to account of the increase of

the average amount of scatter with increasing Y values. The sum of the squares with the appropriate weighting is given by ((Motulsky and Christopoulos, 2003) :

$$SSE = \sum \left[\frac{P_{expt}(t) - P_{model}(t)}{P_{expt}(t)} \right]^2 \qquad \text{(D.2)}$$